5-2005

The Quaternary Tectonic and Structural Evolution of the San Felipe Hills, California

Stefan M. Kirby
Utah State University

THE QUATERNARY TECTONIC AND STRUCTURAL EVOLUTION OF THE SAN FELIPE HILLS, CALIFORNIA

by

Stefan M. Kirby

A thesis submitted in partial fulfillment
of the requirements for the degree

of

MASTER OF SCIENCE

in

Geology

Approved:

UTAH STATE UNIVERSITY
Logan, Utah

2005

ABSTRACT

The Quaternary Tectonic and Structural Evolution

of the San Felipe Hills, California

by

Stefan M. Kirby, Master of Science

Utah State University, 2005

Major Professor: Dr. Susanne U. Janecke
Department: Geology

We examine the transition between extension and strike-slip in the San Felipe Hills, western Salton Trough, southern California using new and compiled geologic mapping, measured stratigraphic sections, magnetostratigraphy, and structural analysis. A 625 m measured section describes the Borrego, Ocotillo, and Brawley formations in the SE San Felipe Hills and constrains a regional disconformity and correlative angular unconformity at ~ 1 Ma. Sedimentation rates for the Brawley Formation above the disconformity range from 1.0 to 1.2 mm/yr, paleoflow was to the ENE. The Brawley Formation consists of three interbedded lithofacies; (1) fluvial and fluvio-deltaic, (2) lacustrine, (3) and eolian deposits. Changes in facies, provenance, and paleoflow, with deposition of Ocotillo and Brawley formations record onset and evolution of cross cutting strike-slip faults other than the San Jacinto fault zone in the western Salton Trough at ~ 1 Ma.

Since deposition of the Brawley Formation (~ 0.5 Ma), rocks of the San Felipe Hills have been uplifted and complexly deformed. New data suggest that strands of the Clark fault persist SE of its previously mapped termination, transferring slip into folded rocks in the central and southern San Felipe Hills. Equivalent right lateral slip from folding for the Clark fault in the San Felipe Hills is 5.6 km. Minimum slip rates for the Clark strand are between 9 and 11 mm/year. Since ~ 0.5 Ma, evolving strands of the San Jacinto fault zone, including the Coyote Creek and Clark faults, have deformed rocks of the San Felipe Hills.

(182 pages)

ACKNOWLEDGMENTS

I would like to thank my wife, Jess, for her untiring support of my work both before and during my time at Utah State University. Without her patience little of this would have been possible. I would also like to thank my primary advisor, Susanne Janecke, for her patient support through out this process. Her broad view points and attention to detail greatly improved the structure and content of this manuscript. Becky Dorsey provided a detailed measured section of the Ocotillo Badlands and many informative discussions both in the field and while revising the thesis. I would like to thank Jim Evans for providing important reviews and discussions of the thesis. Vicki Langenheim graciously provided filtered magnetic and isostatic gravity data and important reviews of the third chapter. Bernie Housen collected and analyzed paleomagnetic data for the Oil Well Wash Section and provided relevant figures for the second chapter. George Jefferson and the staff of Anza-Borrego Desert State park graciously provided free camping and other logistical support. Kris McDougal analyzed microfossils from the Brawley and Borrego formations. Gary Girty provided his detailed mapping and important introduction to the rocks of the San Felipe Hills. Finally I would like to thank many of the graduate students who were friends, confidents, and valuable coworkers both in the field and back in Logan. Funding for this work was provided by NSF grant # EAR-0125497

Stefan M. Kirby

CONTENTS

LIST OF TABLES

LIST OF FIGURES

CHAPTER 1

INTRODUCTION

The evolution of the North American-Pacific plate boundary in the Salton Trough area of southern California is complex and incompletely understood. Within the western Salton Trough early extension was localized on the West Salton detachment fault but sometime after ~2.5-3 Ma cross cutting strike-slip faults replaced the west Salton detachment as the active structures in this area (Axen and Fletcher 1998). The San Jacinto fault zone was the principal cross-cutting dextral strike-slip fault. The relative amount, interaction, and timing of extension and strike-slip motion are poorly constrained in the area.

We examine this transition between extension and strike-slip deformation in the western Salton Trough with new 1:48,000 scale geologic mapping in the San Felipe Hills in approximately 2.5, 7.5 minute quadrangles (Plate 1). This map compiled detailed 1:6,000 scale mapping in the southeast San Felipe Hills (Heitman 2002; Lilly 2003) with new mapping across the rest of the San Felipe Hills. A 625 m detailed measured section describes the Borrego, Ocotillo and Brawley formations in the southeastern San Felipe Hills (Plate 2). A 245 m measured section of the coarse lateral equivalent of the Brawley Formation, the Ocotillo Formation, was described in the Ocotillo badlands to constrain basin-wide changes and lateral facies variation among these units. A major angular unconformity and lateral correlative disconformity beneath these units was constrained structurally and stratigraphically constrained for the first time. The results of the measured sections, map relations, new magnetostratigraphic dating of the Brawley

Formation are presented in chapter 2 and provide new constraints on the initiation and reorganization of the southern San Jacinto fault zone during the last ~ 1 to 1.5 Ma.

Current total plate motion across the plate boundary is broadly distributed east to west at the latitude of the Salton Sea, with much of the slip localized along strands of the San Jacinto fault zone. Previous geologic mapping, microseismicity, focal mechanismsand geophysical data all show significant changes in the characteristics of the San Jacinto fault zone along strike in the western Salton Trough.

The San Jacinto Fault zone is a southeastward widening zone within the western Salton Trough and includes the Coyote Creek, Clark, Superstition Hills, Superstition Mountain faults (Sharp 1967). Initiation of slip on the San Jacinto fault zone to the north near its junction with the San Andreas may have begun at 1.5 Ma (Morton and Matti 1993) or 2.5 Ma (Meisling and Weldon 1989). Within the San Felipe Hills, Plio-Quaternary sediments are strongly deformed by a complex series of folds and faults southeast of the previously mapped termination of the surface trace of the Clark fault. To the south, the Superstition Hills and Superstition Mountain faults may be accommodating slip adjacent to a broad zone of clockwise transrotation (Hudnut et al. 1989). The onset of slip on the southeast portion Clark fault has not been adequately dated. Also, interactions among the active strands of the southern San Jacinto fault zone and in particular the Clark fault, the complex deformation within the San Felipe Hills and transrotation to the south has not been explored by previous studies.

To constrain the structural style, onset of slip, and right-lateral slip amount in the San Felipe Hills, the geologic map was divided into fold domains based on similar fold geometries. Average trend and plunge of fold axes, interlimb angles, strain rates,

shortening, and shortening rates were calculated for each domain. Transects through relevant fold domains were used to calculate the total N-S shortening and amount of equivalent dextral slip on the Clark fault plane oriented 305° NW that is required to produce this amount of shortening. These data along with new and compiled geologic mapping are presented in chapter 3. To constrain the geometries and interactions of the fault strands of the southern San Jacinto fault zone 3 earlier models for the geometry of the Clark fault in the San Felipe Hills and its relation to the Superstition Hills fault to the south are considered in chapter 3. Minimum fault slip rates are calculated, time of reorganization and initiation of the fault zone are identified, and a new kinematic model of the current San Jacinto fault zone are presented in chapter 3.

References

Axen, G.J., and Fletcher, J. M. 1998. Late Miocene-Pleistocene extensional faulting, northern Gulf of California, Mexico and Salton Trough, California. International Geology Review 40:217-244.

Heitman, E. A. 2002. Characteristics of the Structural Fabric Developed at the Termination of a Major Wrench Fault. [M.S. thesis] San Diego State University. San Diego CA, 77p.

Hudnut, K. W.; Seeber, L.; Pacheco, J.; Armbruster, J. G.; Sykes, L. R.; Bond, G. C.; and Kominz, M. A. 1989. Cross faults and block rotation in Southern California; earthquake triggering and strain distribution. Yearbook Lamont–Doherty, Geological Observatory of Columbia University, p. 44-49.

Lilly, D. R. 2003. Structural geology of a transitory left step in San Felipe Hills fault. [M.S. Thesis] San Diego State University. San Diego CA, 91 p.

Meisling, R., and Weldon, K. 1989. Late Cenozoic tectonics of the northwestern San Bernardino Mountains, Southern California. Geological Society of America Bulletin 101:106-128.

Morton, D. M., and Matti, J. C. 1993. Extension and contraction within an evolving divergent strike-slip fault complex: the San Andreas and San Jacinto fault zones

at their convergence in Southern California. *In* R.E. Powell, R.J. Weldon, and J.C. Matti eds, The San Andreas fault system: displacement, palinspastic reconstruction, and geologic evolution. Geological Society of America, Memoir 178, p. 217-230.

Sharp, R.V, 1967, San Jacinto fault zone in the Peninsular Ranges of Southern California. Geological Society of America Bulletin 78:705-729.

CHAPTER 2

STRATIGRAPHY AND DEPOSITIONAL SETTING OF THE BRAWLEY FORMATION: INSIGHTS INTO INITIAL STRIKE-SLIP DEFORMATION IN THE WESTERN SALTON TROUGH[1]

Abstract

The evolution of the North American-Pacific plate boundary in the Salton Trough area is complex and incompletely understood. We examine this evolution and the transition between extension and strike-slip movement in the western Salton Trough with new 1:48,000 scale geologic mapping in the San Felipe Hills in approximately 2.5, 7.5 minute quadrangles (Plate 1). This map compiled new mapping across the San Felipe Hills with detailed 1:6,000 scale mapping in the southeast San Felipe Hills (Heitman 2002; Lilly 2003). A 625 m detailed measured section describes the Borrego, Ocotillo and Brawley formations in the southeastern San Felipe Hills. Magnetostratigraphy in this section shows that the Brawley Formation was deposited between 1.07 Ma and 0.61 Ma $\pm$ 0.02 Ma to 0.52 Ma $\pm$ 0.03 Ma. A 245 m measured section of the coarse lateral equivalent of the Brawley Formation, the Ocotillo Formation, in the Ocotillo Badlands shows rapid westward coarsening of these units.

Plio-Pleistocene sedimentary rocks in the San Felipe Hills, Salton Trough record an abrupt change from older, open, perennial lake beds to cyclic alluvial fan, fluvial-

---

[1] Coauthored by Stefan M. Kirby, Susanne U. Janecke, Rebecca J. Dorsey, Bernard A. Housen, Victoria Langenheim, and Kristin McDougall-Reid.

deltaic, and marginal lacustrine deposits at 1.07 Ma. The ~1680 m thick lacustrine claystone, mudstone, and sandstone of the Borrego Formation in the San Felipe Hills preserve almost no marginal lacustrine deposits and formed in a large perennial lake. A regional disconformity and laterally equivalent angular unconformity at the crest of a 15 km long, east-west trending basement-cored anticline separate the Borrego Formation from the overlying Ocotillo Formation and its fine-grained equivalent, the Brawley Formation. This east-west trending anticline is interpreted as the first evidence for transpressional deformation within the previously transtensional southwest Salton supradetachment basin.

The Ocotillo Formation is dominated by alluvial fan and braided stream facies, with lesser amounts of fluvial and minor lacustrine facies deposited conformably on the underlying Borrego Formation in the Ocotillo Badlands. The Ocotillo Formation fines and thins to east-northeast as it interfingers with the Brawley Formation in the eastern San Felipe Hills.

The Brawley Formation consists of three interbedded lithofacies: fluvial to deltaic sandstone with cross-bedding and weak calcic paleosols; lacustrine mudstone, claystone, and marlstone with 0.5 to 1.5 m deep desiccation cracks, rare evaporite minerals, and locally abundant microfossils; and eolian sandstone with large scale (~ 3-4 m high) high-angle cross stratification. Microfossils include marine and lagoonal forams, and lacustrine ostracods, micromollusks, and charophytes. Sandstones include ~60 % biotite-rich arkose derived from local tonalite plutons (L suite), and ~ 40 % sublitharenite derived from the Colorado Plateau (C suite). Sediment transport was to the E to NNE in the San Felipe Hills. Sedimentation rates in the Brawley Formation average about 1.0

mm/yr ± 0.1 mm/yr to 1.2 mm/yr ± 0.2 mm/yr. Clastic Brawley Formation sediments accumulated in an ephemeral stream and delta system on the western margin of the Salton Trough while evaporites accumulated offshore in the basin center near the southeast Salton Sea (Herzig et al. 1988).

Deposition of the Ocotillo and Brawley formations occurred in a basin controlled by strike-slip faults that cut across the West Salton detachment fault and predate the current, fully formed San Jacinto fault zone. The end of deposition of the Brawley and Ocotillo formations and the first closely spaced folds occurred between 0.61 Ma ± 0.02 Ma and 0.52 Ma ± 0.03 Ma . This abrupt change at ~ 0.6 Ma, south and west of the Salton Sea, reflects reorganization of the basin due to changes in geometry and kinematics of the San Jacinto fault zone in the San Felipe Hills.

Introduction

Tectonic Background

The Late Miocene to Recent evolution of the North American-Pacific plate boundary in the Salton Trough is complex and incompletely understood. Throughout most of this evolution dextral strike-slip motion has occurred on the San Andreas fault system along the eastern margin of the Salton Trough (Atwater 1970; Axen and Fletcher 1998; Oskin and Stock 2003). Within the western Salton Trough early extension was localized on the West Salton detachment fault but sometime after 3 Ma cross cutting strike-slip faults including the San Jacinto fault zone and the Elsinore replaced the west Salton detachment as the active structures in this area (Sharp 1967; Frost et al. 1996; Axen 1998; Axen and Fletcher 1998; Dorsey and Janecke 2002; Steely et al. 2004; Axen

Dibblee (1954, 1984) noted large-scale lithologic relationships, including facies changes and angular unconformities, which hinted at significant changes in basin architecture during deposition of the late Miocene to middle Pleistocene aged stratigraphic section within the San Felipe Hills. Changes in depositional patterns and the presence of an angular unconformity that separates the Ocotillo Formation from older units in some areas (Dibblee 1954, 1984; Reitz 1977) may record a major basin reorganization in the western Salton Trough. The transition from slip on the West Salton detachment fault (Axen and Fletcher 1998) to active slip on strands of the San Jacinto fault zone may have produced the angular unconformity and changes in facies. Complex folding, north-south shortening and faulting of the late Cenozoic stratigraphic section started during the deposition of the upper portion of the sedimentary section, with most deformation postdating the deposition of the Ocotillo and Brawley formations (Dibblee 1954, 1984; Morley 1963; Dronyk 1977; Wagoner 1977; Reitz 1977; Feragen 1986; Wells 1987; Heitman 2002; Lilly 2003; Steely et al. 2004; Kirby et al. 2004; this study) (fig 2-3).

The goal of this study is to better quantify and understand the stratigraphic connection between basin-controlling faults, large folds and the sedimentary section and to examine evidence for the transition from extension and transtension across the now inactive and exhumed West Salton detachment fault system, to on-going strike-slip within the San Jacinto fault zone in the western Salton Trough.

Stratigraphic Overview

The early transtension succession exposed in the San Felipe Hills includes the Latest Miocene (?) to Pliocene marine Imperial Group and its lateral nonmarine

equivalents at Borrego Mountain, and the overlying Pliocene fluvial-deltaic Diablo and Olla formations of the Palm Spring Group (Winker and Kidwell 1996; Axen and Fletcher 1998; Steely et al. 2004) (fig. 2-4). Interfingering with and conformably overlying the Diablo Formation in the San Felipe-Borrego basin is the thick lacustrine Borrego Formation. The Borrego Formation may have been deposited during a poorly dated and understood transition between transtensional deformation and later transpression and strike-slip related deformation or during the final phases of regional transtension on the West Salton detachment fault (Janecke et al. 2004; Dorsey et al. 2004; Steely et al. unpublished data) (fig. 2-4). Altogether this transtensional to transitional succession is up to 4195 m thick and is well exposed in the San Felipe Hills and the Borrego Mountain area (Dibblee 1954, 1984; Morley 1963; Reitz 1977; Wagonner 1977; Dronyk 1977; Feragen 1986; Wells 1987; Heitman 2002; Lilly 2003; this study) (figs. 2-2, 2-3, 2-4). These units were likely deposited in a basin that was at least partially the result of oblique top-to-the-east extensional slip on the west Salton detachment fault (Steely et al. 2004; Axen et al. 2004), because the sandstones and mudstones of the Imperial and Palm Spring groups change laterally into boulder conglomerate of the Canebrake Formation at the detachment fault (Dibblee 1954, 1984; Winker 1987; Winker and Kidwell 1996, 2002; Axen and Fletcher 1998; Dorsey and Janecke 2002; Steely et al. 2004) (figs. 2-2, 2-4). The San Andreas fault on the NE side of the basin probably also localized the basin at this time.

Directly above the Borrego Formation in the San Felipe-Borrego basin there is an abrupt change in lithology and sedimentary environment at the base of the Ocotillo and Brawley formations (Dibblee 1954, 1984; Dorsey 2002; Lutz et al. 2003; this study) (figs.

2-3, 2-4). There are significant lithologic differences between the Ocotillo Formation and the underlying Imperial Group, Diablo and Borrego formations in the San Felipe Hills (Dibblee 1954, 1984; Reitz 1977; Heitman 2002; Lilly 2003; Lutz and Dorsey 2003). The Ocotillo Formation within the Ocotillo and Borrego badlands and the San Felipe Hills is a pebble to cobble conglomerate and pebbly sandstone with lesser fine-grained sandstone and mudstone, whereas the underlying units range from claystone to sandstone (Dibblee 1954,1984; Bartholomew 1967; Reitz 1977; Remieka and Beske-Diehl 1996; Heitman 2002; Lilly 2003; Lutz et al. 2003).

A major basin-wide change in grain size is recorded at the base of the Ocotillo and Brawley formations, but this contact was described as a conformable and nearly imperceptible stratigraphic transition in the eastern San Felipe Hills (Dibblee 1954, 1984; Dronyk 1977; Wagoner 1977). On the south flank of the San Felipe anticline and in the Superstition Hills and Superstition Mountain area this contact is an angular unconformity (Dibblee 1954, 1984; Reitz 1977) (figs. 2-3, 2-4). The nature of this contact and the stratigraphic changes across it in the San Felipe Hills, are the subject of this paper.

Within the western Salton Trough the Ocotillo Formation and its fine-grained lateral equivalent (the Brawley Formation) overlie either an angular unconformity, disconformity, or conformable contact (Dibblee 1954, 1984) (figs. 2-2, 2-3). Previous workers have inconsistently described this contact in and near the San Felipe Hills (Dibblee 1954, 1984; Morley 1963; Bartholomew 1968; Dronyk 1977; Reitz 1977; Wagoner 1977; Feragan 1986; Wells 1987; Heitman 2002; Lilly 2003). In the southwestern San Felipe Hills, an angular unconformity was first described by Dibblee (1954,1984) and later confirmed by other workers (Morley 1963; Reitz 1977; Dorsey et

al. 1999) (figs. 2-3, 2-4). Reitz (1977), Heitman (2002), and Lilly (2003) noted conformable contacts beneath the Ocotillo Formation in Tarantula Wash a short distance east of areas of angular unconformity. In the eastern San Felipe Hills previous workers describe the basal contact of the Brawley formations as conformable with, and nearly indistinguishable from, the underlying Borrego Formation except where the coarse but thin Ocotillo Formation coincides with the contact (Dibblee 1954, 1984; Dronyk 1977; Wagoner 1977; Feragan 1986; Heitman 2002; Lilly 2003). Nearby in the Ocotillo Badlands to the southwest of the study area the Ocotillo Formation is described as conformable with the Borrego Formation with a 20 degree angular unconformity apparent within the lower Ocotillo Formation (Dibblee 1984). To the west-northwest in the Borrego Badlands the basal contact is described as conformable with the underlying Borrego Formation (Dibblee 1954; Remieka and Beske-Diehl 1996; Lutz and Dorsey 2003) but is now recognized as a brief hiatus in a few areas (Lutz, 2005; Lutz et al. 2004). Bartholomew (1968) and Reitz (1977) suggested that some of the Ocotillo Formation is correlative with the terrace and pediment deposits in the Borrego Badlands and the San Felipe Hills respectively.

The lateral equivalent of the Ocotillo Formation, the Brawley Formation, is poorly known. Dibblee (1954, 1984) briefly described it as the lacustrine equivalent of the Ocotillo Formation, and indistinguishable from the underlying Borrego Formation where a thin conglomerate bed at the base of the Brawley Formation is absent. Later workers mostly accepted Dibblee's (1954, 1984) description of the Brawley Formation in the San Felipe Hills. Dronyk (1977) and Feragan (1986), mislocated the Brawley-Borrego contact within the Brawley Formation and described the two units as

indistinguishable. None of these workers completed any systematic study of lithofacies and depositional environment in the Brawley Formation but produced detailed maps of subunits in the Borrego and Brawley formations (Wagoner 1977; Dronyk 1977; Feragan 1986). Prior to this study the Brawley Formation in its exposures in the western Salton Trough was considered to be lithologically similar to the Borrego Formation (Dibblee 1954, 1984; Dronyk 1977; Wagoner 1977).

Structural Overview

The structures controlling basin subsidence in the western Salton Trough have evolved through time and can be subdivided into at least three distinct phases. After a poorly documented phase of extension in Miocene time and deposition of the Red Rock and Elephant Trees formations south of the San Felipe-Borrego basin (Kerr 1984; Winker and Kidwell 1996, 2002; Dorsey and Janecke 2002), the West Salton detachment fault began to slip along the entire west-southwest margin of the basin (Axen and Fletcher 1998; Dorsey and Janecke 2002; Winker and Kidwell 2002; Steely et al. 2004). Development of the first large basins of the western Salton Trough was controlled by oblique, top-to-the-east dextral-normal slip on the west Salton detachment fault in the west and the normal slip component on the San Andreas fault in the east (Frost et al. 1996; Axen and Fletcher 1998; Steely et al. 2004; Axen et al. 2004). The West Salton detachment fault accommodated a significant fraction of strike-slip and produced at least one basin-scale growth anticline with a northwest trend (Steely et al. 2004; Axen et al. 2004). The northwest trend of this syndetachment growth anticline differs from the east-west and north-south trend of folds that formed during the younger phase of transpression and strike-slip deformation (Axen et al. 2004; Kirby et al. 2004; Steely et al. 2004). We

will assume that major east-west trending folds or fold trains are the result of wrench deformation within the San Jacinto fault zone because such orientations are inconsistent with the detachment's predicted and observed strain field, and because such east-west trending folds are active in today's strain field (Anderson et al. 2003).

Later, by Ocotillo time, slip on the San Jacinto fault zone and the southernmost San Andreas fault, the Brawley seismic zone and the Imperial fault were the primary controls on basin architecture (Janecke et al. 2004). A transitional phase of deformation during deposition of the Borrego Formation might predate the present geometry of the San Jacinto fault zone and there is some evidence that parts of the deactivated detachment fault have been utilized by younger strike-slip faults (Pettinga 1991; Axen and Fletcher 1998; Dorsey and Janecke 2002; Axen et al. 2004; Steely et al. 2004).

Currently the San Felipe Hills are surrounded by dextral strands of the southern San Jacinto fault zone (Dibblee 1954, 1984; Sharp 1967, 1981). The Clark fault may enter the study area from the north-west, the Coyote Creek fault is located along the southwestern margin of the study area, the San Andreas fault is ~40 km to the northeast, and the Superstition Mountain and Superstition Hills faults are ~20 km to the south (figs. 2-2, 2-3). Slip on these or other older dextral strands probably created the broad east-plunging San Felipe anticline which dominates the central San Felipe Hills, as well as the innumerable smaller map scale folds throughout the San Felipe Hills (Dibblee, 1984; Heitman 2002; Lilly 2003; Chapter 3) (fig. 2-3).

The San Felipe anticline is a broad east-west trending structure which partially predates deposition of the Ocotillo and Brawley formations (Dibblee 1954, 1984; Chapter 3). Prior work suggests that the San Felipe anticline postdates the deposition of the

Diablo Formation (Dibblee 1954, 1984). The age and geometry of the anticline is refined by this study.

Many open to gentle complex, and more closely spaced folds deform the limbs of the larger San Felipe and Santa Rosa anticlines (Dibblee 1954, 1984; Morley 1963; Reitz 1977; Wells 1987; Feragen 1986; Heitman 2002; Lilly 2003) (fig. 2-3). We will show that these folds all postdate deposition of the Ocotillo and Brawley formations and are consistent with the kinematics of the active strands of the San Jacinto fault zone (Chapter 3).

Methods

To assess stratigraphic and structural relations within the San Felipe Hills new 1:24000-scale geologic mapping was completed and combined with previous detailed mapping in the south central San Felipe Hills (Heitman 2002; Lilly 2003) in approximately 2.5, 7.5 minute quadrangles. Mapping of the angular truncation beneath the Ocotillo Formation in the western San Felipe Hills and south of Squaw Peak is quantified and used to produce a reconstructed cross-section (A-A') of the paleo-San Felipe anticline at the time of initial deposition of the Ocotillo and Brawley formations. The cross-section restores post Ocotillo Formation north-south shortening, but does not restore slip on east-west striking strike-slip faults with uncertain offset. An additional cross section (B-B') was created for a transect just west of A-A' to show the current geometry of the San Felipe anticline. The approximate lateral extent of the angular unconformity beneath the Ocotillo formation was mapped out and compared with the causative structures. A 625 m detailed measured section was described through the

Borrego, Ocotillo and Brawley formations in the south-eastern San Felipe Hills to characterize a disconformity and basin transition, and to provide the first detailed analysis of the depositional environment of the Brawley Formation.

Magnetostratigraphic analysis constrains the age deposition of the Brawley Formation in the San Felipe Hills, and we collected a total of 16 sites, spaced approximately every 40 meters within the measured section, recovering between 4 and 7 samples per site. The drilled samples were oriented using both magnetic and sun compasses; the declinations of the magnetic and sun compass all agreed to within a degree. The magnetizations of the samples were measured using a 2-G 755 DC SQUID magnetometer in a magnetically shielded room at Western Washington University, using an 8 position rotation scheme. The samples were demagnetized using an initial low-temperature treatment accomplished by immersion in liquid nitrogen. Little or no loss of remanence was observed after this treatment. The samples were then either thermally demagnetized (using an ASC-TD 48 oven), with 15 to 22 temperature steps, or by alternating-field (a.f.) demagnetization (using a D-Tech D2000 a.f. demagnetizer), with 5 to 10 mT increments to a maximum field of 200 mT. The paleomagnetic data were analyzed utilizing the PCA technique (Kirschvink 1980) to determine the directions of magnetization components. The directional components were then analyzed using both standard Fisher (1953) statistics, and the bootstrap methods of Tauxe (1998). These results were then correlated with the magnetic polarity timescale of Cande and Kent (1995) to determine the age of the top and bottom of the Brawley Formation, to date the first major phase of growth on the San Felipe anticline, and to determine when the closely spaced folding and related faulting first developed in the area. We compared our data

with the upper 2 Ma of the magnetic polarity timescale because the correlative Ocotillo Formation in the Borrego Badlands yields Irvingtonian fossils and contains the 0.76 Ma Bishop ash (Remieka and Beske-Diehl 1996).

A 224 m of section from the Ocotillo Badlands through the Borrego and Ocotillo formations was described by Dorsey and analyzed for facies, paleocurrents, and provenance. The Oil Well Wash measured section is located 21 km to the east-northeast of the measured section in the Ocotillo badlands. This allows more proximal and distal facies to be compared within the same depositional basin.

Paleocurrent indicators were measured in exposures of the Brawley and Ocotillo formations including the two measured sections. Within the measured section samples were collected and analyzed for microfossils by Kristin McDougall. Sandstone provenance was noted when apparent in hand sample. Sands were subdivided into three groups; Colorado River derived, locally derived, and mixtures of the two.

Results

Outcrop Locations

Within the San Felipe Hills the Ocotillo and Brawley Formations are exposed throughout the southern and eastern portions of the study area (figs. 2-2, 2-3). The primary exposures of Ocotillo Formation form an east-west trending belt along the southern limb of the San Felipe anticline (figs. 2-2, 2-3). On the north limb of the San Felipe anticline in the northwestern portion of the field area there are small exposures of the Ocotillo Formation (fig. 2-3). Other exposures of the Ocotillo Formation exist, immediately to the south and north of the study area, in the Ocotillo and Borrego

Badlands and the Seventeen Palms area (Dibblee 1954, 1984; Pettinga 1991) (fig. 2-2). South of Squaw Peak the Ocotillo Formation extends eastward as this unit interfingers with the Brawley Formation in the southeastern San Felipe Hills (figs. 2-2, 2-3).

Outcrops of the Brawley Formation form an east-west trending belt east of the Powerline fault in the southern San Felipe Hills. In the eastern San Felipe Hills exposures of the Brawley Formation lie near and east of California State Highway 86, and extending nearly to the Salton Sea (figs. 2-2, 2-3). To the south of the San Felipe Hills the Brawley Formation has been uplifted and exposed in the Superstition Hills and Superstition Mountain areas (Dibblee 1954, 1984) (Fig. 2-2). The Brawley Formation is in the subsurface to the east and south of the study area (Severson 1987; Herzig et al. 1988).

In the southeast portion of the San Felipe Hills, east of the Powerline fault, the Brawley interfingers with and grades westward into the Ocotillo Formation (Dibblee 1954,1984; this study) (figs. 2-2, 2-3). The contact between the two units was placed above the highest conglomerate or pebbly sandstone (Girty pers. comm. 2003; this study). A thin (5-25 m) widespread tongue of conglomerate and pebbly sandstone, mapped as Ocotillo Formation, makes up the basal unit of the finer-grained Brawley Formation in the southeastern San Felipe Hills (Dibblee 1954, 1984; Heitman 2002; Lilly 2003) (figs.2-3, 2-5). This basal conglomerate is replaced in the north by a locally derived sandstone and grit in the eastern San Felipe Hills.

Borrego Formation

The Borrego Formation in the San Felipe Hills is up to 1680 m thick in the eastern San Felipe Hills, and has a sharp upper contact with the overlying Ocotillo and Brawley

formations. The base of the Borrego Formation is transitional as it interfingers with the underlying fluvial-deltaic Diablo Formation. In the north and central San Felipe Hills a transitional map unit was used to identify areas where Diablo and Borrego lithologies interfinger in nearly equal amounts.

The Borrego Formation in the San Felipe Hills and Ocotillo Badlands consists of fine-grain lacustrine claystone, mudstone, and siltstone with widely spaced interbedded sandstones. The total volume of sandstone is less than fifty percent, usually much less than fifty percent (figs. 2-5, 2-6; plate 2). Red finely laminated to massive marly claystone, and mudstone are the primary lithology of the Borrego Formation. Lesser grey claystone and thin marl up to 0.5 m thick are also present (figs. 2-5).

Sandstone beds in the Borrego Formation are up to 4 m thick and dominantly sublitharenite derived from the Colorado River (Guthrie 1991; Winker and Kidwell 1996). The middle of the Borrego Formation in the eastern San Felipe Hills contains several discontinuous beds up to 2 m thick of pebbly sandstone, with clasts dominated by tonalite. In the southeastern San Felipe Hills a laterally continuous bed of conglomerate that contains clasts of Diablo Formation sandstone and oyster shell fragments from the marine Imperial Group is traceable for several kilometers in the middle to upper Borrego Formation.

The Borrego Formation appears internally conformable at our map scale and does not show evidence for syndepositional growth in the San Felipe Hills. Growth may be apparent within the Borrego Formation to the north and northwest in the Borrego Badlands (Dorsey unpublished data 2003). Landsat imagery that shows possible convergence of beds within the Borrego Formation on the north flank of the San Felipe

anticline coincides with a zone of structural convergence and numerous dextral faults (plate 3). Further stratigraphic work within the Borrego Formation throughout the western Salton Trough is necessary to clarify these relationships.

The uppermost Borrego Formation was measured in the lower part of both the Ocotillo Badlands section and the Oil Well Wash section. This portion of the Borrego Formation is exposed in the southeastern and eastern San Felipe Hills and the core of the anticline in the Ocotillo Badlands beneath the Ocotillo and Brawley formations (figs. 2-3, 2-5, 2-6; plate 2). Both of the sections started in the upper Borrego Formation. The Oil Well Wash measured section describes up to 128.5 m of the Borrego Formation and the Ocotillo Badlands measured section describes 21.5 m.

The Borrego Formation in both sections is dominated by claystone with lesser mudstone and sandstone. In the Oil Well Wash section the claystone is gray to red or pink and finely laminated to massive with thin up to several cm thick yellow weathering marl. Sandstone in the Oil Well Wash measured section is composed of fine- to medium-grained sublitharentite, which is characteristic of Colorado River-derived sediments (Guthrie 1991) (fig. 2-5; plate 2). Sandstone beds are up to 5 m thick but more commonly only 2-3 m thick displaying low-angle cross stratification and planar stratification. Thin 10 cm thick gray silty-marl beds are also present in the Borrego Formation. The upper 5 m of the Borrego Formation consists of interbedded very fine-grained sandstone, siltstone, and thin 1-2 cm thick laminated micrite. One prominent interval of desiccation cracks in red claystone occurs in the upper 15 m of the Borrego Formation in Oil Well Wash.

The upper Borrego Formation in the Ocotillo Badlands is dominated by massive to finely laminated red claystone (fig. 2-15). One 2 m thick bed of horizontally stratified pebbly sandstone is interbedded in red claystone 5 m below the contact with the Ocotillo Formation. Clast composition of this bed is dominated by tonalite from the eastern Peninsular Ranges. No soil structures or desiccation cracks were observed in the uppermost Borrego Formation in the Ocotillo Badlands and the contact with the overlying Ocotillo Formation is interbedded and conformable.

Microfossils in the Borrego Formation included ostracods, micromollusks, diatoms, rare planktonic forams, and plant fragments (fig. 2-5; table 2-1) (McDougall unpublished data 2004). Microfossil assemblages indicate freshwater to occasionally brackish water lacustrine conditions. The Borrego Formation accumulated in a quiet and relatively clear, shallow (< 20 m), near-shore environment in a pool/lake/lagoon setting (McDougall unpublished work 2004). Water for this system was provided by saline (marine) and freshwater sources (McDougall unpublished work 2004).

The rocks of the Borrego Formation accumulated in a perennial lacustrine setting with sandstone representing more proximal facies and claystone and mudstone representing distal, open lacustrine facies and near shore environments. Further work is necessary to characterize the sandstone facies in the Borrego Formation, but work to date shows few marginal lacustrine deposits in the San Felipe Hills.

Ocotillo Formation

Overview

The base of the Ocotillo Formation is a angular unconformity in the western San Felipe Hills and is a disconformity in the east, where the Ocotillo Formation interfingers

with the Brawley Formation to the east and north (figs. 2-5, 2-6, 2-7). To the south throughout the Ocotillo Badlands and in the measured section, the Ocotillo Formation overlies the Borrego Formation along a sharp but conformable contact that has no apparent soil development or erosional relief (figs. 2-3, 2-6). Clasts of the underlying Borrego Formation are not present in the basal beds of the Ocotillo Formation. The contact is diffcult to place in some areas.

Outcrops of the angular unconformity beneath the Ocotillo Formation occur principally in the western San Felipe Hills as a relatively narrow east-west belt on the southern limb of the San Felipe anticline. The area underlain by angular unconformity extends east to Tarantula Wash and probably continues to the west beyond the study area. To the east of Tarantula Wash the Ocotillo Formation overlies the Borrego Formation in disconformity (fig. 2-3). In the Tarantula Wash area the base of the Ocotillo Formation changes laterally from an angular unconformity to a disconformity across a 200-500 m distance (fig. 2-3). This defines the eastern extent of angular unconformity (fig. 2-3). On the north limb of the San Felipe anticline there is one outcrop of the Ocotillo Formation lying in angular unconformity on the Diablo Formation (fig. 2-3). 1Onelies in disconformity on the transitional Diablo to Borrego unit (fig. 2-3). Near Seventeen Palms, ~5 km to the north (Fig. 2-9), there are more extensive exposures of the Ocotillo Formation that appear to be conformable on the Borrego Formation (Dibblee 1984; Pettinga 1991; Bartholomew 1968). Post-Ocotillo folding and faulting has obscured the contact relations of several outcrops of the Ocotillo Formation between Seventeen Palms and the northwest edge of the study area and we have not studied them.

A well exposed section of the Ocotillo Formation was measured (by Rebecca Dorsey) in the northern Ocotillo badlands. The Ocotillo Formation is 223.5 m thick in the section there, but map data suggest a total thickness of ~450 m in the northern Ocotillo badlands (fig. 2-6). The Oil Well Wash section contains just 16.5 m of distal Ocotillo Formation (fig. 2-5).

Facies and sedimentary patterns

The Ocotillo Formation is characterized by conglomerate, pebbly to gritty sandstone, sandstone, and lesser fine grain siltstone and mudstone (fig. 2-6). Within the San Felipe Hills, moderately lithified pebbly arkosic sandstone is the dominant lithology of the Ocotillo Formation, but medium-grained sandstone to mudstone are also important components of the lower Ocotillo Formation. Sedimentary structures include shallow channel fills with imbricated clasts and horizontal to low-angle stratification. The Ocotillo Formation includes interbedded C-suite and L-suite sandstones, with L-suite dominating over C-suite. Recycled clasts of the Diablo Formation with lesser amounts of the Imperial Group, are common.

In the Ocotillo badlands, the base of the Ocotillo Formation was placed at the base of the lowest conglomerate bed greater than 2 m thick (fig. 2-6). Directly above its basal contact with the Borrego Formation, the Ocotillo Formation consists of massive to horizontally stratified pebble to cobble conglomerate. Above the contact distinct beds of sandy matrix-supported pebble to cobble conglomerates showing low-angle cross stratification and occasional shallow channel scours generally less than 1m thick dominate the measured section (fig. 2-6).

A interval of red claystone and mudstone with lesser siltstone and sandstone begins abruptly at 48.5 m in the measured section continuing up section to 77.5 m (fig. 2-6). Bioturbation and gastropods were noted in the lower portion of this section. Sand-filled desiccation cracks up to 1 m deep are present immediately below a planar bedded sandstone interval near 65 m (fig. 2-6).

Conglomerate and pebbly sandstone overlie a sharp contact above a finer-grained section between 58.5 and 77.5 m (fig. 2-6). These beds are horizontally stratified and similar to the section above the base of the Ocotillo Formation (fig. 2-6). Above this, from 90 to 109 m the section contains fine-grained cross-bedded sandstone with Colorado River provenance (fig. 2-6). At 101.5 m in this interval these sandstones are interbedded with lesser red mudstones. The relative abundance and thickness of mudstone beds increases up section in this otherwise sandy section (fig. 2-6).

Above 109 m pebble to occasionally cobble conglomerate dominate, with intervals of coarse sandstone and pebbly sandstones (fig. 2-6). The pebbly sandstone is commonly crudely bedded showing weakly developed horizontal stratification with stringers of pebbles set in sand-dominated beds. Minor claystone and mudstone beds up 2 m thick are interbedded with these deposits (fig. 2-6). Fine-grained deposits include grey to white bedded and rippled siltstone and peach to red mudstone and claystone which is several meters thick. Several mudstone and claystone beds display well developed polygonal desiccation cracks (figs. 2-6, 2-8).

Provenance

The Ocotillo Formation in the Ocotillo Badlands is dominated by granular sub-rounded very coarse to coarse white plagioclase, quartz and biotite grains, which are

likely derived from nearby uplifts of the eastern Peninsular Ranges (fig. 2-6). Sands with similar compositions have been linked to the eastern Peninsular Ranges to the west by previous workers (Guthrie 1991; Winker and Kidwell 1996). Up to 90 % of sandstone in the measured section has a local source (fig. 2-6). Small intervals (8%) of the section contained Colorado River derived and mixed local and Colorado River-derived sediments (up to 2%). Colorado River-derived sands are restricted to the lacustrine and fluvial-deltaic intervals between 50 and 100 m (fig. 2-6).

Composition of pebble to cobble sized clasts are fairly uniform. Clasts include tonalite, Diablo Formation, metasedimentary schists and marbles, mylonites, and gneiss (fig. 2-6). Tonalite clasts dominate the section. Clasts of the Diablo formation are overall less common, though locally abundant, and are present throughout the section. Mylonite, metasedimentary, and gneiss clasts were noted both near the base and top of the section. Just above the base of the Ocotillo Formation, clasts include tonalite from the eastern Peninsular Ranges and up to 30 % recycled clasts of the Diablo Formation sandstone (figs. 2-6, 2-9). Ocotillo Formation to north and northeast in the San Felipe Hills has a similar overall clast composition.

Paleoflow

Clast imbrications were measured at 6 intervals in the measured section. Tilt-corrected mean paleoflow was easterly based on 34 pebble imbrications (fig. 2-10).

Environment of deposition

Based on grain size, sedimentary structures, and facies we infer that the upper 130 m of Ocotillo Formation was formed in a proximal to distal alluvial fan and bajada

setting. The lower 110 m of Ocotillo Formation consists of alternating lacustrine, fluvial, deltaic, and alluvial fan deposits (fig. 2-6). Alluvial fan environments are characterized by the horizontally stratified pebbly sandstones and pebble to cobble conglomerates, with low-angle cross stratification and shallow channel fills (figs. 2-6, 2-9). Evidence for lacustrine deposition is limited to a 77.5 m thick transitional zone in the lower Ocotillo Formation, where Borrego and Ocotillo lithofacies alternate. This interval contains lacustrine fauna including gastropods and fine grain interlaminated mudstone and claystone. Fluvial to deltaic deposition is indicated by cross bedding and fining-up trends between 86 and 109 m (fig. 2-6). Facies association and sedimentary structures between exposures of the Ocotillo Formation in the San Felipe Hills, and the Ocotillo and Borrego badlands are similar and likely represent deposition in alluvial fans that prograded into and interfingered with finer basinal deposits which were either fluvial or lacustrine (this study; Lutz and Dorsey 2003).

San Felipe anticline

Angular relations beneath the angular unconformity underlying the Ocotillo Formation in the western San Felipe Hills define a large east-west trending anticline in the underlying Borrego and Diablo formations and Imperial Group which probably formed just prior to deposition of the Ocotillo Formation across it (fig. 2-11). Based on the age of the rocks beneath the angular unconformity, the angularity of the contact, and the younging direction beneath the unconformity the anticline is roughly 10 km north to south and 14 km from the western edge of the study area to the eastern tip. The anticline likely extends to the west to Borrego Mountain for a total east-west length of 24 km. The anticline coincides with the large east-west trending San Felipe anticline which

deforms the Ocotillo and Brawley formations as well as the underlying Imperial Group, Diablo and Borrego formations (fig. 2-12).

In cross-section the reconstructed anticline has a longer (7 km) north limb whereas the south limb is only 3 km in length (fig. 2-11). The Diablo Formations dips 28° to the north beneath flat lying Ocotillo Formation on the north limb of the anticline (fig. 2-11). Pre-Ocotillo beds on the southern limb of the anticline dip from 16 to 24° (fig. 2-11). Structural offset between the southern San Felipe Hills and the Ocotillo Badlands imply north-side-up thrust fault or similar structure separating these two areas (fig. 2-11). The exact dimensions of the southern limb are poorly constrained because the conformable contact between the Ocotillo and Borrego formations in the Ocotillo Badlands is located southwest across a major strand of the Coyote Creek fault with up to 2 kilometers of slip (fig. 2-11). The interlimb angle of the San Felipe anticline beneath the reconstructed angular unconfomity was at most 128° just prior to deposition of the Ocotillo Formation. Using the modern strain rate of $32.0 \pm 2.4\text{^}10^{-8}$ per year from GPS data sets (Anderson et al., 2003) over a similar spatial area and orientation to that of the reconstructed anticline the anticline could have formed in 285,500 ± 19,700 years.

A 2.7 mGal gravity high coincides very well with the San Felipe anticline mapped at the surface and defines the subsurface extent of the basement-cored part of the San Felipe anticline. This correspondence shows that the basement is coupled to the overlying sedimentary section at the scale of the San Felipe anticline. The anticline appears to end or be truncated either at the Powerline fault or ~ 2-3 km to the east in the central San Felipe Hills (fig. 2-13). To the west the gravity signal of the San Felipe anticline extends along trend 6 km to the west of Borrego Mountain on the southwest side

of the Coyote Creek fault. The extent of the gravity high corresponds well with the position of both the modern and ancient, pre-Ocotillo and Brawley formations, San Felipe anticline (fig. 2-13).

Brawley Formation

Overview

The base of the Brawley Formation in the eastern San Felipe Hills is defined here by the first trough cross-bedded locally derived sandstone in erosional contact with underlying red claystone, mudstone, and lesser sandstone of the Borrego Formation (fig. 2-14). The basal sandstone of the Brawley Formation is commonly overlain by a red mudstone or claystone up to 20 m thick which may also have within it a white silty marl interbed up to 1 m thick. The location of the contact was later confirmed using Landsat data acquired after the contact had been traced in the field.

The grain size of the lowermost Ocotillo and Brawley formations decreases to the north and east above the disconformity in the eastern San Felipe Hills. Recycled clasts of the underlying Borrego Formation and adjacent Diablo Formation are common in the lowermost Ocotillo and Brawley formations in the eastern San Felipe Hills and are typically 1 cm in diameter, ranging up to 2-3 cm in diameter. Throughout most of the San Felipe Hills the contact has been extensively folded and faulted by deformation that postdates deposition of the Brawley Formation (fig. 2-3).

Four hundred and eighty meters of the Brawley Formation, and 128.5 m of the Borrego Formation were measured and described in Oil Well Wash in the south-east portion of the study area (figs. 2-3, 2-5, 2-15). The section was described and measured in three distinct intervals that are separated by younger folds and faults. Section legs 1

and 2 were directly correlated by laterally following bedding on foot and on aerial photos around a east-northeast plunging anticline (figs. 2-5, 2-15). Section legs 2 and 3 were correlated across the Extra fault zone using a prominent series of marls and an overlying channel complex at 480 m as a marker (figs. 2-5, 2-15). This marker couplet could also correlate with a marl and sandstone interval at 415 m in leg 2, but this correlation is not preferred because of a poor stratigraphic match above the marker couplet. If this alternate correlation is correct, the base of the Bruhnes normal would lie at 435 m in the measured section instead of at 480 m.

Facies and sedimentary patterns

The measured section in Oil Well Wash is 625 m thick. The lower 128.5 m consists of upper Borrego Formation and the upper 496.5 m contain Ocotillo and Brawley formations (fig. 2-5; plate 2). A thin tongue of the Ocotillo Formation, 16.5 m thick, separates the Brawley Formation from the Borrego Formation in this area (figs. 2-3, 2-5, 2-15; plate 2). Strata of the Brawley Formation are conformable and lack observable growth strata. The contact between the Ocotillo and Brawley formations is conformable.

Basal beds of the Ocotillo Formation overlie a disconformable contact with Borrego Formation in this section and locally contain pebble to occasional tonalite cobbles. The Ocotillo Formation fines up from the basal unconformity to 145 m in the section and consists of horizontally stratified, locally derived sandstone. Massive mudstones of the lowermost Brawley Formation conformably overlie this tongue of the Ocotillo Formation.

Throughout the Brawley Formation buff to tan-orange weathering fine- to medium-grained sandstone is the dominant lithology. Sandstone is characterized by buff

color, general lack of consolidation, and a variety of well developed sedimentary structures that include tabular and trough cross bedding, climbing and tabular ripples, large scale high-angle cross stratification, channel fills, and convolute laminations (figs. 2-16, 2-17, 2-18, 2-19; plate 2). Lesser amounts of red, finely laminated to massive, claystone and mudstone up to 3-4 m thick with well developed downward tapering sand-filled cracks up to 1.5 m deep are also characteristic of the Brawley Formation (figs. 2-5, 2-20, 2-21; plate 2).

Channel-fill structures occur in the sandstone-dominated portions of the Brawley Formation, with good exposures between 425 m and 450 m in the measured section (fig. 2-5). Channel fills in the Brawley Formation generally fine upward to siltstone and mudstone and typically occur in beds 2–6 m wide and 1-4 m high (figs. 2-5, 2-16). Rip-up mud pebbles and rare cobbles and armored mudballs are common in the base of channel fills (fig. 2-22). Several channel complexes up to 20 m thick exist as vertically stacked channel-fill deposits. Climbing ripples and trough cross bedding are well developed and common within the channel fills (fig. 2-17). Soft sediment deformation consisting of folded laminations are present in some channel fills (fig. 2-18). Similar lithologies dominate the section from 156 m to 450 m.

From 260 m to 400 m fine- to very fine-grained sandstone which commonly displays large scale (3-4 m) high angle cross stratification is present in the measured section (figs. 2-19). Stacked sets of steep and tabular foresets up to 10-15 m thick are characteristic of this section. Sandstone in these deposits is well sorted and contains thin segregated interbeds of biotite. Thin, 1 m or less, lenticular and discontinuous interbeds

of massive to laminated mudstone and claystone are also present in this part of the section (fig. 2-5; plate 2).

Red to red-brown mudstone and claystone are interbedded with sandstone in the measured section. Thickness of these beds ranges from less than 1 m up to 3-4 m (fig. 2-5; plate 2). These deposits are massive to laminated and show rare burrow mottling. Mudstone and claystone is dominant in the section between 145 m and 156 m and above 480 m where they are interbedded with sandstone, marl and siltstone (fig. 2-5; plate 2).

Marl consists of grey to whitish silty to muddy carbonate-rich layers that commonly have abundant microfossils visible in hand sample including forams, ostracods, and gastropods (fig. 2-18). Typical individual marl beds are 20-30 cm thick. Intervals of stacked marl beds reach 2 m in thickness and make useful stratigraphic markers. Locally-dervied sandstone is commonly associated with marly intervals. Sedimentary structures in marl include soft sediment deformation, bioturbation, and occasional cross stratification. Marl usually is associated with claystone and mudstone but several are abruptly overlain by channel sandstones.

Mudstone and claystone of the Brawley Formation commonly contain sand-filled desiccation cracks. The cracks are typically well developed and downward tapering, and filled from above with locally derived sands (figs. 2-20, 2-21). Examination of some sand-filled cracks reveals faint sub-horizontal laminations. The cracks are up 1.5 m deep and up to 40 cm wide. When seen in plan view the desiccation cracks are commonly polygonal and up to 1-2 m across, and cross-sectional view generally show regularly spaced (up to 1-2m) vertically oriented sand-filled cracks which occur throughout a given mudstone or claystone bed. Soil features in the claystone and mudstone of the Brawley

Formation are weakly developed and represented by small calcic rhizo-concretions and irregular rounded calcic nodules up to 3 cm in length (fig. 2-23).

Microfossil results

Portions of the the Brawley Borrego formations in the Oil Well Wash measured section and elsewhere in the eastern San Felipe Hills were sampled and analyzed for microfossils (McDougall unpublished data 2004). Fossil assemblages within the Brawley Formation range from fresh water to brackish to saline water forms and included; forams, micromollusks, ostracods, echinoids, and chara (fig. 2-5; table 2-1; plate 2). Plant fragments were also noted in several samples. The foram species is a saline to brackish water type (McDougall unpublished data 2004). All other microfossils are fresh water types. The Borrego Formation has a slightly different fossil assemblage which was characterized by planktonic forams, micromollusks, ostracods, and diatoms (table 2-1).

Provenance

Sandstone of the Brawley Formation in the Oil Well Wash section contains up to ~57 % locally derived sandstones (L-suite) based on the presence of plagioclase, quartz and biotite grains derived from the Eastern Peninsular Ranges to the west (fig. 2-5, 2-22). Lesser (up to 36 %) Colorado River derived sandstones (C-suite) and minor (up to 7 %) mixed local and Colorado River derived sandstones characterize the Brawley Formation in Oil Well Wash (fig. 2-5). L-suite and C-suite sandstone beds alternate on a 5 m scale with relatively little mixing of the two petrofacies.

Paleoflow

The Brawley Formation contains many well developed paleocurrent indicators such as channel scours, foresets, ripples, and trough and planar cross beds. For this study paleoflow was measured primarily from channel axes, cross bedding and small scale climbing ripples at various locations in the San Felipe Hills (fig. 2-24). The tilt-corrected mean of the 51 measurements was 50° or north-easterly (fig. 2-24).

Environment of deposition

Two thirds of the Brawley Formation in Oil Well Wash consists of fluvial and fluvial deltaic facies, as indicated by conspicuous cross-bedded sandstone channel fills that fine up into mudstone with desiccation cracks and rare weak paleosols. Fluvial and fluvial-deltaic facies dominate the section from 156 m to 450 m. Within this section were brief periods of lacustrine deposition and longer intervals of eolian deposition.

Eolian sandstone units are interbedded with the fluvial and fluvial deltaic deposits between 260 m to 400 m in the section (fig. 2-5; plate 2). These deposits record sand dunes up to 4 m high and overall eastward dune migration. Similar facies patterns have been interpreted in the rock record as being deposited on the arid margin of ephemeral lacustrine systems (Rogers and Astin, 1991). Other evidence for arid conditions during deposition of the Brawley Formation include deep desiccation cracks and development of weak calcic paleosols. Both features are indicative of soil formation under arid conditions (Wright 1986). The intervals which show the most evidence for extended subareal exposure and soil formation correspond well with intervals of eolian deposition (fig. 2-5; plate 2).

Lacustrine deposits comprise ~ 20 % of the Brawley Formation in Oil Well Wash (fig. 2-5). Prominent lacustrine intervals are present between 145 m and 157 m and above 475 m where they are interbedded with fluvial-deltaic deposits. Lesser intervals of lacustrine deposition exist between 157 m and 475 m (fig. 2-5; plate 2). The most diagnostic lithofacies in the lacustrine association are fossiliferous marls and massive to laminated claystones and mudstones. Lacustrine conditions are supported by the lacustrine fauna identified in these marls and elsewhere in the Brawley Formation. Lacustrine conditions and subareal arid conditions alternated, producing the common well-developed sand-filled desiccation cracks (figs. 2-5, 2-25; plate 2). The largest desiccation cracks occur in the lacustrine intervals.

Water chemistry of the Brawley Formation lacustrine system varied from fresh to brackish. Brackish water chemistry is required at times in the Brawley lake to support the shallow marine to lagoonal marine forams preserved there. This probably developed during the periodic drying out of the lake basin, consistent with other studies of the Brawley lake history (Herzig et al. 1988).

Paleomagnetic Results

Fourteen of the paleomagnetic sampling sites along Oil Well Wash in the upper Borrego and Brawley formations preserve a stable primary magnetization. The uppermost Borrego Formation is reversely magnetized, and the lower 145.5 m of the Brawley Formation has a normal polarity (fig. 2-5; plate 2). About 206 m in the middle part of the Brawley Formation are reversely magnetized and the upper 145 m return to a normal polarity that we infer to be the Bruhnes subchron from regional relations(fig. 2-5; plate 2). This correlation with the magnetic time scale is further supported by work to the

north on the Ocotillo Formation which used the presence of the Bishop ash (0.76 Ma) and unique fossil assemblages to correlate this portion of the time scale to these rocks. This correlation places the base of the Jaramillo event at the disconformity between the Ocotillo and Brawley formations and the Borrego Formation. The coincidence of the reversal with the disconformity allows us to date the contact very precisely at 1.07 Ma.

We recognize two distinct grades of paleomagnetic data quality in our specimens. Class I data have well-defined second-removed vector components with a maximum angular deviation (MAD) of less than 25° (fig. 2-25). Class II data have poorly defined second-removed components, with MAD >25°, and commonly do not trend towards the origin of the orthogonal vector plots (fig. 2-26). Many of the specimens with Class II data have well-defined great circles that allowed for qualitative evaluation of the polarity of the second-removed magnetization components (figs. 2-26, 2-27). One site (03Qb19) has well-defined (Class I) magnetization vectors, which point either shallowly up, or shallowly down (fig. 2-28). We interpret these directions to represent a recording of a transitional field, most likely associated with an excursion or short-lived polarity event, and so will not include this mean direction in our analysis.

There are six sites with enough Class I data to calculate site mean directions (fig. 2-29). With one exception (Site 03Qb18), all of these sites have well-defined mean directions, with k> 15. The α_{95} values are high, due to the low number of Class I samples in these sites. The site mean directions are moderately clustered in in-situ coordinates, but become markedly better clustered after tilt-correction (fig 2-29). The in-situ mean direction (after inverting the polarity of Site 03Qb32) is D = 6.8, I = 50.3, k = 27.8, α_{95} =

12.9, N = 6. After correcting for bedding tilt, the mean of these directions is D = 8.5, I = 61.1, k = 51.0, α_{95} = 9.5, N = 6.

Age Constraints and Sedimentation Rates of the Brawley Formation

The results of the paleomagnetic sampling and correlation indicate that the base of the Ocotillo and Brawley formations at 128.5 m in the measured section coincides with the Matuyama-Jaramillo reversal (1.070 Ma) and that the base of the Bruhnes normal (0.780 Ma) lies at 480 m (fig. 2-5; plate 2). The age of the rocks above and below these two tie points can be estimated from sediment accumulation rates.

Magnetic reversals were placed at the midpoints between sample points of opposite polarity, except for the two reversals described above (plate 2). The top of the Jaramillo normal subcron (0.990 Ma) was detected at 274 m $\pm$ 36 m (fig. 2-5; plate 2). The base of the Jaramillo subchron would lie at 135 m $\pm$ 30 m if it were halfway between the sample points. Instead the base of the Jaramillo was placed 6.5 m lower in the section at the disconformity between the Ocotillo and Borrego formations at 128.5 m because this reversal coincides with the basal Ocotillo Formation in the other two localities that have been analyzed in the Borrego Badlands and Ocotillo Badlands (Brown et al. 1991; Lutz and Dorsey 2003) (fig. 2-5; plate 2). The coincidence of this reversal and the major lithologic change at the contact is best explained if the Ocotillo Formation represents an abrupt basin-wide change. Altogether the magnetostratigraphy shows that the onset of deposition of the Ocotillo and Brawley formations in the southeastern San Felipe Hills was at 1.070 Ma.

The base of the Bruhnes normal was interpreted to lie at 480 m between 03Qb24 and 03Qb21based on a stratigraphic and paleomagnetic correlation of section leg 3 to

section leg 2 (figs. 2-5, 2-15; plate 2). If section leg 3 is not correlated into leg 2, the reversal would be interpreted to lie at 448 ± 34 m, halfway between 03Qb25 and 03Qb24. We calculate sedimentation rates using the preferred and alternate positions of the reversals.

Applying the age constraints of 1.070 Ma and 0.780 Ma to the 351.5 m of the section between 128.5 m and 480 m yields a time averaged sedimentation rate of 1.2 ± 0.1 mm/yr. Alternate placement of the reversals at 135 ± 30 m and 448 ± 34 m yields a sedimentation rate of 1.1 ± 0.2 mm/yr. This is the overall rate for the constrained interval. Two other rates within this interval can be calculated using the top of the Jaramillo normal subchron at 0.990 Ma. Using the preferred correlation of the base of the Jaramillo at 128.5 m and the top of the Jaramillo 274 ± 36 m the sedimentation rate over this chron is 1.8 ± 0.4 mm/yr (fig. 2-5; plate 2). For the alternate correlation at 135 ± 30 m and 274 ± 36 m the rate is 1.7 ± 0.8 mm/yr.

The reversed subchron between the Jaramillo and the Bruhnes normals yields a sedimentation rate of 1.0 ± 0.2 mm/yr using the preferred correlations at 274 ± 36 m and 480 m (fig. 2-5; plate 2). Using the alternate correlation at 274 ± 36 m and 448 ± 34 m a rate of 0.8 ± 0.3 mm/yr is calculated.

Although these rates are computed from only a portion of the lower to middle Brawley Formation it likely can be applied to the entire measured section because of the similarities in depositional environments. By doing this a rough age can be calculated for the top of the Brawley Formation at 625 m (fig. 2-5; plate 2). Using the preferred correlation of the base of Bruhnes normal at 480 m and the two preferred rates previously

calculated of 1.2 $\pm$ 0.1 mm/yr and 1.0 $\pm$ 0.2 mm/yr, the age of the top of the Brawley Formation is estimated to be 0.66 $\pm$ 0.01 Ma and 0.64 $\pm$ 0.03 Ma (fig. 2-5; plate 2).

The total thickness of the Brawley and Ocotillo formations may be greater than the 480 m exposed in Oil Well Wash. Up to 550 m of the Brawley Formation is inferred from map relations located north and east of the measured section. By applying the preferred sedimentation rates of 1.2 $\pm$ 0.1 mm/yr and 1.0 $\pm$ 0.2 mm/yr to this additional thickness, the end of Brawley sedimentation within the San Felipe Hills ranges from 0.61 $\pm$ 0.02 Ma to 0.52 $\pm$ 0.03 Ma.

Discussion

The Ocotillo Formation in the Ocotillo Badlands and the San Felipe Hills is dominated by locally derived pebble to cobble conglomerates and pebbly sandstones with lesser sandstones and minor mudstones and claystones. Clast composition of the coarse beds is dominated by tonalite from the eastern Peninsular Ranges with lesser but common recycled clasts of Diablo Formation sandstones. Both tonalite and Diablo Formation clasts may have been sourced from uplifts to west and south in the Fish Creek and Vallecito mountains. In the Ocotillo Badlands paleoflow is easterly supporting western sources for the tonalite and recycled Diablo Formation clasts. Some sediment may have had a source on the west most uplifted end of the San Felipe anticline near Borrego Mountain.

Alluvial fan and bajada facies dominate the Ocotillo Formation and differ from the underlying lacustrine Borrego Formation. This change in depositional environment is significant and could have resulted from either tectonic or climatic variations. The

presence of recycled clasts of the older Diablo Formation and the underlying angular unconformity beneath the Ocotillo Formation in the western San Felipe Hills support tectonic influences as the driver of change in depositional environment at the onset of deposition of the Ocotillo Formation.

Angularity and location of the angular unconformity below the Ocotillo Formation and the age of the subcrop relation show that 1) the angular unconformity overlies the basement-cored part of the San Felipe anticline and 2) it defines the extent of the anticline just prior to 1.07 Ma. The San Felipe anticline at 1.07 Ma was a broad east trending anticline which stretched from at least Borrego Mountain in the west to central San Felipe Hills (~24 km) and was 10 km north to south. The orientation and scale of this fold are consistent with wrench deformation produced by northwest-striking dextral strike-slip faults with a maximum horizontal stress oriented north-south. The fold has continued to grow in the current dextral strain field since the end of deposition of the Brawley Formation.

The base of the Brawley Formation is a disconformity in the San Felipe Hills, which commonly displays 1-2 m of erosional relief. This suggests a regional drop in base level just prior to deposition of the fluvial to fluvial-deltaic Brawley Formation over the persistently lacustrine Borrego Formation. We infer a structural cause for this major change. The mapped extent, contact relations, lithology, and depositional environment of the Brawley Formation documented in this study differ from those of previous workers (Dibblee 1954, 1984; Wagoner 1977; Dronyk 1977; Feragen 1986). Previous workers in the eastern San Felipe Hills placed this contact 1-3 km farther to the east in the northeastern San Felipe Hills (Dibblee 1954, 1984; Dronyk 1977).

The fluvial, fluvial-deltaic, eolian, and lacustrine conditions which existed during deposition of the Brawley Formation represent an arid fluvial-lacustrine system. Arid lacustrine settings are typically associated with thick evaporite deposits (Boggs 2001). Lacustrine intervals in the Brawley Formation contain common well-developed sand-filled desiccation cracks and thin silty marlstone interbedded with eolian and fluvial deposits, but only one documented evaporite bed. Similar-aged evaporite deposits have been described in time correlative deposits farther to the east in drill cores and at Durmid Hills east of the Salton Sea and shows that the basin axis was to the east during the deposition of the Brawley Formation (Herzig et al. 1988). The presence of significant desiccation cracks maybe the result of longer periods of flooding produced by the episodic infilling of the Salton Trough by a major river system.

The facies and sedimentary structures in the Brawley Formation represent important paleoclimate indicators for the period of deposition. The presence of calcic paleosols, common well-developed desiccation cracks, and significant sections of eolian sandstone deposits in the middle of the Oil Well Wash section record semi-arid to arid conditions during deposition of the Brawley Formation (Plummer and Gostin 1981; Weinberger 2001). Climate during Brawley time may have been similar to the modern arid conditions of the Salton Trough and suggest desert conditions in this area at least since approximately 1 Ma.

Provenance during deposition of the Brawley Formation differs significantly from that in the underlying Borrego and Diablo formations (fig. 2-30). Previous workers have shown that sandstone provenance of the Borrego and Diablo formations in the San Felipe Hills is dominated by Colorado River sourced sand and mud (Guthrie 1991; Winker

1987; Winker and Kidwell 1996). However C-Suite sandstone in the Brawley Formation probably was recycled from the older Borrego and Diablo formations. Recycled clasts of Diablo Formation sandstone just above the base of the Brawley Formation indicate sediment recycling began synchronously with deposition of the Brawley Formation. Because paleoflow in the Brawley Formation was toward the northeast and the mouth of the Colorado River sediment was located far to the southeast during Brawley deposition it is highly unlikely that sediment was transported directly into the study area from the Colorado River. Much of the sand-size sediment in the Brawley Formation may be recycled from nearby uplifts, including the now denuded and uplifted Fish Creek and Vallecito Mountains. Overall northeastward fining of the Ocotillo and Brawley formations and overall east-northeast paleoflow supports the interpretation that recycled sediment was transported from uplifts to west and southwest of the San Felipe Hills (figs. 2-31, 2-32).

A paleogeographic reconstruction of the Ocotillo and Brawley formations shows a west to east lateral change in depositional environments (fig. 2-31). Alluvial fan and bajada deposits in the southwestern San Felipe Hills and Ocotillo badlands change eastward into fluvial-deltaic and lacustrine deposits (figs. 2-31, 2-32). Grain size decreases to the east towards the lacustrine depocenter which is centered near the modern Salton Sea (figs. 2-31, 2-32). The San Felipe anticline is a large east-west trending structure which may have partially partitioned the San Felipe-Borrego Basin. The position of the Brawley delta was likely located just south of the San Felipe anticline and the stream feeding this delta may have flowed along the axis of the syncline just to the south (fig. 2-31). West and south of the Ocotillo Badlands and the San Felipe Hills

dextral and or normal faulting along the front of the current Vallecito and Fish Creek mountains may have produced uplift and denudation of these areas, and thereby supplied much of the sediment for the Ocotillo and Brawley formations. Generally east-northeast paleoflow is documented away from the mountain blocks (figs. 2-31, 2-33).

Facies contrast across the disconformity further support changes in base level between Borrego and Brawley time. During deposition of the Borrego Formation in the San Felipe Hills, claystone and mudstone accumulated in a relatively deep-water lacustrine setting. Near-shore lithofacies are uncommon. This contrasts with fluvial to fluvial-deltaic, eolian, and intermittent near shore lacustrine facies of the Brawley Formation in the eastern San Felipe Hills. Prior to 1.07 Ma the Borrego Formation had a major depocenter in the San Felipe Hills and Borrego Badlands. The basin center shifted abruptly eastward at about 1.07 Ma at the end of Borrego deposition and before deposition of the Ocotillo and Brawley formations.

The drop in base level and the shift to fluvial, fluvial-deltaic, and alluvial fan and bajada facies at the onset of deposition of the Ocotillo and Brawley formations could have been caused by a shift to a drier climate. However, the correlation of the facies change with a disconformity and angular unconformity that coincides with the San Felipe anticline, and the presence of significant amounts of recycled sediment within the Ocotillo and Brawley formations strongly support tectonic deformation and its resultant base level change as the primary driver of these changes. Climate records for the late Pliocene to Pleistocene in the southwestern United States show dramatic drying during the early Pleistocene at approximately 1.5 Ma (Smith 1994). This does not correlate with the 1.070 Ma disconformity, angular unconformity, and conformable contact and

suggests that the upper Borrego Formation was possibly deposited during arid conditions. Thus the change in sedimentation is unlikely to have been the result of climate change.

The basic control on the position of fine and coarse-grained facies in a tectonically active basin is the balance between subsidence and sediment influx (Boggs 2001). A major progradation of coarse grained facies, such as that recorded by the Ocotillo and Brawley Formations, is likely the result of changes in both subsidence and sediment influx. Increased sediment influx may have been produced by new and or active tectonically driven interbasin and basin margin uplifts such as the San Felipe anticline and Fish Creek-Vallecito Mountains. The shift in basin architecture was therefore likely caused by change or reorganization of the basin controlling faults.

The locations and kinematics of the faults that controlled this tectonic transition is still being investigated (Steely, Janecke, and Langenheim, in progress). However we do conclude that the controlling structures were not part of the older West Salton detachment fault system. East-west trending San Felipe anticline is likely the result of transpressional deformation and is unexpected for the early phase of transtension on the West Salton detachment fault. The Coyote Creek strand of the San Jacinto fault zone offsets the San Felipe anticline and is therefore a younger structure. There is no evidence for slip on the currently active strands of the San Jacinto fault system during deposition of these early syn-transtension units, including the Imperial and Palm Spring groups, and Borregoormation in the San Felipe Hills. If slip occurred on the Coyote Creek and Clark strands of the San Jacinto fault zone during deposition of the Ocotillo and Brawley formations it is expected that unconformities and or growth strata would be observable on the closely spaced folds in the study area. None have been noted at map scale within the

study area in the Ocotillo, Brawley, and Borrego formations in the study area but broad tilting adjacent to faults is not truled out by our data set. Altogether these data show that the growth of the San Felipe anticline and the drop in regional base-level at the onset of deposition of the Ocotillo and Brawley formations may have been the result of strike-slip on now inactive strands of the San Jacinto and/or the San Felipe fault zones. The fault at the northeast edge of the Vallecito and Fish Creek mountains was apparently one of these ancient strands (fig. 2-30) but other structures may have been involved in this reorganization. At the end of Brawley Formation (0.61 $\pm$ 0.02 Ma to 0.52 $\pm$ 0.03 Ma) uplift halted deposition in the San Felipe Hills, closely spaced east-west, north-south, and south-east trending folds developed, the San Felipe anticline tightened and a network of interconnected strike-slip faults of the modern Clark strand of the San Jacinto fault zone propagated from the SE Santa Rosas (Lutz 2005) into the San Felipe Hills (fig. 2-3). This deformation continues today and is described in Chapter 3.

Conclusions

Basin analysis is a powerful tool for understanding the evolution of plate boundary fault systems. Evidence for the initiation or reorganization of the San Jacinto fault zone exists within the Pleistocene stratigraphic section of the San Felipe Hills. A regional disconformity and correlative angular unconformity and changes in depositional patterns at 1.07 Ma was coeval with strike-slip related deformation in the southwestern Salton Trough. Deposition of the Ocotillo and Brawley formations was probably produced by now inactive strike-slip faults in the area, possibly by slip on the original strands of the San Jacinto fault zone.

The angular unconformity beneath the Ocotillo Formation in the western San Felipe Hills defines a large east plunging basement-cored anticline which corresponds well with the modern San Felipe anticline. The interlimb angle of this fold was ~ 130 ° based on a reconstructed cross section of the structure just prior to deposition of the Ocotillo Formation. The orientation and scale of this fold are consistent with wrench deformation produced by northwest striking dextral strike-slip faults. The west Salton detachment fault must therefore have stopped slipping as a single transtensional structure by this time.

The angular unconformity correlates eastward with a regional disconformity beneath the Ocotillo and Brawley formations in the eastern San Felipe Hills magnetostratigraphically dated at 1.07 Ma. The San Felipe anticline formed shortly before 1.07 Ma and provides the first clear evidence that strike-slip deformation of the San Jacinto-Elsinore system had supplanted the older West Salton detachment fault.

The Ocotillo Formation just south of the San Felipe Hills in the Ocotillo Badlands is locally conformable on the underlying lacustrine Borrego Formation. This unit is dominated by pebble to cobble locally derived conglomerates, dominated by locally tonalite clasts and commonly containing recycled clasts of the underlying Diablo Formation. Paleoflow was easterly based on clast imbrications.

The Ocotillo Formation interfingers and fines to the east northeast into the Brawley Formation in the southeastern San Felipe Hills (figs. 2-3, 2-32; plate 1). These two formations represent proximal to distal parts of the same depositional basin, with deposition ranging from alluvial fan and bajada deposits of the Ocotillo Formation to the fluvial-deltaic to lacustrine deposits of the Brawley Formation.

Previous workers characterized the Brawley Formation as the lacustrine lateral equivalent of the Ocotillo Formation (Dibblee 1954, 1984; Dronyk 1977; Wagoner 1977). Instead the Brawley Formation in the eastern San Felipe Hills and measured in Oil Well Wash is dominated by locally derived and recycled Colorado River derived fluvial and fluvial-deltaic deposits with lesser eolian and lacustrine intervals. A regional disconformity separates the Brawley Formation from the underlying Borrego Formation throughout the eastern San Felipe Hills. The disconformity at the base of the Brawley Formation in the eastern San Felipe Hills has been magnetostratigraphically dated for the first time at 1.07 Ma. The Brawley Formation in the eastern San Felipe Hills is 500 to 550 m thick. Sedimentation rates (uncorrected for compaction) calculated for the Brawley Formation in Oil Well Wash were 1.2 ± 0.1 mm/yr and 1.0 ± 0.2 mm/yr. Brawley Formation sediments were supplied from nearby intrabasin and basin margin uplifts which shed mostly Diablo Formation and occasional Imperial Group deposits and intermixed these sediments with locally derived arkoses.

The abrupt alternation of lacustrine, fluvial-deltaic, and eolian intervals in the Brawley Formation was likely driven by the occasional flooding of the Salton Trough due to aggrading and channel switching of the Colorado River delta which sent water northward into the Salton Trough. Occasional brackish conditions and a connection with the Gulf of California to the south for the Brawley lake are suggested by the presence of marine forams intermixed with more typical lacustrine microfossils. Large desiccation cracks and weak calcic paleosols formed and 4 m high sand dunes were deposited during intervening dry periods.

Modern deposition patterns in the central Salton Trough show similar highly episodic patterns to the Brawley Formation however the depocenter is more tightly focused on the floor of the Salton Trough. There is significant north-south shortening in the San Felipe Hills, the style and magnitude which was not apparent during the deposition of the Ocotillo and Brawley formation. This suggests that the current configuration of the strands of the southern San Jacinto fault system is no older than the top of the Brawley Formation between 0.61 Ma $\pm$ 0.02 Ma to 0.52 Ma $\pm$ 0.03 Ma.

The sedimentary rocks exposed within the San Felipe Hills record the late Miocene to recent evolution of the North American-Pacific plate boundary in the western Salton Trough. Early oblique extension on the west Salton detachment fault was replaced by later transpression and strike-slip on strands of the San Jacinto fault zone. This transition is recorded by the deposition of the Ocotillo and Brawley formations over the Borrego and Diablo formations and the Imperial Group in the San Felipe Hills. Subsequent changes in the kinematics and geometry of the San Jacinto fault zone have deformed this succession within the San Felipe Hills.

References

Anderson, G. C.; Agnew, D. C.; and Johnson, H. O. 2003. Salton Trough Regional Deformation Estimated from Combined Trilateration and Survey-Mode GPS Data: Bulletin of the Seismological Society of America 93:2402-2414.

Atwater, T. 1970. Implications of plate tectonics for the Cenozoic tectonic evolution of western North America. Geological Society of America Bulletin 81:3513-3536.

Axen, G.J. 1998. Implications of late Cenozoic detachment faulting along the northeastern Peninsular Ranges, California, and Baja California. Geological Society of America, Abstracts with Programs 30:4.

Axen, G.J., and Fletcher, J. M. 1998. Late Miocene-Pleistocene extensional faulting,

northern Gulf of California, Mexico and Salton Trough, California. International Geology Review 40:217-244.

Axen, G.; Kairouz, M.; Steely, A.N.; Janecke, S.U.; and Dorsey, R.J. 2004. Structural expression of low-angle normal faults developed in wrench settings: an example from the West Salton detachment system. Geologica Society of America, Abstracts with Programs 36:37.

Bartholomew, M. J. 1968. Geology of the southern portion of the Fonts Point quadrangle and the southwestern portion of the Seventeen Palms quadrangle, San Diego County, California. [M.S. Thesis], University of Southern California, Los Angeles, California, 59 p.

Boggs, Sam, Jr. 2001. Principles of sedimentology and stratigraphy. Third edition. Princeton, Prentice Hall, 726 p.

Brown, N.N.; Fuller M.D.; and Sibson R.H. 1991. Paleomagnetism of the Ocotillo Badlands, southern California, and implications for slip transfer through an antidilational fault jog. Earth and Planetary Science Letters 102:277-288.

Cande, S.C., and Kent, D.V. 1995. Revised calibration of the geomagnetic polarity timescale for the Late Cretaceous and Cenozoic: Journal of Geophysical Reseach, B, Solid Earth and Planets 100:6093-6095.

Dibblee, T.W., Jr. 1954. Geology of the Imperial Valley region, California. *In* R.H. Jahns ed, Geology of southern California. California Division of Mines Bulletin 170: 21-28.

Dibblee, T.W. 1984a. Stratigraphy and tectonics of the San Felipe Hills, Borrego Badlands, Superstition Hills and vicinity. *In* , C.A. Rigsby ed, The Imperial Basin; tectonics, sedimentation and thermal aspects. Pacific Section SEPM Field Trip Guidebook 40:31-44.

Dibblee, T. W. 1984b. Stratigraphy and tectonics of the Vallecito-Fish Creek mountains, Vallecito badlands, Coyote mountains, Yuha desert, southwestern Imperial basin, *In* , C.A. Rigsby ed, The Imperial Basin; tectonics, sedimentation and thermal aspects. Pacific Section SEPM Field Trip Guidebook 40:59-79.

Dickinson, W. R. 1996. Kinematics of transrotational tectonism in the California Transverse Ranges and its contribution to cumulative slip along the San Andreas transform fault system, Geological Society of America, Special Paper 305, p. 1-46

Dorsey, R. J. 2002. Stratigraphic record of Pleistocene initiation and slip on the Coyote Creek fault, lower Coyote Creek, southern California, *In* A. Barth ed, Tectonic evolution southern and Baja California, Sonora and Environs. Boulder, Co. Geological Society of America. Special Paper 365, p. 251-269.

Dorsey, R. J.; Janecke, S. U.; Kirby, S.; Axen, G.; and Steely, A. N. 2004. Pliocene Lacustrine Transgression in the Western Salton Trough, Southern California: Implications for Regional Tectonics and Evolution of the Colorado River Delta. Geological Society of America Abstracts with Programs 36:317.

Dorsey, R.J., and Janecke, S.U. 2002. Late Miocene to Pleistocene West Salton detachment fault and basin evolution, Southern California; new insights. Geological Society of America, Abstracts with Programs 34:248.

Dorsey, R.J.; Seeber, L.; and Steckler, M.S. 1999. Stratigraphic constraints on a block rotation model for the Salton Trough; preliminary insights and hypotheses. Eos, Transactions, American Geophysical Union 80:715.

Dronyk, M. P. 1977. Stratigraphy, structure and a seismic refraction survey of a portion of the San Felipe Hills Imperial Valley, California. [M.S. Thesis], University of California, Riverside. Riverside, CA, 141 p.

Feragen, E.S. 1986. Geology of the southeastern San Felipe Hills, Imperial Valley, California. [M.S. Thesis], San Diego State University. San Diego CA, 144 p.

Fisher, R. A. 1953. Dispersion on a sphere. Proc. R. Soc. London, Ser. A 217:295–305.

Frost, E. G.; Fattahipour, M. J.; and Robinson, K. L. 1996. Emerging perspectives on the Salton Trough region with an emphasis on extensional faulting and its implications for later San Andreas deformation. *In* P.L Abbott and D.C. Seymour, eds, Sturzstroms and Detachment Faults, Anza-Borrego Desert State Park, California. South Coast Geological Society, Annual Field Trip Guide Book 24:81-122.

Guthrie, L. L. 1991. An internally standardized study of the Cenozoic sand and sandstone compositions, Salton basin, southern California: Implications for the rift basin evolution with emphasis on the Palm Spring and Imperial formations. [M.S. Thesis], San Diego State University. San Diego CA, 180p.

Heitman, E. A. 2002. Characteristics of the Structural Fabric Developed at the Termination of a Major Wrench Fault. [M.S. thesis], San Diego State University. San Diego CA, 77p.

Herzig, C. T.; Mehegan, J. M.; and Stelting, C. E. 1988. Lithostratigraphy of the State 2-14 Borehole; Salton Sea Scientific Drilling Project. Journal of Geophysical Research 93:12,969-12,980.

Hudnut, K. W.; Seeber, L.; Pacheco, J.; Armbruster, J. G.; Sykes, L. R.; Bond, G. C.; and Kominz, M. A. 1989. Cross faults and block rotation in Southern California; earthquake triggering and strain distribution. Yearbook Lamont–Doherty,

Geological Observatory of Columbia University, p. 44-49.

Janecke, S.U.; Kirby, S.M.; Langenheim, V.E.; Housen, B.; Dorsey, R.J.; Crippen, R.E.; and Blom, R.G. 2004. Kinematics and evolution of the San Jacinto fault zone in the Salton Trough: progress report from the San Felipe Hills Area. Geological Society of America, Abstracts with Programs 36:37.

Jennings, C. W. 1977. Geologic Map of California. State of California, Resources Agency, Dept. of Conservation, scale 1:750,000.

Johnson, N. M.; Officer, C. B.; Opdyke, N. D.; Woodard, G. D.; Zeitler, P. K.; and Lindsay, E. H. 1983. Rates of late Cenozoic tectonism in the Vallecito-Fish Creek basin, western Imperial Valley, California. Geology 11:664-667.

Kerr, D. R. 1984. Early Neogene continental sedimentation in the Vallecito and Fish Creek Mountains, western Salton Trough, California. Sedimentary Geology 38:217-246.

Kirby, S. M.; Janecke, S. U.; Dorsey, R. J.; Housen, B. A.; and McDougall, K. 2004. A 1.07 Ma change from persistent lakes to intermittent flooding and desiccation in the San Felipe Hills, Salton Trough, southern California. Geological Society of America Abstracts with Programs 37:318.

Kirschvink, J.L. 1980. The least squares line and plane and the analysis of paleomagnetic Data. Geophysical Journal of the Royal Astronomical Society 62:699-718.

Lilly, D. R. 2003. Structural geology of a transitory left step in San Felipe Hills fault. [M.S. Thesis], San Diego State University. San Diego CA, 91 p.

Lutz, A.T., and Dorsey, R.J. 2003. Stratigraphy of the Pleistocene Ocotillo Formation, Borrego Badlands, Southern California; basinal response to evolution of the San Jacinto fault zone. Geological Society of America, Abstracts with Programs 35:580.

Lutz, A.T. 2005. Tectonic controls on Pleistocene basin evolution in the central San Jacinto fault zone, southern California. [M.S. thesis], University of Oregon. Eugene Oregon, 136 p.

Morley, E.R. 1963. Geology of the Borrego Mountain quadrangle and the western portion of the Shell Reef quadrangle, San Diego County, California. [M.S. Thesis], University of Southern California. Los Angeles, California, 138 p.

Morton, D. M., and Matti, J.C. 1993. Extension and Contraction within an evolving divergent strike-slip fault complex: the San Andreas and San Jacinto fault Zones at their convergence in Southern California, *In* R. E. Powell, R. J. Weldon, and J.C. Matti eds, The San Andreas fault system: displacement, palinspastic

reconstruction, and geologic evolution. Geological Society of America, Memoir 178, p. 217-230.

Nicholson, C.; Seeber, L.; Williams, P.; and Sykes, L. R. 1986. Seismic evidence for conjugate slip and block rotation within the San Andreas fault system, southern California. Tectonics 5:629-648.

Oskin, M., and Stock, J. 2003. Marine incursion synchronous with plate-boundary localization in the Gulf of California. Geology 1:23-26.

Petersen, M. D.; Seeber, L.; Sykes, L. R.; Nabelek, J. L.; Armbruster, J. G.; Pacheco, J.; and Hudnut, K. W. 1991. Seismicity and fault interaction, southern San Jacinto fault zone and adjacent faults, Southern California: implications for seismic Hazard. Tectonics 10:1187-1203.

Pettinga, J.R. 1991. Structural styles and basin margin evolution adjacent to the San Jacinto fault zone, Southern California. Geological Society of America, Abstracts with Programs 23:257.

Platt, N. H., and Wright, V. P. 1991. Lacustrine carbonate: facies models, facies distributions and hydrocarbon aspects. *In* P. Anadon, L. Cabrera, and K. Kelts eds, Lacustrine facies analysis. Blackwell Scientific Publications, Oxford, p. 57-74.

Plummer, P. S., and Gosten, V. A. 1981. Shrinkage cracks: desiccation or synaresis? Journal of Sedimentary Petrology 51:1147-1156.

Reitz, D. T. 1977. Geology of the western and central San Felipe Hills, northwestern Imperial County, California. [M.S. Thesis], University of Southern California. Los Angeles, California, 155 p.

Remieka, P., and Beske-Diehl, S. 1996. Magnetostratigraphy of the western Borrego Badlands, Anza-Borrego Desert State Park, California: implications for stratigraphic age control. *In* P.L Abbott and D.C. Seymour eds, Sturzstroms and Detachment Faults, Anza-Borrego Desert State Park, California. South Coast Geological Society, Annual Field Trip Guide Book 24:209-220.

Rogers, D. A., and Astin T. R. 1991 Ephemeral lakes, mud pellet dunes and wind blown sand and silt: reinterpretations of Devonian lacustrine cycles in north Scotland. *In* P. Anadon, L. Cabrera, and K. Kelts eds, Lacustrine facies analysis. Blackwell Scientific Publications, Oxford.

Severson, L. C. 1987. Analysis of seismic reflection data from the Salton Trough. [M.S. Thesis] University of Southern California. Los Angeles, CA, 141 p.

Sheridan, J. M.; Weldon, R. J. II.; Thornton, C. A.; and Rymer, M. J. 1994. Stratigraphy

and deformational history of the Mecca Hills, Southern California. *In* S.F. McGill, and T.M. Ross eds, Geological investigations of an active margin. Geological Society of America , Cordilleran Section Annual Meeting 27:319-325.

Sharp, R.V. 1967. San Jacinto fault zone in the Peninsular Ranges of Southern California. Geological Society of America Bulletin 78:705-729.

Sharp, R.V. 1981. Variable rates of late Quaternary strike slip on the San Jacinto fault zone, Southern California. Journal of Geophysical Research 86:1754-1762.

Smith, G. A. 1994. Climatic influences on continental deposition during the late-stage filling of an extensional basin, southeastern Arizona. Geological Society of America Bulletin 106:1212-1228.

Steely, A.N.; Janecke, S.U.; Dorsey, R.J.; and Axen, G. 2004. Evidence for late Miocene-Quaternary low-angle oblique strike-slip faulting on the West Salton detachment fault, southern California. Geological Society of America, Abstracts with Programs 36:37.

Tauxe, L. 1998. Paleomagnetic principles and practice. Dordrect, Netherlands, Kluwer Academic Publishers, 299 p.

Wagoner, J. L. 1977. Stratigraphy and sedimentation of the Pleistocene Brawley and Borrego formations in the San Felipe Hills area, Imperial Valley, California, U.S.A. [M.S. Thesis], University of California, Riverside. Riverside, CA, 128 p.

Winker, C.D. 1987. Neogene stratigraphy of the Fish Creek - Vallecoti section, southernCalifornia: implications for early history of the northern Gulf of California andColoradodelta. [Ph.D. dissertation], University of Arizona. Tucson, 494 p.

Winker, C. D., and Kidwell, S. M. 1996. Stratigraphy of a marine rift basin: Neogene of the western Salton Trough, California. P.L. Abbot and J.D. Cooper, eds, Field Conference Guide, Pacific Section AAPG, GB 73, Pacific Section S.E.P.M., Book 80, p. 295-336.

Winker, C. D., and Kidwell, S. M. 2002. Stratigraphic evidence for ages of different extensional styles in the Salton Trough, Southern California: Geological Society of America, Abstracts with Programs 34:83-84.

Wells, D.L. 1987. Geology of the eastern San Felipe Hills, Imperial Valley, California: implications for wrench faulting in the southern San Jacinto fault zone. [M.S. thesis] San Diego State University. San Diego, California, 140 p.

Weinberger, R. 2001. Evolution of polygonal patterns in straitified mud during desiccation: the role of flaw distribution and layer boundaries. GSA Bulletin 113:20-31.

Wright, P. V. 1986. Paleosols their recognition and interpretation. Princeton, N. J., Princeton University Press, 307 p.

Table 2-1. Microfossil results. Microfossil numbers correspond with those on plate 2. Fossil indentification is from McDougall unpublished work (2004).

Microfossil sample #	Formation	Fossil ID
1	Brawley	Forams, ostracods, micromollusks
2	Borrego	Forams (planktonic), micromollusks, diat
3	Borrego	Barren
4	Brawley	Plant Fragments
5	Brawley	Barren
6	Brawley	Forams?, ostracods
7	Brawley	Forams?, ostracods, shell fragments
8	Brawley	Forams, ostracods, micromollusks
9	Brawley	Forams?, ostracods
10	Brawley	Barren
11	Brawley	Forams?, ostracods, chara, echinoids?
12	Brawley	Ostracods
13	Brawley	Barren
14	Brawley	Forams, ostracods, abundant chara, Tintin
15	Brawley	Forams?, ostracods, chara, plant fragmer
16	Brawley	Forams, ostracods
17	Brawley	Barren
18	Brawley	Forams, ostracods, chara, micromollusk
19	Brawley	Forams, ostracods, chara
20	Brawley	Barren
21	Borrego	Ostracods, diatoms?
22	Brawley	Diatoms?, shell fragments?

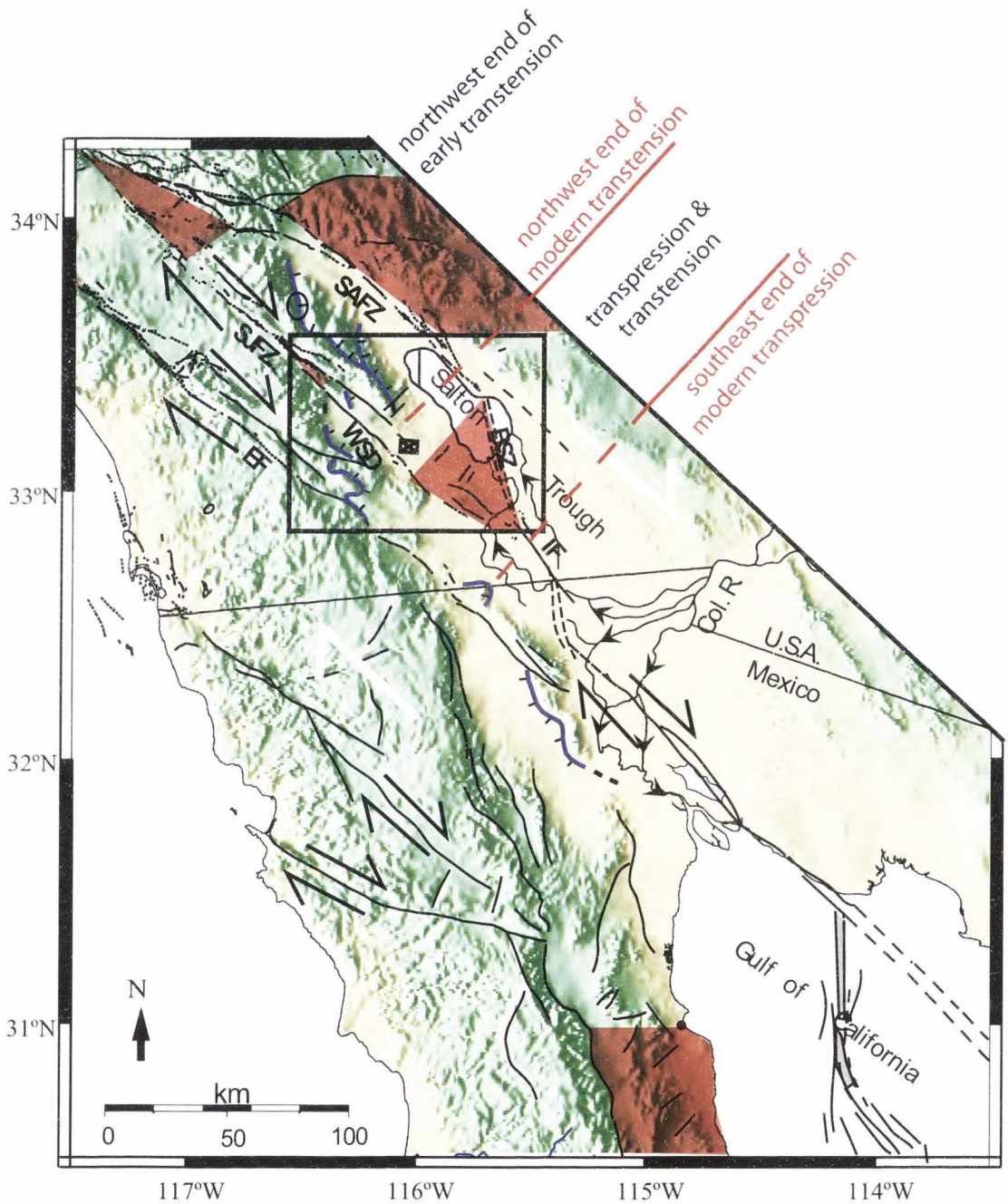

Figure 2-1. Tectonic overview of southern California. Areas of active block rotation are shaded red (Nicholson et al. 1986; Hudnut et al. 1989; Oskin and Stock 2003). Strike-slip faults are in black; SAFZ=San Andreas fault zone, SJFZ=San Jacinto fault zone, IF=Imperial fault, SJFZ=San Jacinto fault zone, EF=Elsinore fault. BSZ=Brawley Seismic Zone. Oblique-slip detachment faults are in blue including the WSD=West Salton detachment. Fault locations are from Jennings (1977), and Axen and Fletcher (1998). Box is approximate location of figure 2-2.

Figure 2-2. Overview of the western Salton Trough. Black box is extent of gravity map in figure 2-13. Dashed black box is the extent of the study area figure 2-3. CCF, Coyote Creek fault; CF, Clark fault; SAF, San Andreas fault; SHF, Superstition Hills fault; SMF, Superstition Mountain fault; EF, Extra fault; ERF, Elmore Ranch fault; IF, Imperial fault; BSZ, Brawley Seismic zone; DH, Durmid Hills; SFH, San Felipe Hills; OC, Ocotillo Badlands; BB, Borrego Badlands; FCB, Fish Creek-Vallecitos basin; FCM, Fish Creek Mts.; PM Pinyon Mountains; CM, Coyote Mountain; C Mts.,Coyote Mountains; SM, Split Mt.; SYM, San Ysidro Mts.; VM,Vallecito Mts.; TBM, Tierra Blanca Mountains; WP, Whale Peak; YR, Yaqui Ridge. Modified from Axen and Fletcher (1998)

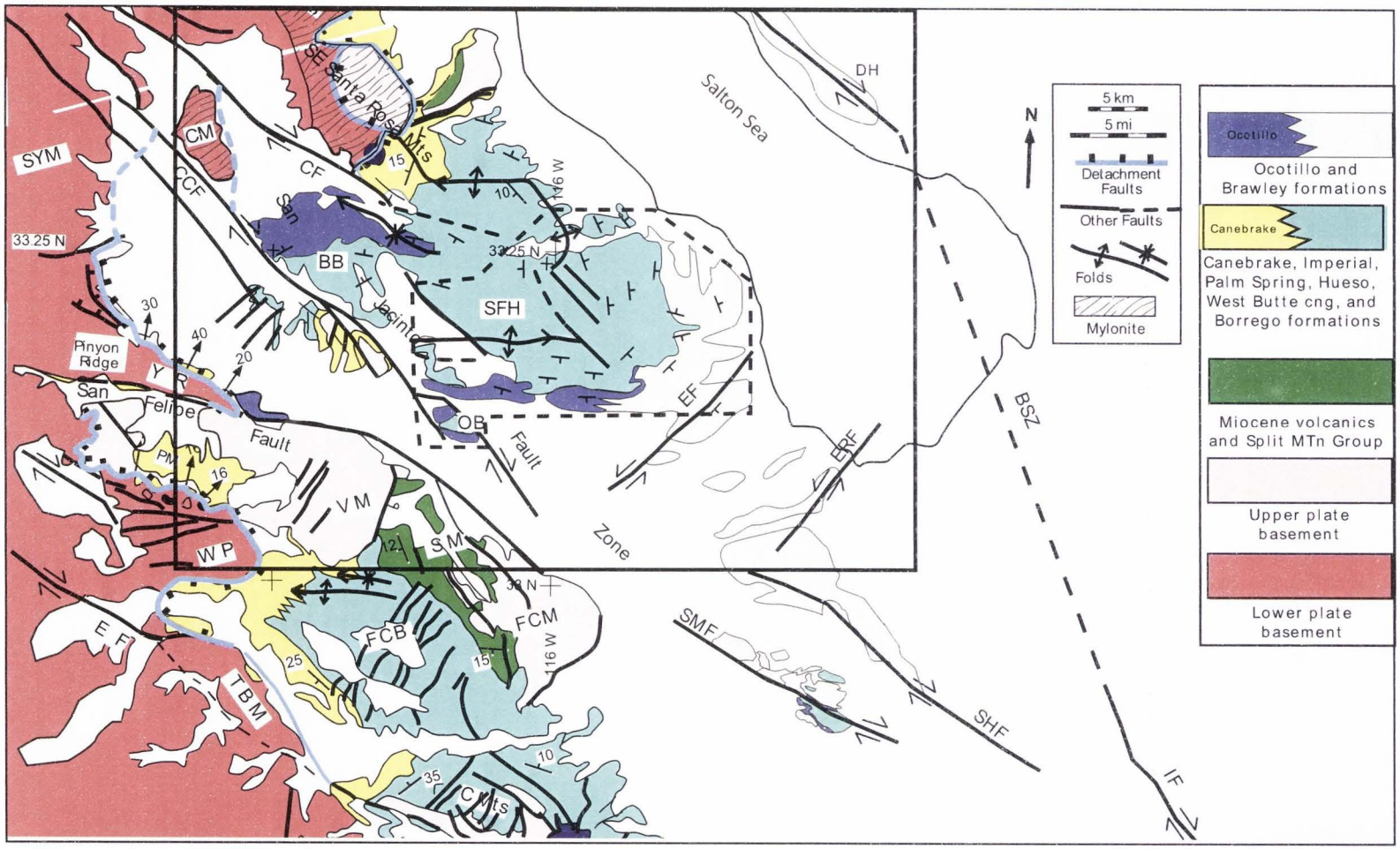

Figure 2-2. Overview of the western Salton Trough.

Figure 2-3. Simplified geology of the San Felipe Hills. Compiled from new unpublished mapping by Kirby, Janecke, Dorsey and Steely (2003) and Girty, Heitman, and Lilly (2002) shown by dashed blue box. Faults are shown in blue and folds in black.. Major strike-slip faults within the study area include the SFHF (San Felipe Hills fault), the DF (Dump fault), the CCF (Coyote Creek fault), the PWF (Powerline fault), and the SDF (Sand Dunes fault). The trend of the major SFA (San Felipe Anticline) is shown in black. Outcrops of angular unconformity between the Ocotillo Formation and the underlying units is shown in yellow on the limbs of the San Felipe anticline. Black dashed line is approximate extent of the San Felipe anticline just prior to deposition of the Ocotillo Formation. The extent of disconformity at the base of the Ocotillo and Brawley formations is shown in red. A to A' is the location of the reconstructed cross section for figure 2-11. Location of cross section B-B' (Fig. 2-12) is shown. Black box corresponds to position of figure 2-15. Star represents location of the Ocotillo Badlands measured section in figure 2-6. Approximate position of San Felipe wash is shown by the black dashed line. Red dashed lines are state highways.

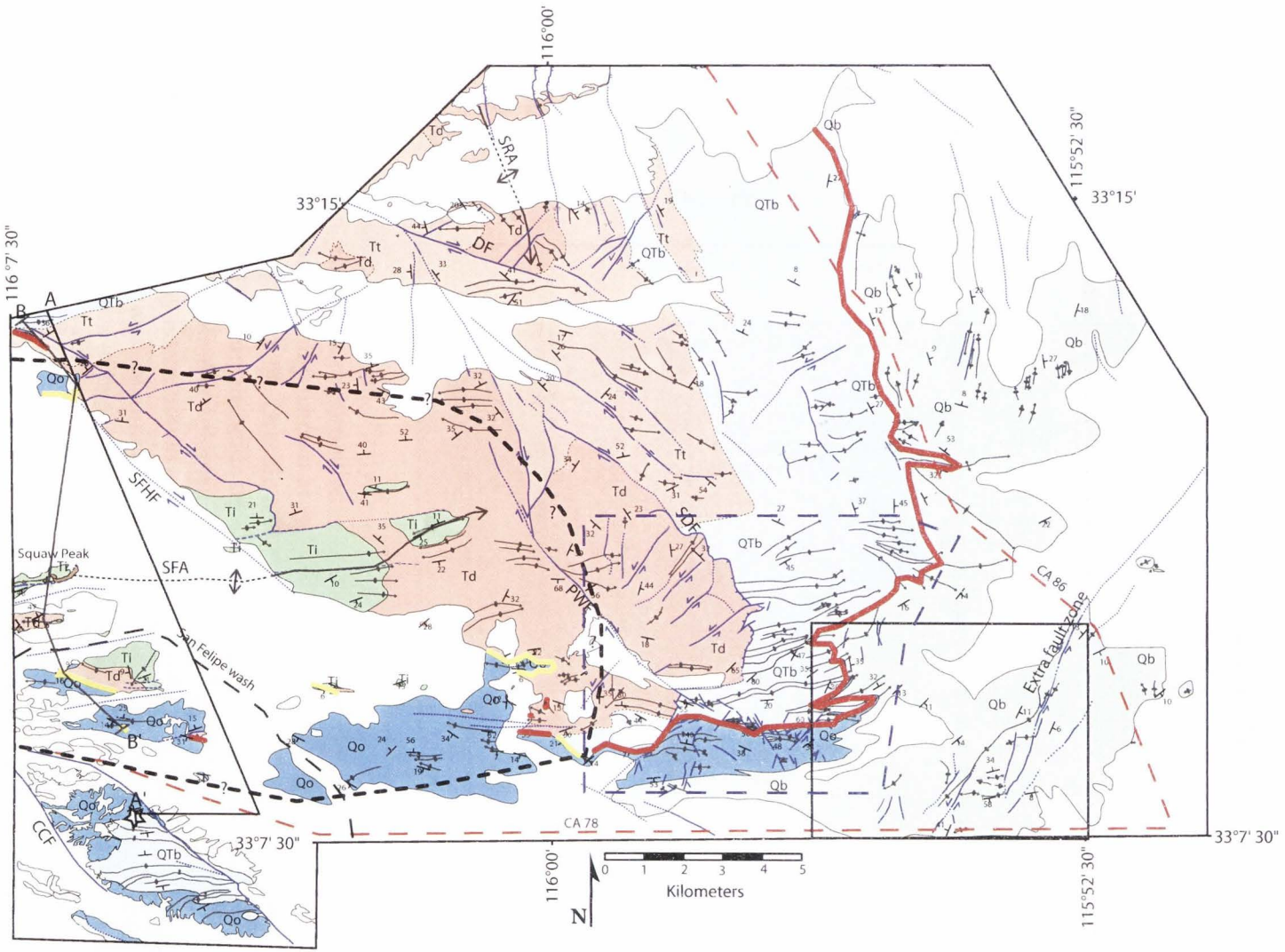

Figure 2-3. Simplified geology of the San Felipe Hills.

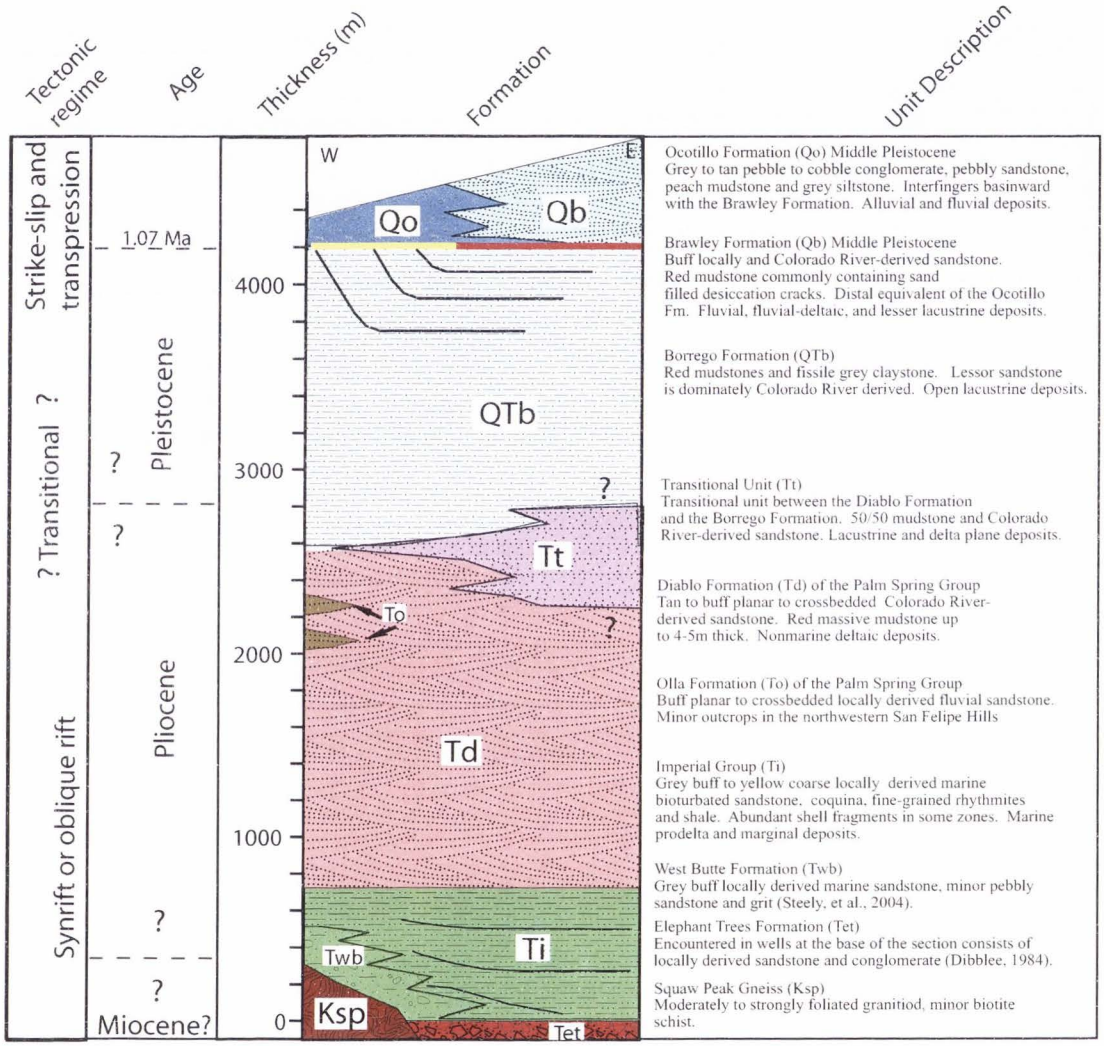

Figure 2-4. Stratigraphic column. Early synrift succession is the Imperial Group to Diablo Formation. The Borrego Formation is a transitional unit. Above these units, across an angular unconformity (shown in yellow) in the west and disconformity (shown in red) in the east are the Ocotillo and Brawley formations which were likely deposited during onset or reorganization of slip on strands of the San Jacinto fault zone. The coarse Ocotillo Formation conglomerate and sandstone interfinger with the finer sandstone of the Brawley Formation to the east within the San Felipe Hills. The 1.07 Ma age of the unconformity was determined paleomagnetically by this study. Other ages are approximate based on work of this study and previous work nearby by Johnson et al. (1983), Remieka and Beske-Diehl (1996),Winker and Kidwell (1996), and Steely et al. (2004). Growth may be apparent in the Imperial-aged deposits just to the west (Steely et al., 2004). Unit thickness's are minima based on mapping from this study. Units match those in figure 2-3.

Figure 2-5. Oil Well Wash measured section summary. Age constraints are shown relative to provenance, depositional environment, and sedimentary structures. Major changes in facies, provenance, and sedimentary structures occur across the regional disconformity (black line) separating the Ocotillo and Brawley formations from the underlying Borrego Formation. Base of the Jaramillo normal was placed at the disconformity because of magnetostratigraphy in the Borrego Badlands which tightly constrains the onset of Ocotillo deposition (Lutz, 2005). The base of the Bruhnes normal was placed at 480 m based on stratigraphic correlation of the section legs 2 and 3 across the Extra fault zone. The thin dashed line is position of the other possible correlation which is not preferred because of a stratigraphic mismatch. Microfossils include; fp, planktonic Forams; f, Forams; o, Ostracods; m, Mollusks; p, plant fragments; c, Chara; e, Echinoids; d, Diatoms. Reference polarity timescale is from Cande and Kent (1995).

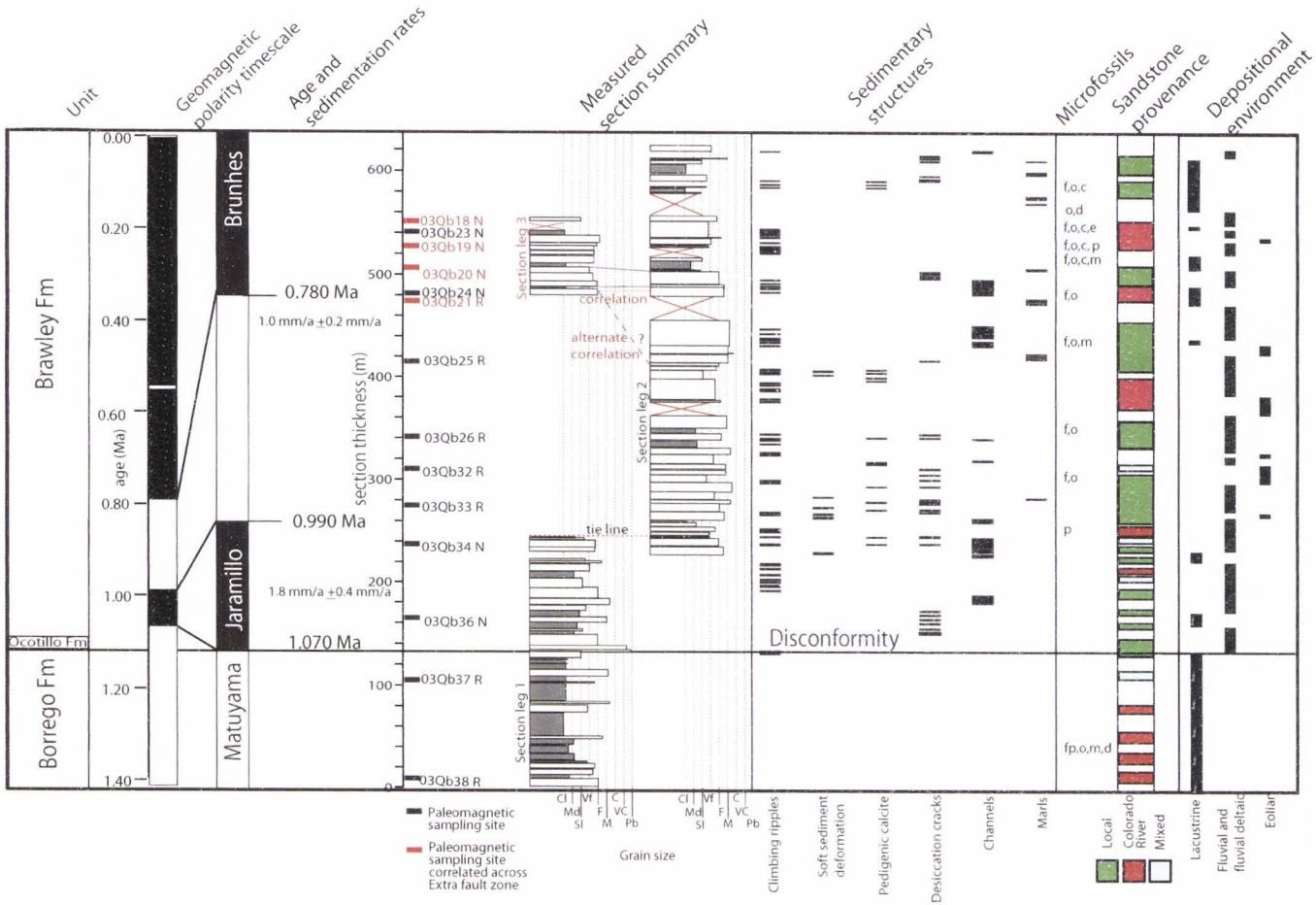

Figure 2-5. Oil Well Wash measured section summary.

Figure 2-6. Ocotillo Badlands measured section summary. Major changes in facies, provenance, and sedimentary structures occur across the conformable contact, shown in black, separating the Ocotillo Formation from the underlying Borrego Formation. Grain sizes are as follows; Cl, claystone; Md, mudstone; Sl, siltstone; Vf, very fine grain sandstone; F, fine grain sandstone; M, medium grain sandstone; C, coarse grain ssandstone; Vc, very coarse grain sandstone; Pb, pebble conglomerate; Cb, cobble conglomerate. Grey fill are siltstone or finer, pattern fill is pebble conglomerate or coarser. Onset of Ocotillo deposition is marked by sharp increase in grain size to pebble or cobble conglomerates. Location of section is shown on figure 2-3.

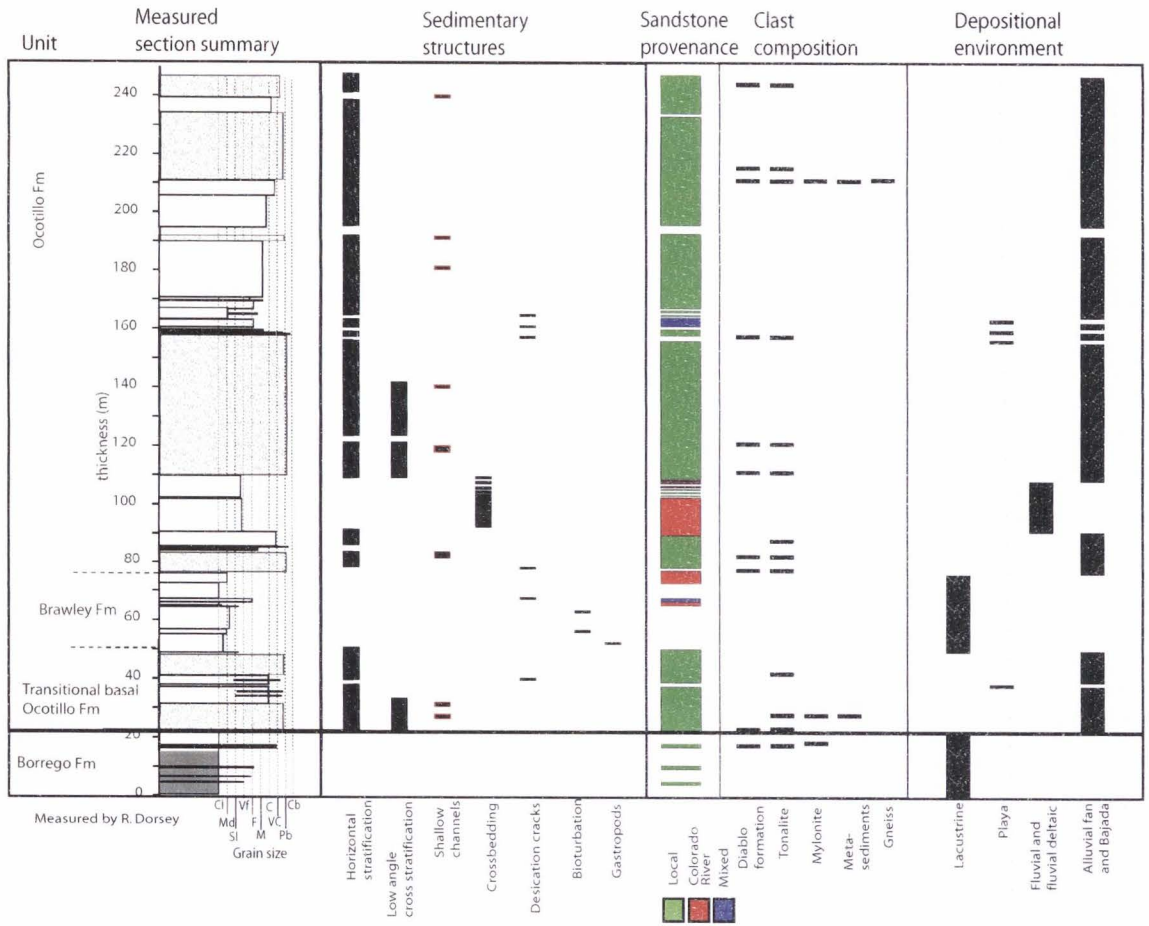

Figure 2-6. Ocotillo Badlands measured section summary.

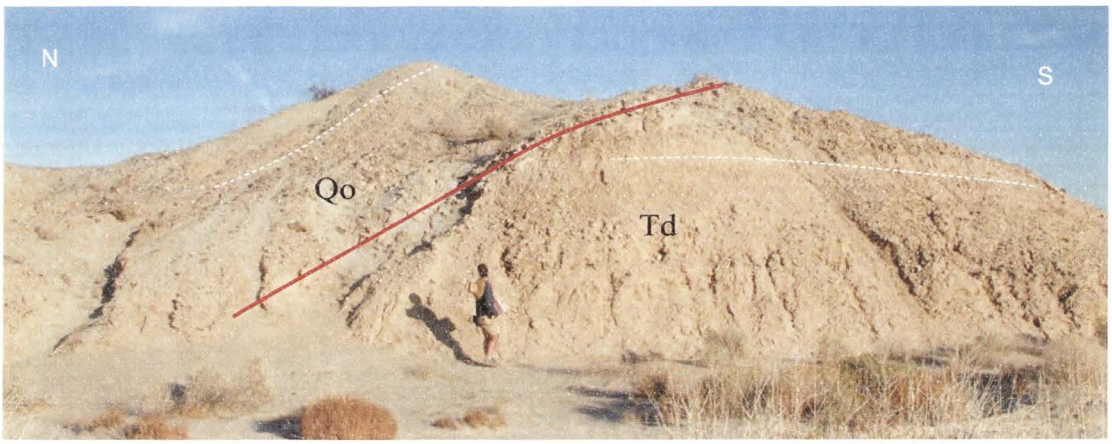

Figure 2-7. Angular unconformity in the southern San Felipe Hills. Angular unconformity between north-dipping Ocotillo Formation (Qo) and south-dipping Diablo Formation (Td) in Tarantula Wash on the south limb of the San Felipe anticline.

Figure 2-8. Plan view of polygonal sand filled desication cracks in red mudstone of the Ocotillo Formation. Location is south of the San Felipe Hills in the Ocotillo Badlands. Hand shovel is 60 cm long.

Figure 2-9. Photo of conglomerate in the Ocotilllo Formation with numerous recycled clasts of Palm Spring Formation sandstones. Arrows point to Palm Spring clasts. Location is just south of the study area in the Ocotillo Badlands, from 80 m in the measured section (Fig. 2-6).

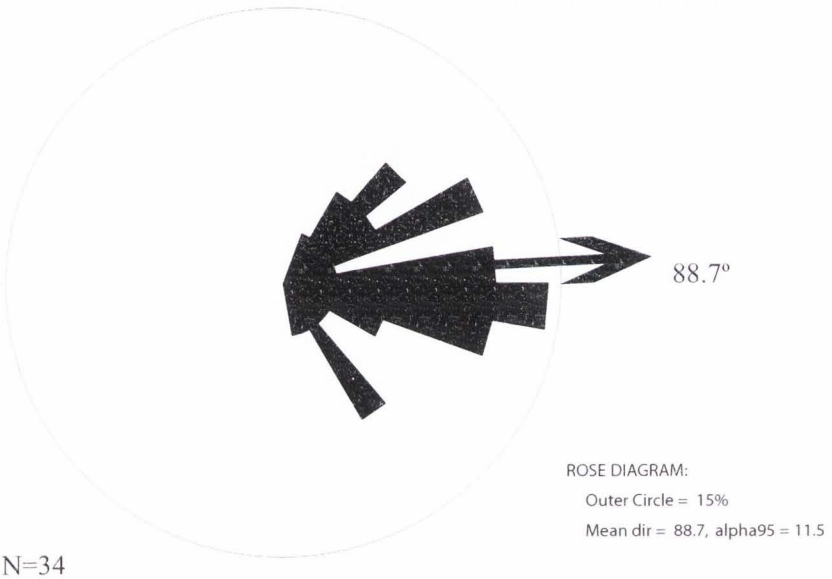

Figure 2-10. Paleocurrents for the Ocotillo Formation. Paleoflow was measured from clast imbrications within the Ocotillo Formation in the Ocotillo Badlands. Mean direction = 88.7°.

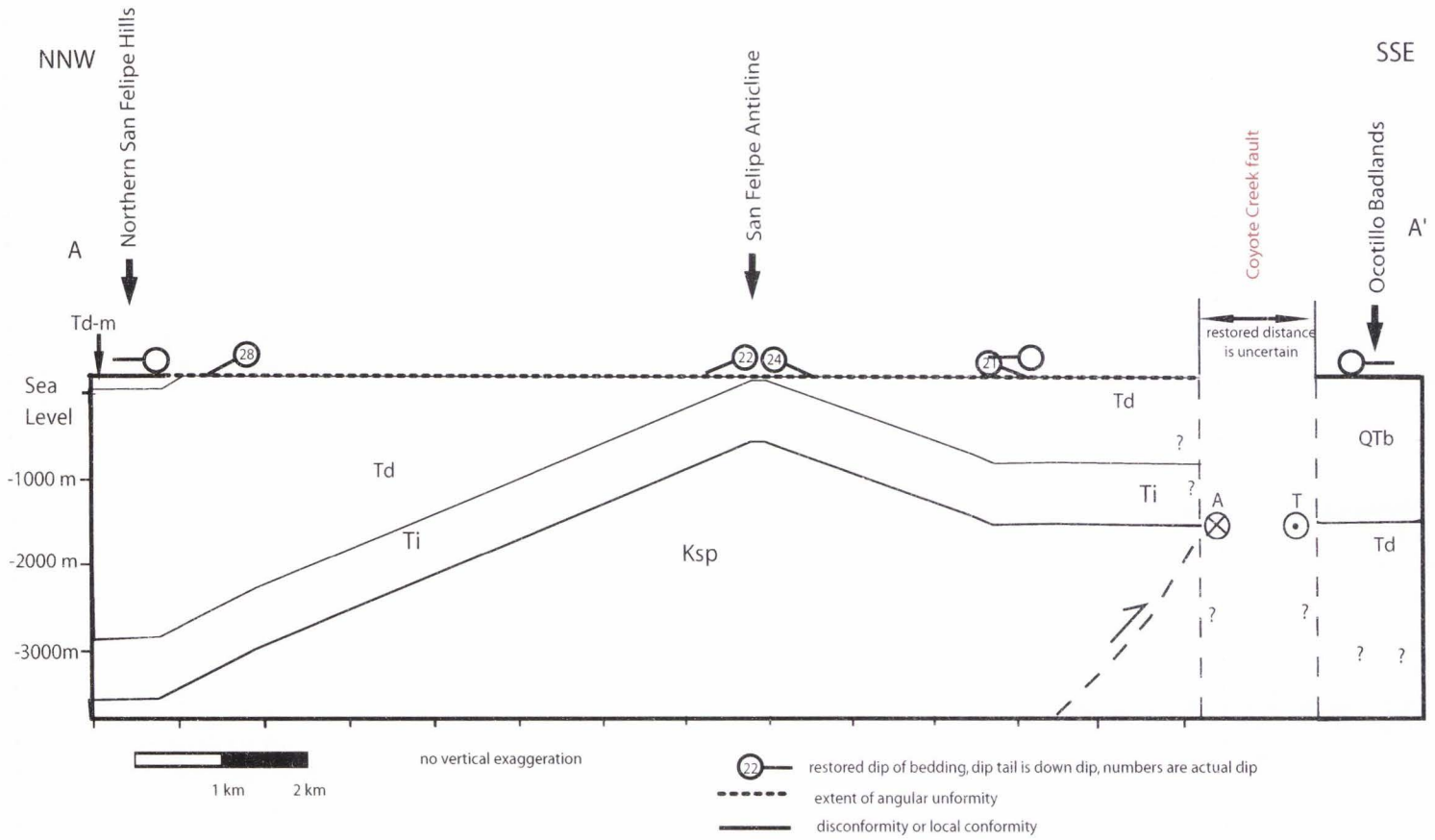

Figure 2-11. Cross section A. Reconstructed cross section of the San Felipe anticline in the western San Felipe Hills at 1Ma created from the angular relations between the Ocotillo Formation and the older units beneath it. Offset across the Coyote Creek fault along the south limb of the San Felipe anticline is unconstrained. Offset across the Coyote Creek fault on the north limb of the San Felipe anticline may be 4 km based on offset gravity signals (Langenheim unpublished data). Units correspond with those used in Figs. 2-3, 2-4. Dip tadpoles without numbers indicate flat sub-Ocotillo Formation bedding. See Fig. 2-3 for location of cross section.

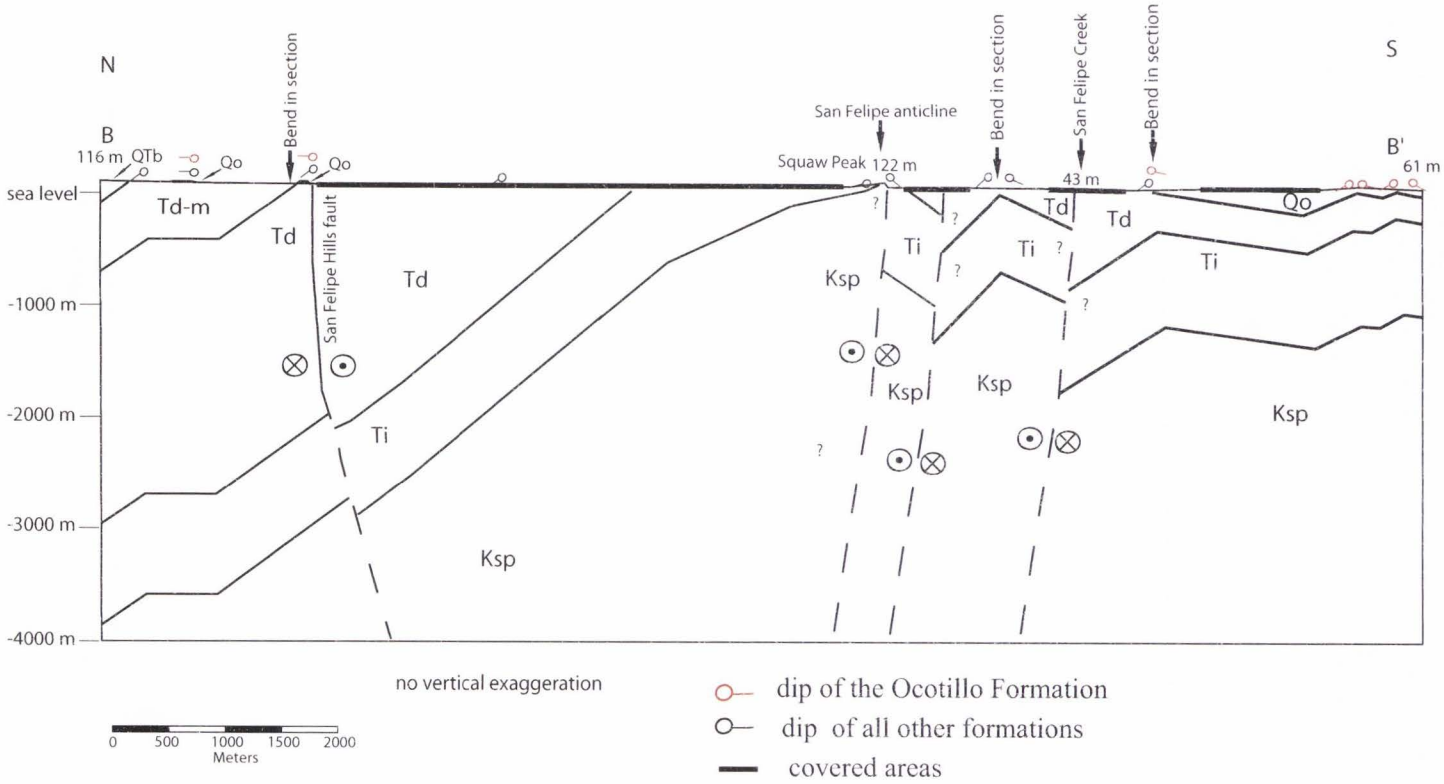

Figure 2-12. Cross section B. North-south cross section in the western San Felipe Hills through the modern east trending San Felipe anticline. Units include the KSP (Squaw Peak basement), Ti (Imperial Group), Td (Diablo Formation), QTd-m (muddy Diablo transitional unit), QTb (Borrego Formation), and the Qo (Ocotillo Formation). Black tadpoles represent the dips of all units except the Ocotillo Formation. Red tadpoles represent the dip of the Ocotillo Formation. Units correspond with those used in Figs. 2-3, 2-4. See Fig. 2-3 for location of cross section.

Figure 2-13. Isostatic gravity anomalie map. Approximate extent of the study area is shown by black dashed box. Extent of surficial angular unconformity beneath the Ocotillo Formation is shown be the white dash. The gravity signal of the San Felipe anticline (SFA) extends east past the Powerline fault (PWF). The gravity signal of the south plunging Santa Rosa anticline (SRA) is apparent. Major faults are shown in white including the Clark fault, CF; Coyote Creek fault, CCF; Extra fault zone, EFZ; Elmore Ranch fault, ERF; Superstition Hills, SHF. Relevant exposures of Plio-quarternary rocks include the Borrego badlands, BB; and the Ocotillo badlands, OB. State highways are shown by the red dashed lines. Gravity data is courtesy of Langenheim unpublished work (2004).

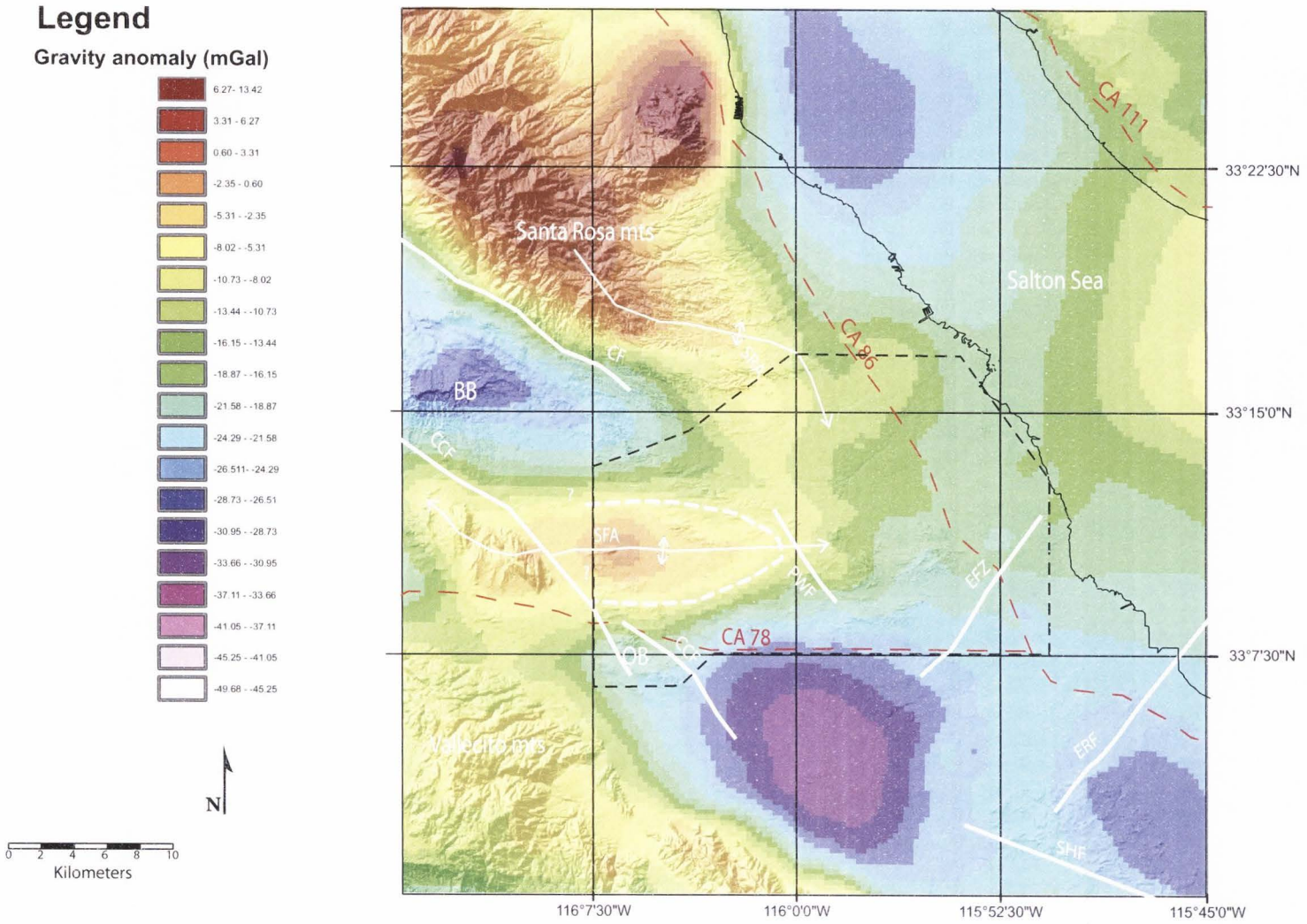

Figure 2-13. Isostatic gravity anomaly map.

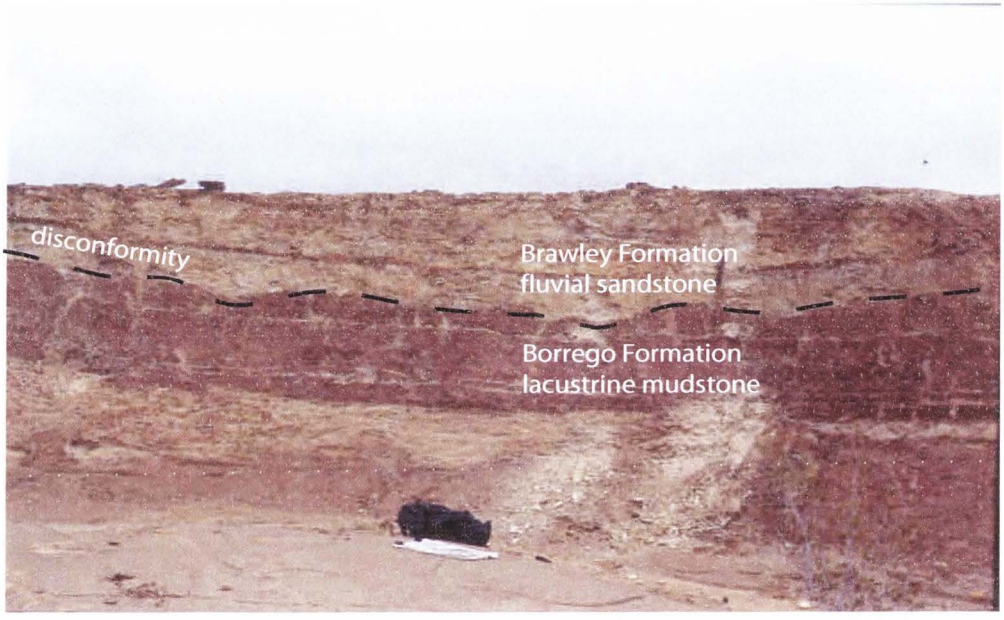

Figure 2-14. Disconformity in the eastern San Felipe Hills. Erosional contact between the basal locally derived coarse grit of the Brawley Formation and the red lacustrine mudstones of the upper Borrego Formation. Location is 10 km north of the Oil Well Wash measured section in the eastern San Felipe Hills. Backpack in foreground for scale.

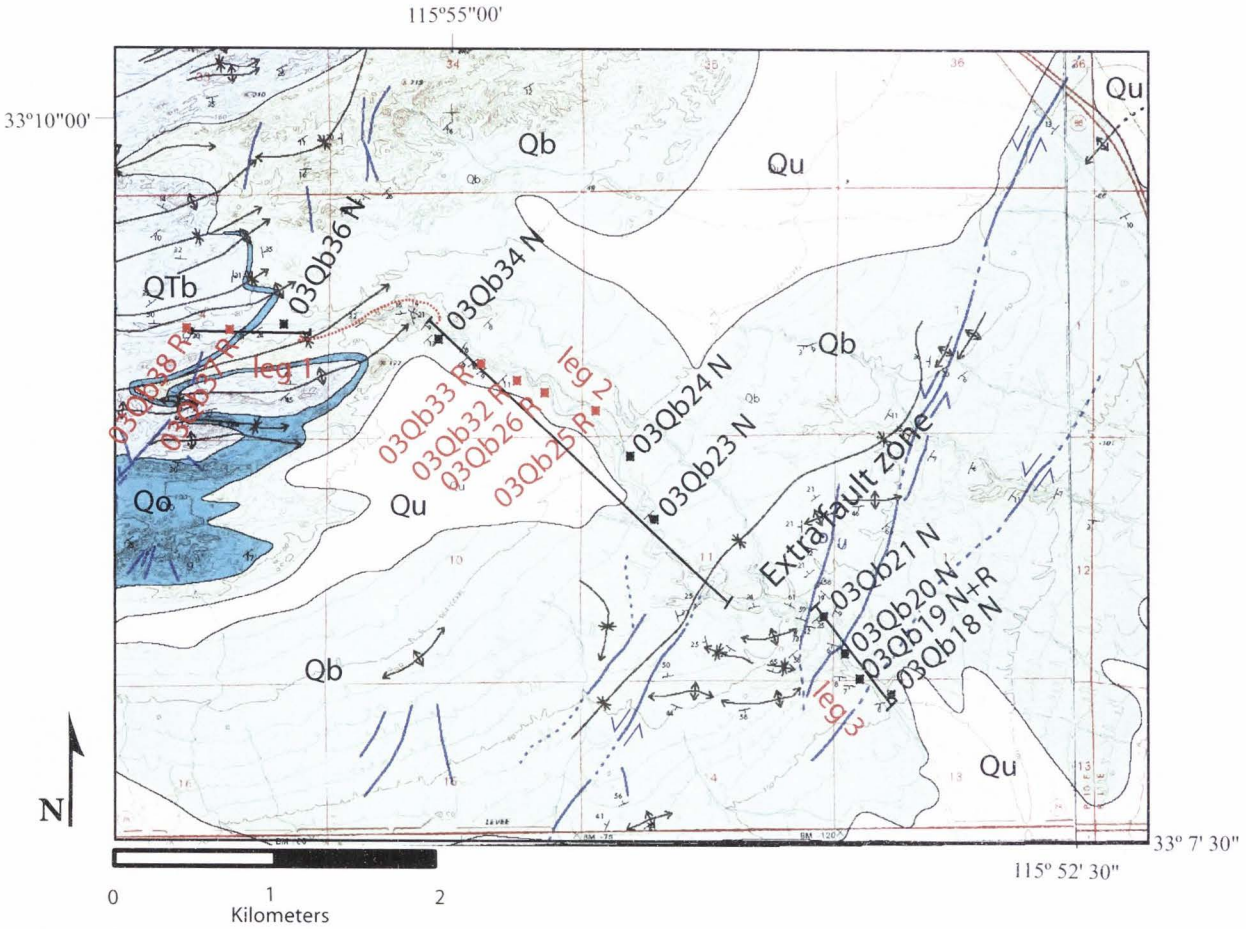

Figure 2-15. Oil Well Wash measured section location map. Faults are in blue and include the left lateral Extra fault zone. Folds are in black. Black bars represent approximate extent of segments of the measured section. Red dashed line represents stratigraphic tie line around structures. Crosses are approximate position of paleomagnetic sampling sites, red represents reversed polarity and black represents normal polarity. Site numbers correspond to those in figure 2-5 and plate 2. Qb=Brawley Formation, Qo= Ocotillo Formation, QTb= Borrego Formation, and Qu=undivided Holocene deposits.

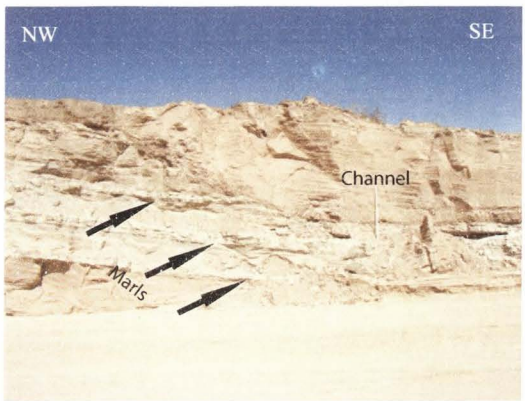

Figure 2-16. Channel fill in te Brawley Formation. Location is 483 m in the Brawley Formation. White scale bar is 2m. Arrows indicate prominent beds of silty marl that are up to 40 cm thick.

Figure 2-17. Climbing ripples in the Brawley Formation. Climbing ripples in poorly consolidated very fine-grained locally derived sandstone.

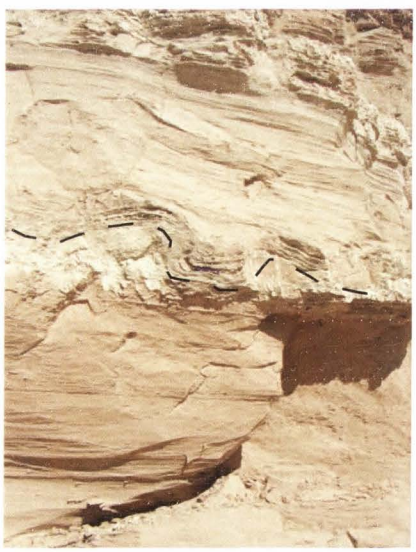

Figure 2-18. Soft sediment deformation in the Brawley Formation. Soft sediment deformation in the lowest marl bed in figure 2-16. Width of view is appoximately 1m.

Figure 2-19. Eolian deposits in the Brawley Formation. Foresets are approximately 3-4m in length.

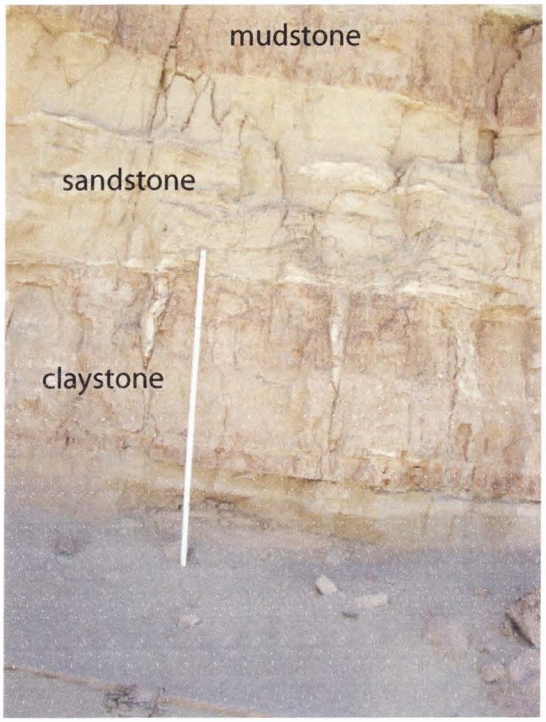

Figure 2-20. Large desiccation cracks in the Brawley Formation. Cross sectional view of large downward tapering desiccation cracks in red claystone. Photo is from 524 m in Brawley Formation along Oil Well Wash. Scale is 2m.

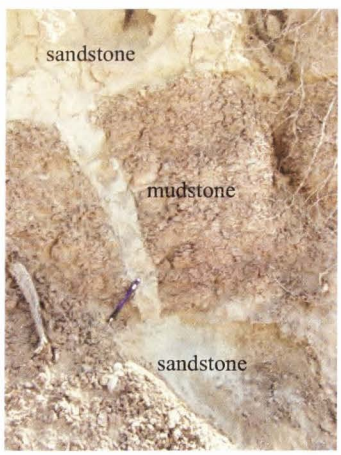

Figure 2-21. Close up of desiccation cracks in the Brawley Formation. Cross sectional view of small desiccation crack filled with locally derived sands. Pencil for scale. Many cracks traverse the full thickness of a mudstone or claystone.

Figure 2-22. Locally derived sandstone in the Brawley Formation. Granular locally derived sandstone with mudstone clasts at base of channel fill. White grains are plagioclase weathered from Peninsular Ranges basement. Pencil for scale.

Figure 2-23. Paleosols in the Brawley Formation. Calcite nodules developed in a red mudstone. Downward tapering sand filled desication cracks are apparent. Photo is from 404 m in the Oil Well Wash measured section. Pencil for scale.

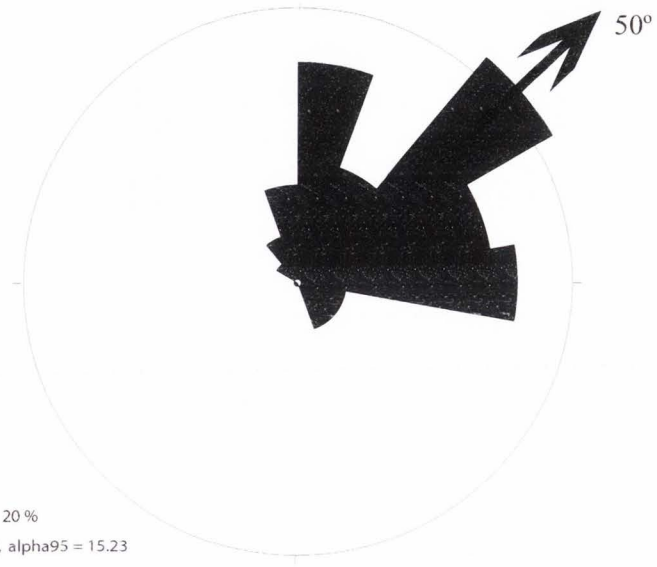

a)

N=51

ROSE DIAGRAM:

Outer Circle = 20 %

Mean dir = 50, alpha95 = 15.23

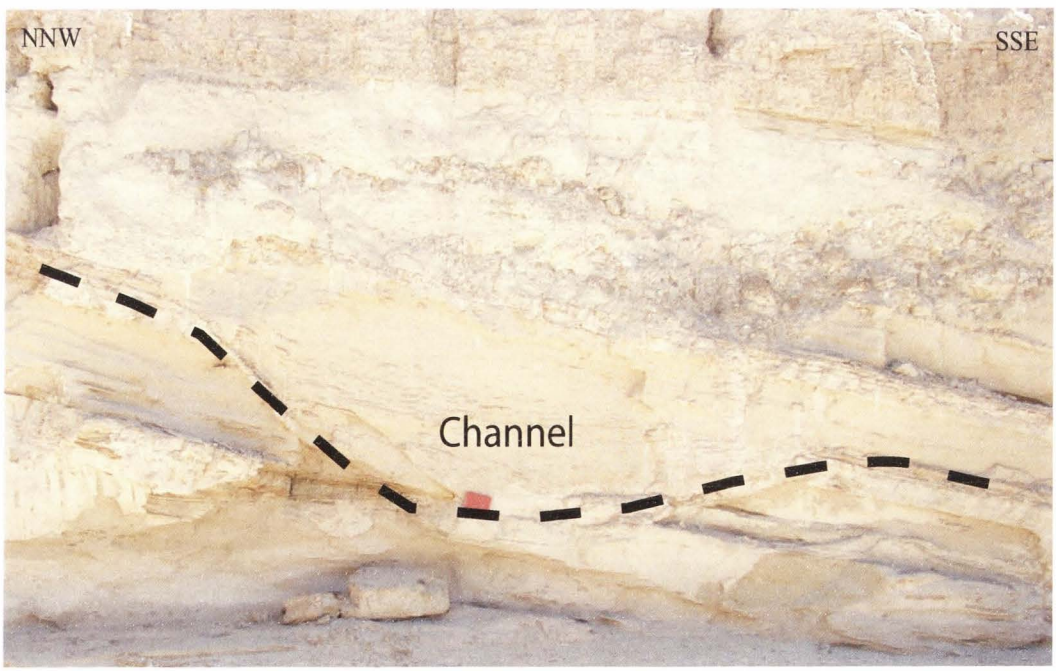

b)

Figure 2-24. Paleocurrents for the Brawley Foramtion. a) Paleocurrents from the Brawley Formation throughout the eastern San Felipe Hills. Mean direction = 50° Paleoflow was measured from channel fills structures similar to the one shown in b) when additional sedimentary structures such as ripples and or trough crossbeds could be measured to determine unique flow direction. Additional measurements were taken on crossbeds and ripples. Orange field notebook for scale.

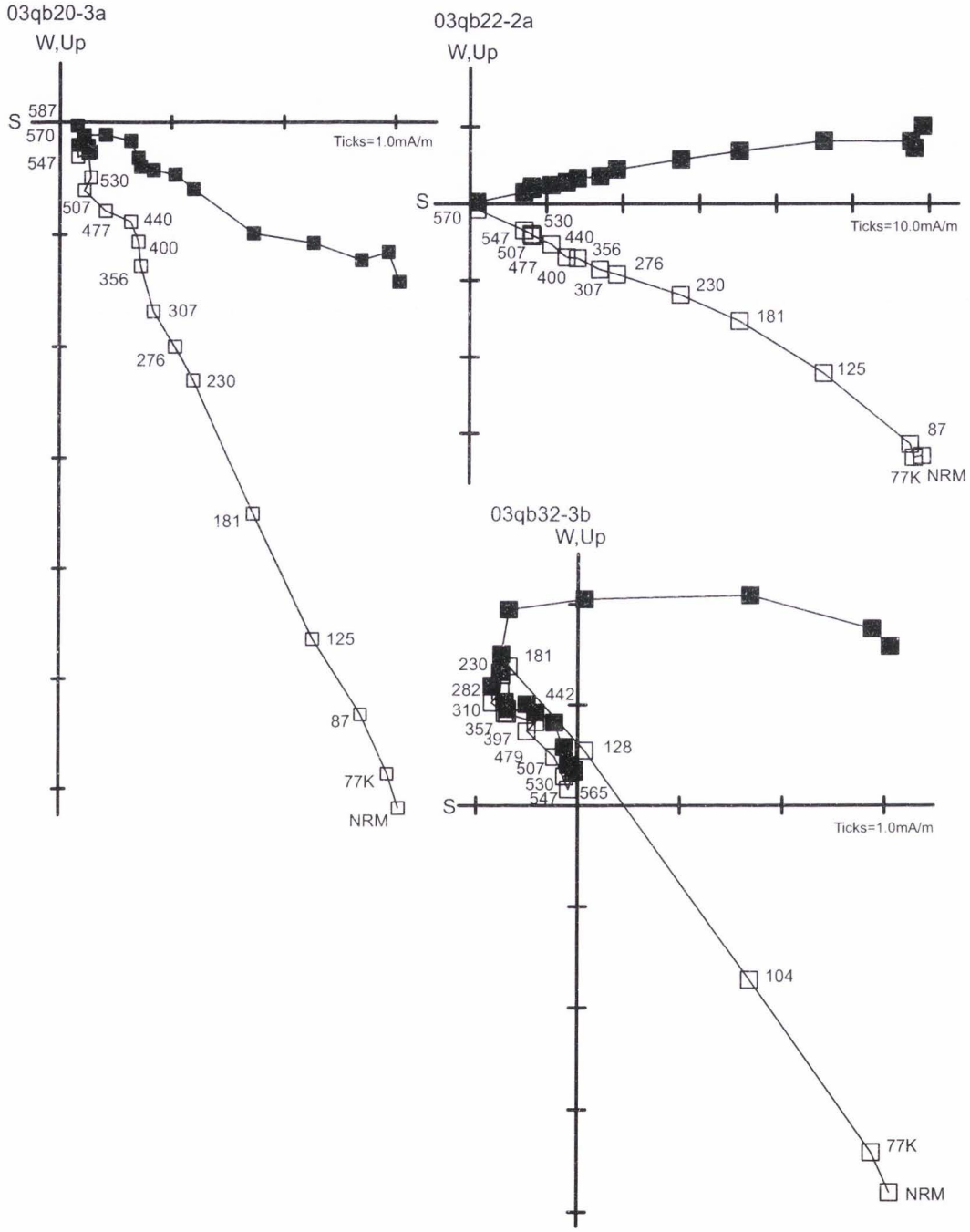

Figure 2-25. Demagnetization diagrams for class 1 data. These sites have a well defined second-removed vector components.

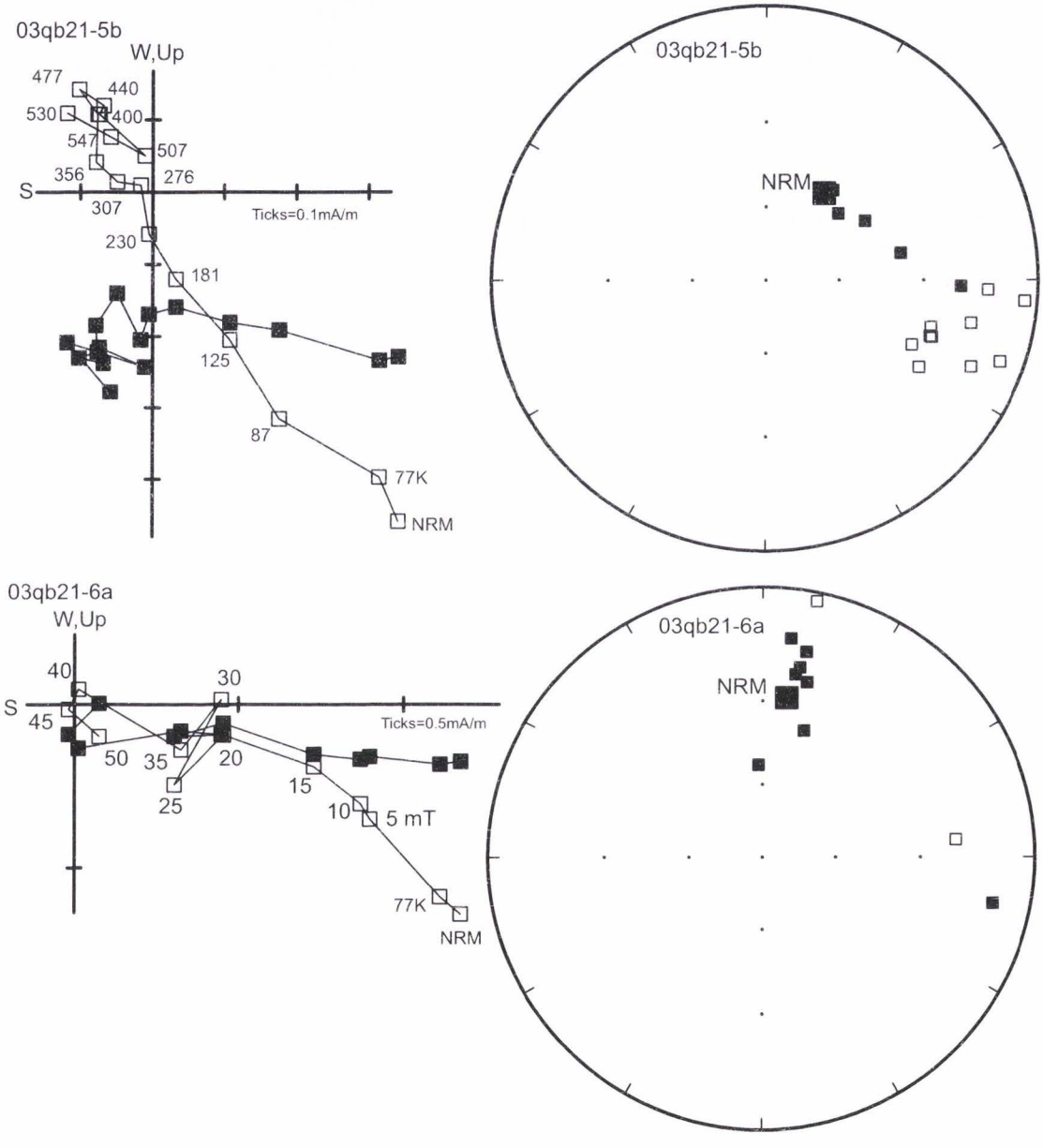

Figure 2-26. Demagnetization diagrams for class 2 data. These sites had a poorly defined second removed components, and commonly do not trend towards the origin of the orthogonal vector plots.

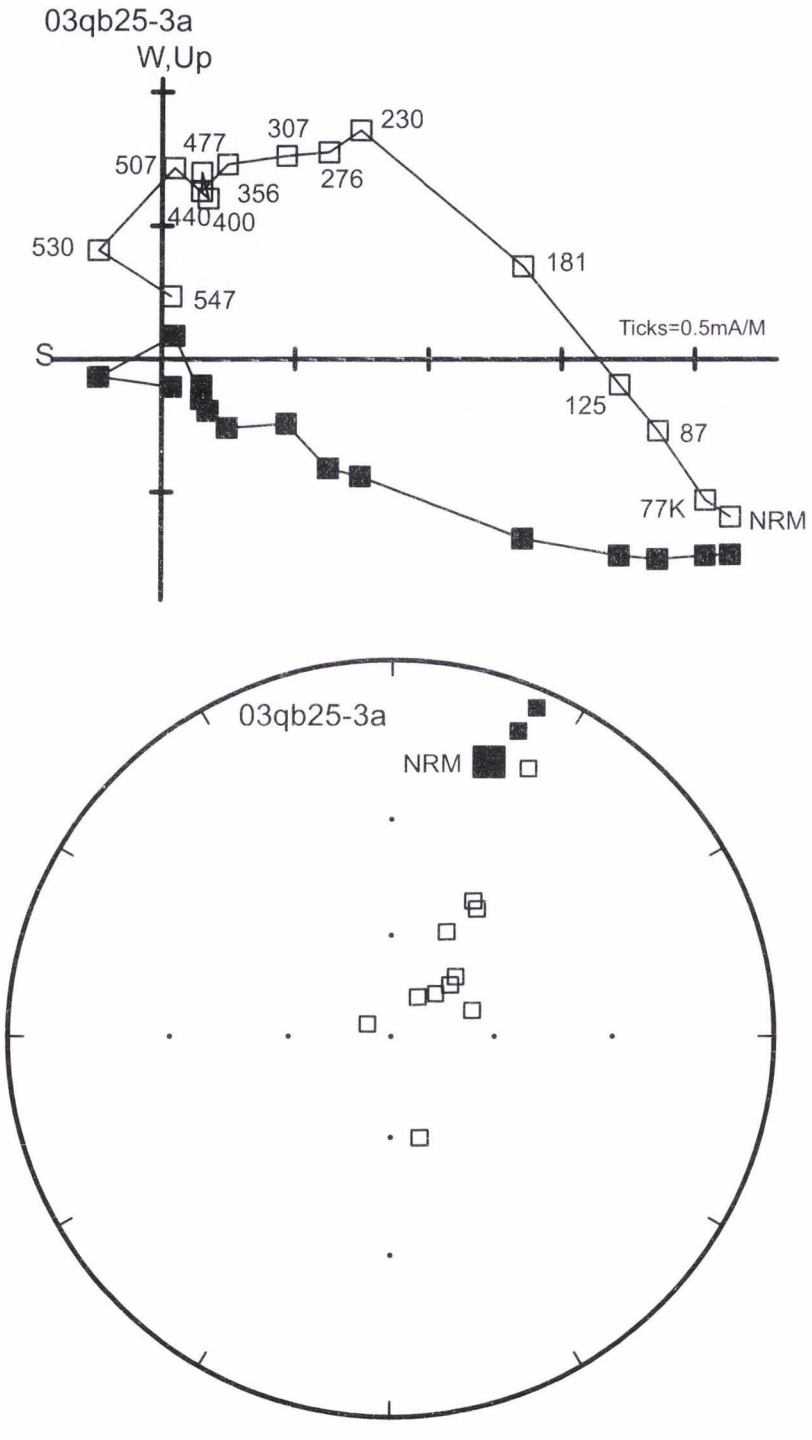

Figure 2-27. Class 2 data specimen polarity. Class 2 specimens which have a well defined great circle were qualitatively assessed for polarity.

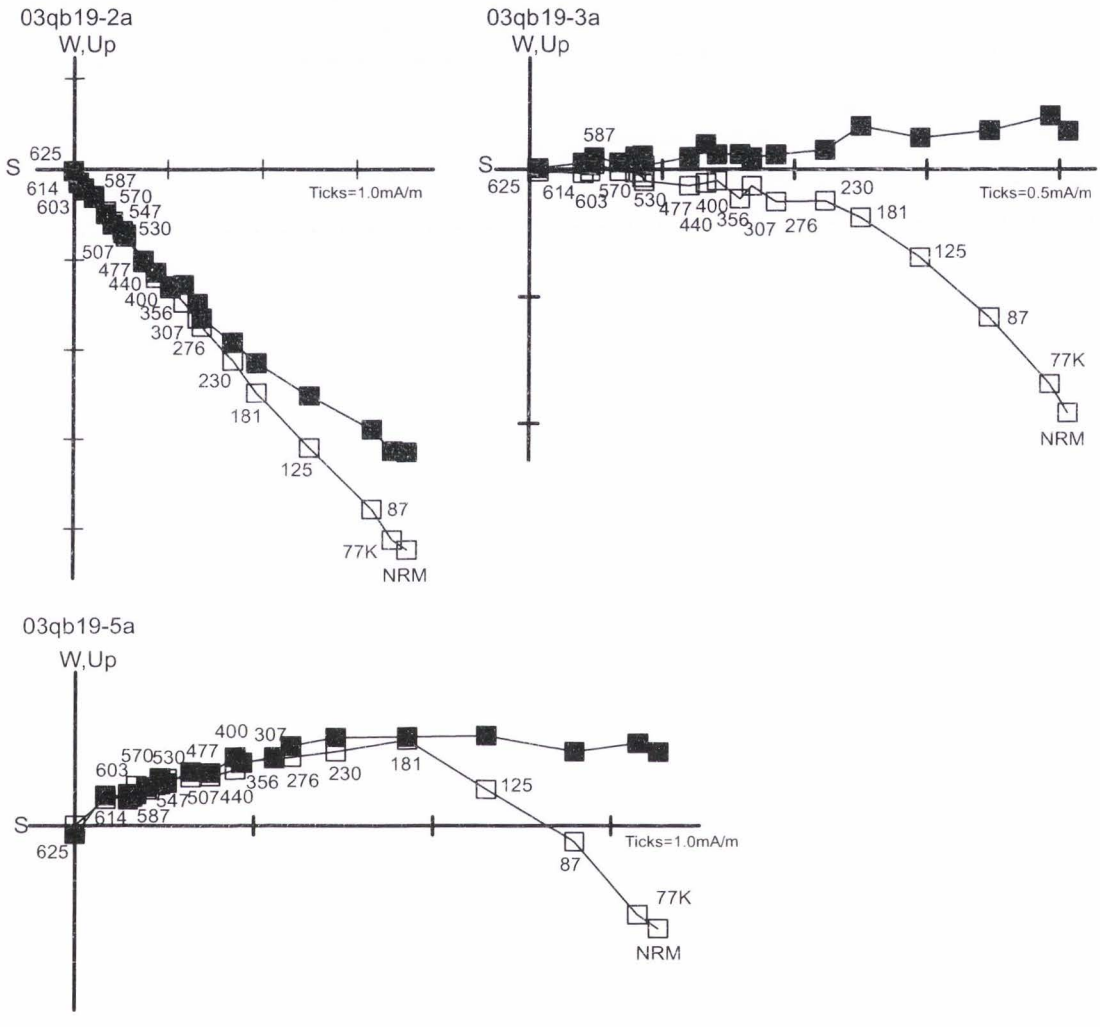

Figure 2-28. Transitional field sites. Sites which shows well defined magnetization vectors which point either shallowly up, or shallowly down. This is interpreted to represent a period of transitinoal field.

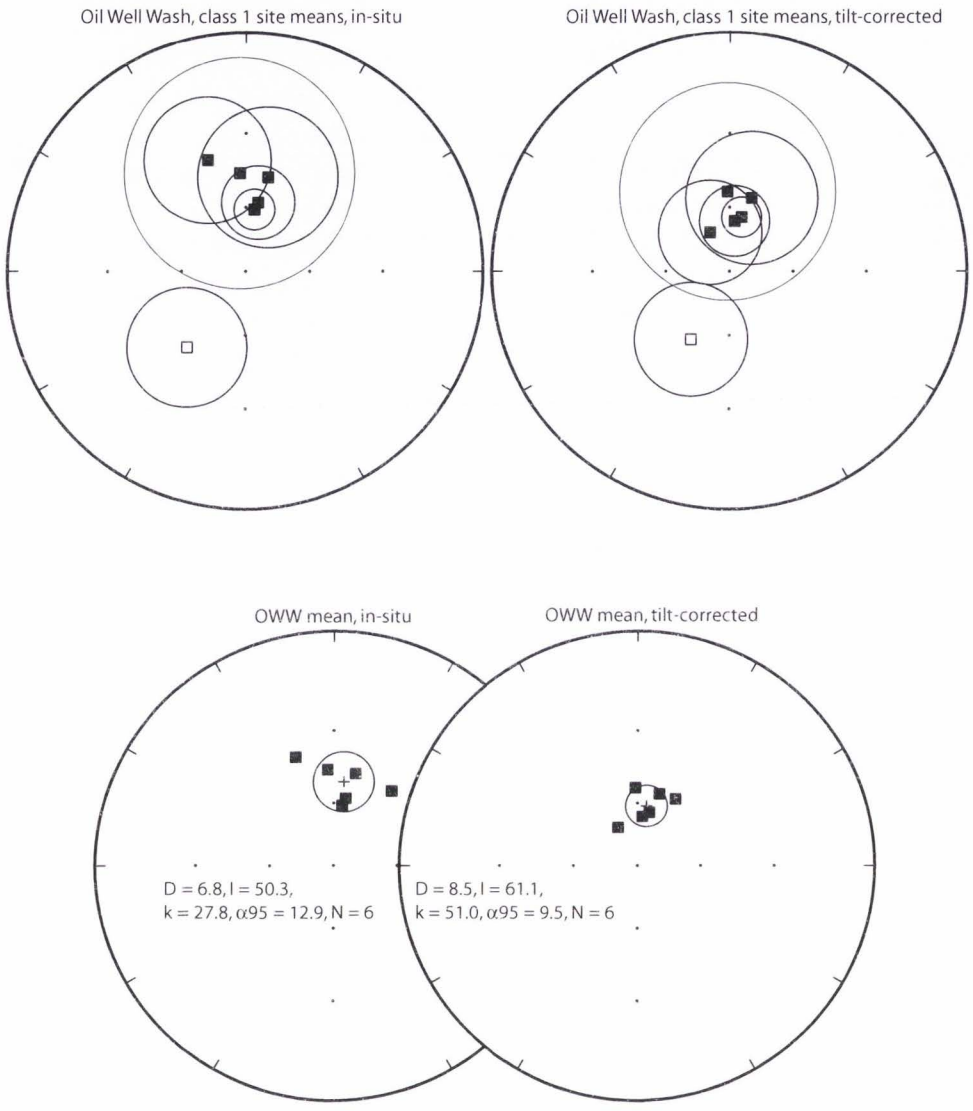

Site	N / No	Declination	Inclination	k	$_{95}$	Bed s/d
03Qb18	3 / 4	356.5	45.3	9	43.8	075/08
03Qb20	4 / 4	10.1	57.4	33.4	16.1	113/09
03Qb22	4 / 4	341	37.7	15.8	23.8	077/32
03Qb23	3 / 3	13.2	46	20.3	28.1	085/09
03Qb32	3 / 3	217.4	-46.2	27.1	24.2	165/10
03Qb34	3 / 3	7.8	60.7	184.5	9.1	061/04

Figure 2-29. Class 1 data site means. Site mean directions from class 1 sites. Directions are given in in-situ coordinates, N/No are the number of accepted sample directions/ number of demagnetized samples, k is the Fisher clustering parameter, 95 is the radius of 95% confidence about the mean directionSite mean directions are moderately clustered in in-situ coordinates. Site mean directions are better clustered after tilt correction.

Figure 2-30. Tectonic and stratigraphic summary. Units and their approximate ages are shown to the left. Italics represent inferred ages primarily from correlation with paleomagnetically dated units to the south in the Fish Creek Basin (Winker and Kidwell 1996; Johnson et al. 1983). Regular type represents constrained age from this study. Paleoflow is north when straight up and shows a 180 degree reversal between the Brawley Formation and the underlying units. Active faults show major structures which likely controlled basin architecture at a given time. Numbers represent data source (1, this study; 2, Steely et al. 2004; 3, Axen and Fletcher 1998; 4, Morton and Matti 1993; 5, Lutz 2005).

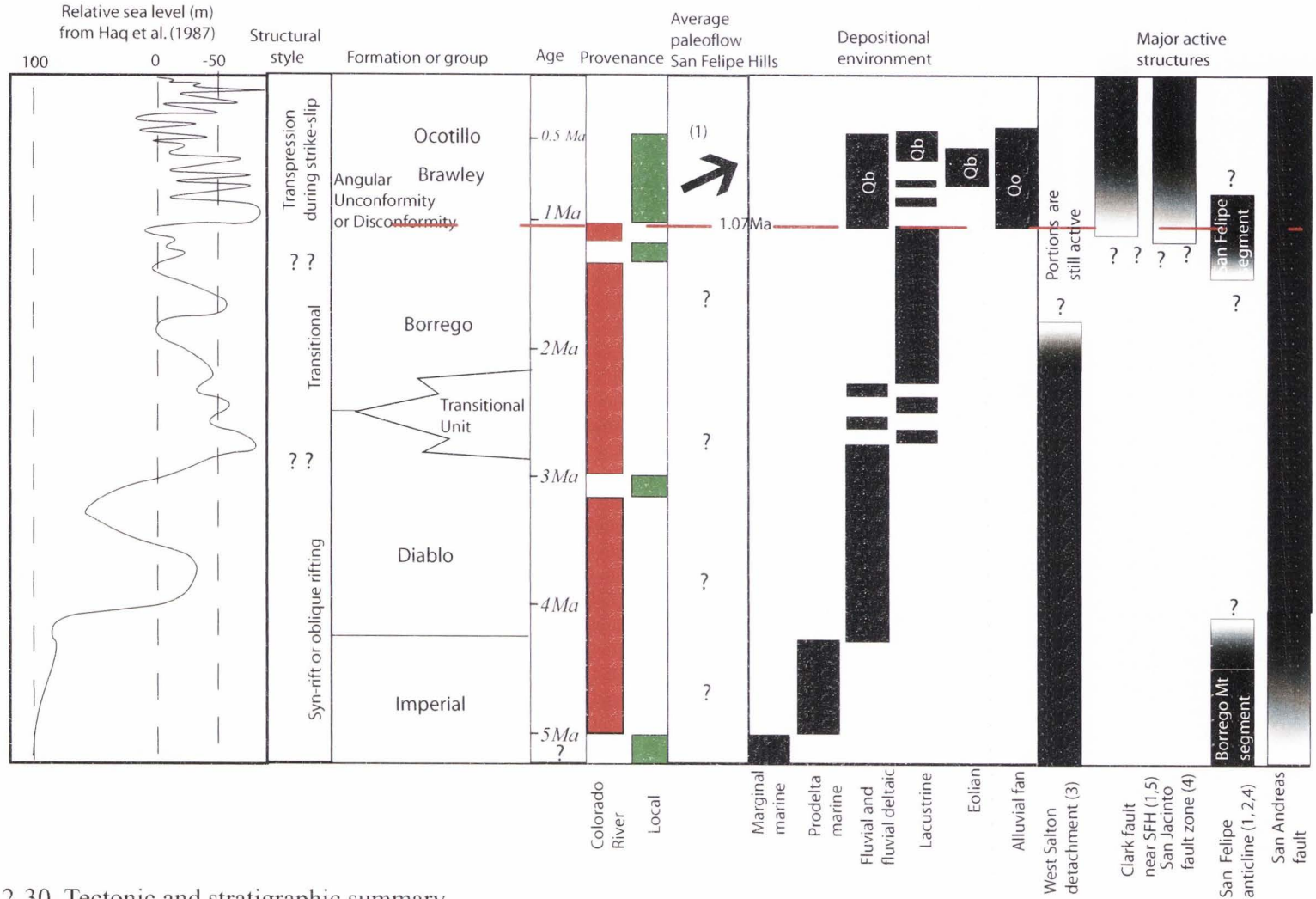

Figure 2-30. Tectonic and stratigraphic summary.

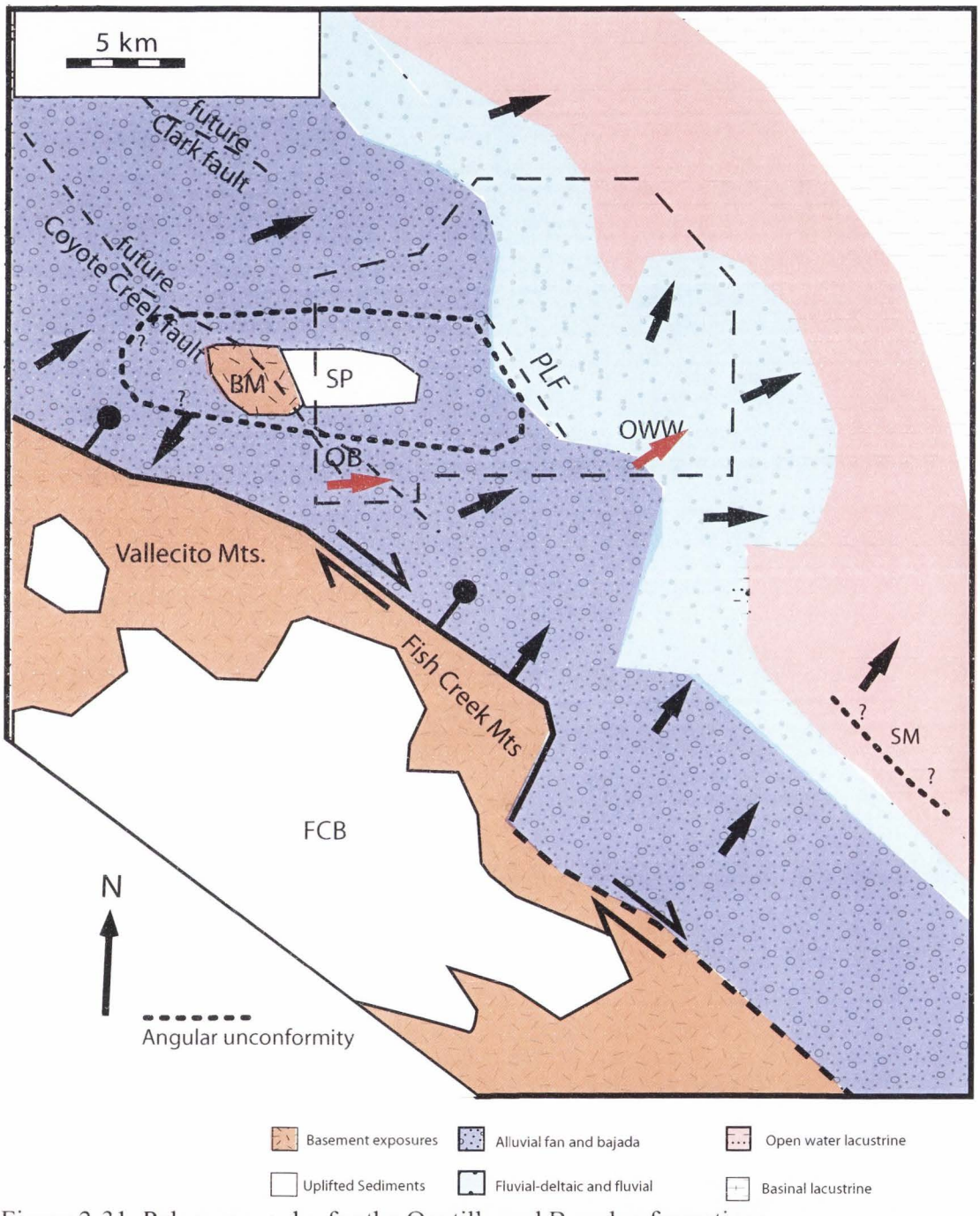

Figure 2-31. Paleogeography for the Ocotillo and Brawley formations. Paleogeography of the San Felipe Hills during deposition of the Ocotillo and Brawley formations just after 1 Ma. SFA, San Felipe anticline; BB, Borrego badlands; OB, Ocotillo badlands; OWW, Oil Well Wash; SP, Squaw Peak; FCB, Fish Creek basin; BM, Borrego Mountain; PLF, Powerline fault; SM, Superstition Mountains. Black arrows show infered direction of sediment dispersal. Red arrows show actual sediment dispersal. Black dotted line is the extent of sub-Ocotillo Formation angular unconformity. Black dashed box is the extent of the study area.

Figure 2-32. Comparison of Oil Well Wash and Ocotillo badlands measured sections. Black line represents the base of the Ocotillo Formation from both sections. This transition was dated at 1.070 Ma in Oil Well Wash. Grain sizes are as follows; Cl, claystone; Md, mudstone; Sl, siltstone; Vf, very fine grain sandstone; F, fine grain sandstone; M, medium grain sandstone; C, coarse grain ssandstone; Vc, very coarse grain sandstone; Pb, pebble conglomerate; Cb, cobble conglomerate. Grey fill represents siltstone or finer, pattern fill represents pebble conglomerate or coarser. Onset of Ocotillo deposition is marked by sharp increase in grain size to pebble or cobble conglomerates at both locations. In the Oil Well Wash section this corresponds with a regional disconformity in the Ocotillo Badlands no disconformity is apparent. Measured Ocotillo Formation thickness in the Ocotillo badlands is at least 243.5 m and in the Oil Well Wash section is only 22.5 m thick showing dramatic eastward fining of the Ocotillo and Brawley formations. The Ocotillo Badlands section is located 20 km west of the Oil Well Wash section. Comparison of depositional environments shows basinward changes from alluvial fan and bajada deposition to finer grain fluvial-deltaic and marginal lacustrine deposits.

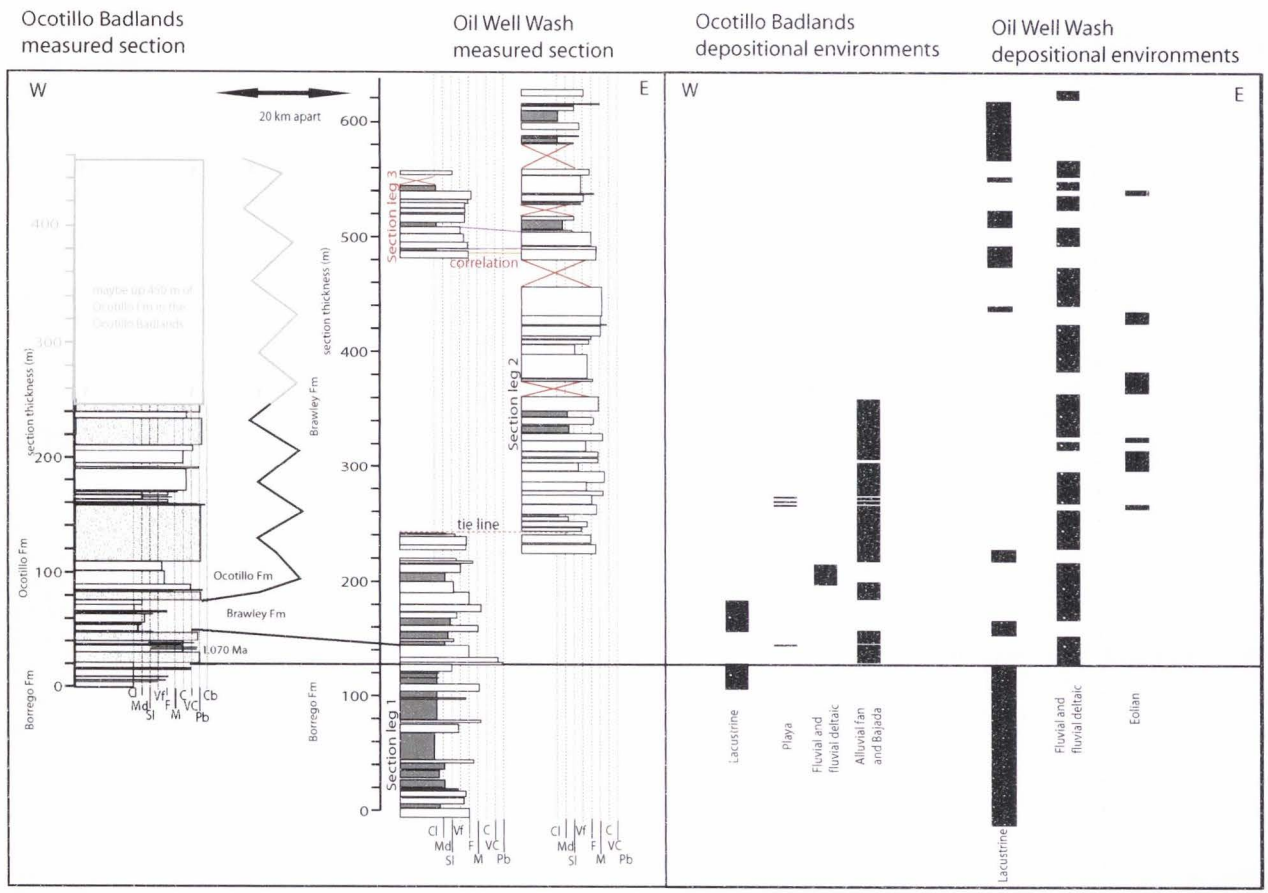

Figure 2-32. Comparison of Oil Well Wash and Ocotillo badlands measured sections.

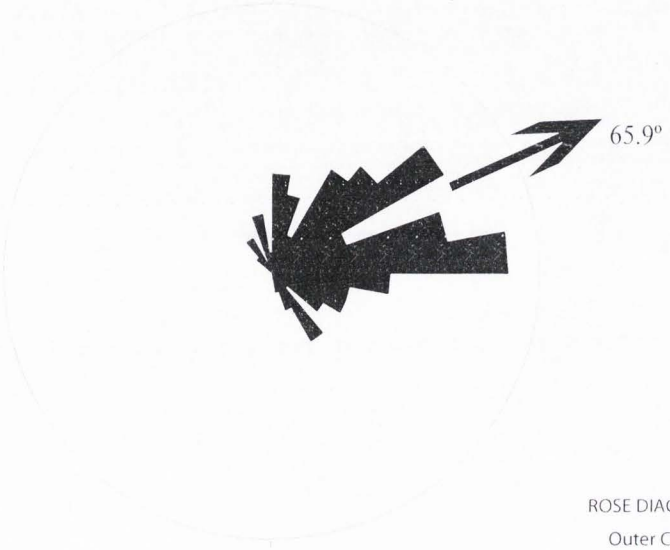

Figure 2-33. Combined paleocurrents for the Ocotillo and Brawley formations. Mean direction = 65.9°

CHAPTER 3

MIDDLE PLEISTOCENE TO RECENT STRUCTURAL EVOLUTION OF THE SAN JACINTO FAULT ZONE IN THE SAN FELIPE HILLS AREA, CALIFORNIA[2]

Abstract

The current transform plate boundary within southern California is a broad zone of northwest-striking dextral faults. Total plate motion across the plate boundary is broadly distributed east to west at the latitude of the Salton Sea, with much of the slip localized along strands of the San Jacinto fault zone. Previous geologic mapping, microseismicity, seismic reflection, gravity, magnetic, and trilateration data all show significant changes in the characteristics of the San Jacinto fault zone along strike in the western Salton Trough. Interactions among the active strands of the southern San Jacinto fault zone and in particular between the Clark fault and other strands, the complex deformation within the San Felipe Hills and the importance of sinistral faulting to the south have been poorly constrained by previous studies. The rocks in the San Felipe Hills record the evolution of the San Jacinto fault zone at the latitude of the southern Salton Sea.

In the western Salton Trough right-lateral separation along the Clark fault and the Santa Rosa fault is 15 km based on an offset of the Cretaceous Eastern Peninsular Ranges

---

[2] Coauthored by Stefan M. Kirby, Susanne U. Janecke, Victoria E. Langenheim, Rebecca J. Dorsey, and Bernard Housen.

mylonite zone [*Sharp*, 1967], yet a fault tip was identified just a few kilometers southeast of the offset mylonite. To the southeast in the San Felipe Hills, Plio-Quaternary sediments are strongly deformed by a complex series of folds and faults south-east of the previously mapped termination of the surface trace of the Clark fault. New data suggest that the Clark fault probably persists into the central San Felipe Hills as an incompletely mapped horsetail fan and en echelon fault zone, and the San Jacinto fault zone recently began to accommodate strain in a broad rotational zone southeast of the San Felipe Hills.

Based on structural analysis, folds in the San Felipe Hills were divided into domains with similar geometries. Two transects through relevant fold domains were used to calculate the total shortening and amount of equivalent dextral slip on the Clark fault plane oriented 305° NW required to produce this amount of shortening. Total equivalent slip on the Clark fault plane is 5.62 km based on analysis of an eastern transect, and represents roughly a third of the right separation documented to the northwest. Folding along this transect may have begun no earlier than the end of deposition of the internally conformable Brawley Formation in the southeastern San Felipe Hills at 0.61 Ma $\pm$ 0.02 Ma to 0.52 Ma $\pm$ 0.03 Ma. Our analysis based on the spatial extent, amount of shortening from folding and the time constraints give slip rates on the Clark fault ranging from 9.5 $\pm$ 0.3 mm/year to 10.8 $\pm$ 0.7 mm/year. This suggests a significant component of plate boundary motion at this latitude has been localized on the Clark strand of the San Jacinto fault zone since at least 0.5 Ma.

The southeast San Felipe Hills preserve the most intensely folded sedimentary rocks in the area, and is interpreted as the boundary zone between the domain of dextral slip and wrench folding to the northwest and a broad domain of clockwise block rotation

to the southeast. The rotating domain transfers slip from the Coyote Creek and Superstition strands to the Imperial and Brawley zones in the east and southeast [*Hudnut et al.*, 1989; *Seeber and Armbruster*, 1999], our work shows that it also captures slip from the Clark strand.

Introduction

Tectonic Background

The current transform plate boundary within southern California is a broad zone of major northwest-striking dextral fault systems, including the San Andreas, Elsinore, and San Jacinto fault systems [*Atwater*, 1989]. Total plate motion across the plate boundary is broadly distributed east to west at the latitude of the Salton Sea, with much of the slip localized along the strands of the San Jacinto fault zone to the southwest and the San Andreas fault to the northeast [*Atwater*, 1989; *Rockwell et al.*, 1990] (Figures 3-1, 3-2). Southward the San Andreas fault steps right to the Imperial fault across the north-northwest trending Brawley Zone which interact with the San Jacinto fault zone further to the west via a series of northeast-striking left lateral faults [*Nicholson et al.*, 1986; *Hudnut et al.*, 1989; *Frost et al.*, 1996; *Magistrale*, 2002] (Figures. 3-1, 3-2). The southern San Jacinto fault zone may be slipping at rates that equal or exceed the southern San Andreas fault at this latitude but this interpretation is controversial [*Kendrick et al.*, 1994; *Meade and Hager 2005*]. Despite the relative importance of the San Jacinto fault zone to total plate boundary motion at the latitude of the western Salton Trough, the geometries and kinematics of this fault zone are incompletely known.

The southeastern San Jacinto fault zone in the western Salton Trough is characterized by several short, divergent fault strands which accommodate dextral strike-slip. These include the Buck Ridge fault, the Clark fault and the Coyote Creek fault in the northwest and the Superstition Mountain and Superstition Hills faults to the southeast [*Dibblee*, 1954, 1984a, 1984b; *Sharp*, 1967, 1981] (Figure 3-2). Slip rates and fault geometries of strands of the southern San Jacinto probably evolved through time within the western Salton Trough but the specifics of the possible changes are uncertain [*Bartholomew*, 1970; *Pettinga*, 1991; *Dorsey*, 2002; *Janecke et al.*, 2004; *Kirby et al.*, 2004; *Lutz*, 2005].

Lying along strike of the San Jacinto fault zone in the western Salton Trough, are spatially extensive exposures of folded and faulted late Miocene to Pleistocene sedimentary rocks in the San Felipe Hills [*Dibblee*, 1954, 1984a; *Dronyk*, 1977; *Reitz*, 1977; *Feragen*, 1986; *Wells*, 1987; *Heitman*, 2002; *Lilly*, 2003]. The structures within the San Felipe Hills should show the nature and extent of the interaction between strands of the San Jacinto fault zone at this latitude. However, the geometric and kinematic details of the faults which drive deformation in the San Felipe Hills and the relation to the San Jacinto fault zone to the northwest and southeast are poorly known (for example compare) [*Dibblee*, 1954, 1984a; *Dronyk*, 1977; *Reitz*, 1977; *Feragan*, 1986; *Wells*, 1987; *Heitman*, 2002; *Lilly*, 2003]. This study provides new structural and geophysical data about the San Jacinto fault zone and clarifies the complex geometry of the San Jacinto fault zone in the western Salton Trough.

Early strike-slip motion at the latitude of the Salton Trough was localized on the southern San Andreas fault, which appears to have been actively accommodating dextral

slip in the Salton Trough starting after localization of the North American/ Pacific Plate boundary in the Gulf of California at ~6.3 Ma [*Atwater*, 1970; *Oskin and Stock*, 2003]. During this time structures in the western Salton Trough accommodated regional oblique extension across the West Salton detachment fault [*Frost et al.*, 1996; *Axen and Fletcher*, 1998; *Steely et al.*, 2004] (Figures 3-1, 3-2). Strike-slip on strands of the San Jacinto fault zone began much later [*Meisling and Weldon*, 1989; *Morton and Matti*, 1993; *Weldon et al.*, 1993] and evolved over time [*Janecke et al.*, 2004; *Kirby et al.*, 2004]. To the north, near its intersection with the San Andreas fault, slip on the San Jacinto fault began after 1.5 Ma perhaps as recently as 1.2 Ma [*Morton and Matti*, 1993]. A separate analysis assuming constant slip rates of 10 mm/yr across the entire fault zone points to a 2.5 Ma inception of the San Jacinto fault zone [*Morton and Matti*, 1993]. Data presented here provides important geometric and time constraints on the development of the San Jacinto fault zone at this latitude and revise long-term geologic slip rates.

Structural Background

The current configuration and interrelation of the strands of the southern San Jacinto fault zone has been the focus of much research [*Sharp*, 1967, 1972, 1975; *Nicholson et al.*, 1986; *Rockwell et al.*, 1990; *Petersen et al.*, 1991; *Seeber and Armbruster*, 1999; *Dorsey*, 2002; *Hudnut et al.*, 1989; *Anderson et al.*, 2003]. Previous geologic mapping, and geophysical data sets all show changes in the geometry and kinematics of the San Jacinto fault zone along strike in the southwestern Salton Trough [*Dibblee*, 1954, 1984a; *Sharp*, 1967, 1981; *Bartholomew*, 1970; *Nicholson et al.*, 1986; *Severson*, 1987; *Seeber and Armbruster*, 1989; *Hudnut et al.*, 1989, *Pettinga*, 1991; *Magistrale*, 2002; *Anderson et al.*, 2003].

Early work on the San Jacinto fault zone in the western Salton Trough was completed by *Dibblee* [1954, 1984a] and *Sharp* [1967, 1981]. Both of these workers mapped the San Jacinto fault zone as a series of southeastward-divergent discontinuous fault strands as it enters the western Salton Trough from the northwest [*Dibblee*, 1954, 1984a; *Sharp*, 1967, 1975, 1981] (Figure 3-2). Changes in fault zone geometry are most pronounced as the strands of the southern San Jacinto splay southeast-ward into the western Salton Trough and distribute slip among several active faults [*Dibblee*, 1954, 1984a; *Sharp*, 1967, 1981] (Figures 3-1, 3-2). Most of the dextral slip accommodated by the San Jacinto fault zone within the Salton Trough was assumed to be carried on the Coyote Creek, Superstition Mountain, and Superstition Hills faults [*Dibblee*, 1954,1984a; *Sharp*, 1967] (Figure 3-2). Other major strands which enter the Salton Trough from the northwest include the Buck Ridge fault and the Clark fault [*Dibblee*, 1954, 1984a; *Sharp*, 1975]. Offset across the Buck Ridge fault and its kinematic relations to the San Jacinto fault zone are incompletely understood [*Sharp*, 1967]. The Clark strand, which may be the dominant structure of the San Jacinto fault zone farther to the northwest in the Peninsular Range, was not considered to be the dominant fault strand in the Salton Trough and was thought to terminate south of the Santa Rosa Mountains some 10 km northwest of the San Felipe Hills (Figure 3-2) [*Dibblee*, 1954, 1984a; *Sharp*, 1967, 1972, 1975, 1981; *Bartholomew*, 1970; *Pettinga*, 1991].

Total right-lateral slip across the San Jacinto fault zone northwest of the Salton Trough in the Eastern Peninsular Range is up to 24 km [*Sharp*, 1967; *Bartholomew*, 1970; *Matti and Morton*, 1991]. To the southeast in the Salton Trough, the Coyote Creek strand near Coyote Mountain was thought to have up to 6 km of right lateral offset

[*Sharp*, 1967; *Dorsey*, 2002], but newer work suggests offset of about 4 km [*Janecke et al.*, 2005]. To the northeast, the Clark fault has at least 15 km of right separation on the basis of offset east-dipping Cretaceous mylonite zone [*Sharp*, 1967; *Bartholomew*, 1970] (Figure 3-2). A significant component of southwest-side-down slip across the Clark or Santa Rosa faults in Clark Valley would reduce the actual strike-slip component of slip but there are few data to assess these dip slip components. Early work by *Bartholomew* [1970] postulated that much of the separation apparent on the Clark fault southeast of Coyote Mountain (Figure 3-6) could be the result of a connection between the NW Clark fault and SE Coyote Creek fault along the north-striking East Coyote Mountain fault.. New data which shows similar ~ 4 km offset along the NW and central Coyote Creek fault may preclude this possibility [*Janecke et al.*, 2005]. Later work has not focused on Bartholomew's hypothesis; although several other stepover models have been proposed for the Clark and Coyote Creek faults [*Janecke et al.*, 2003]. Timing of initiation of the Clark fault is also poorly known but critical to understanding the evolution of the San Jacinto fault zone.

South and southeast along strike of the San Jacinto fault zone significant changes in kinematics and structural geometries occur [*Hudnut et al.*, 1989]. Several fault strands including the dextral northwest striking Superstition Hills and Superstition Mountain faults which may bound the southwest edge of a zone of clockwise block rotation southeast of the San Felipe Hills. These rotating blocks are bounded by the Superstition Hills and Superstition Mountain faults to the southwest, and by northeast-striking sinistral faults such as the Elmore Ranch and Extra faults on the northwest and by the north-northeast-striking Brawley Seismic zone on the east-northeast [*Hudnut et al.*, 1989;

Seeber and Armbruster, 1999; *Magistrale*, 2002] (Figures 3-1, 3-2). Block rotation appears to accommodate dextral slip across the southwestern Salton Trough southwest of the termination of the San Andreas fault and northwest of the termination of the Imperial fault [*Seeber and Armbruster*, 1999]. Duration, magnitude, and timing of initiation of block rotation, however, is poorly constrained [*Hudnut et al.*, 1989; *Seeber and Armbruster*, 1999].

The northwestern boundary of block rotation is inconsistently located in different studies, but is assumed to be located approximately in the central San Felipe Hills, and extending southwest from the southern tip of the San Andreas fault to the Coyote Creek fault in the southwest [*Hudnut et al.*, 1989; *Seeber and Armbruster*, 1999]. None of the kinematic models for this latitude of the San Jacinto fault zone adequately explain the complex deformation in the San Felipe Hills, and or interpret the relationship of the Clark fault with the province of block rotation further to the southeast.

Southeast of the previously mapped termination of the Clark fault in the San Felipe Hills, numerous workers have shown extensive folding and faulting of the latest Miocene to Pleistocene stratigraphy over a ~ 550 km^2 area [*Dibblee*, 1954, 1984a; *Morley*, 1963; *Dronyk*, 1977; *Reitz*, 1977; *Wagoner*, 1977; *Feragen*, 1986; *Wells*, 1987; *Heitman*, 2002; *Lilly*, 2003; *Janecke et al.*, 2003; *Kirby et al.*, 2004] (Figures. 3-2, 3-3, 3-4). Exposures of deformed late Miocene to Pleistocene stratigraphy stretch from the Salton Sea in the east to Borrego Mountain in the west, and from California State Highway 78 in the south to the Truckhaven Road in the North. Prior to this study only the work by *Dibblee* [1954, 1984a] covered this entire area. All other previous work was

limited to smaller portions of the San Felipe Hills area [*Morley*, 1963; *Dronyk*, 1977; *Reitz*, 1977; *Wagoner*, 1977; *Wells*, 1986; *Feragen*, 1987; *Heitman*, 2002; *Lilly*, 2003].

The east-plunging San Felipe anticline forms the backbone of the San Felipe Hills and exposes Cretaceous age foliated plutonic rocks and some older metasedimentary rocks and late Miocene to early Pliocene marine Imperial Group at its core [*Dibblee*, 1954, 1984a; *Morley*, 1963; *Reitz*, 1977] (Figures 3-3, 3-4). Entering the San Felipe Hills from the north is the south to southeast-plunging Santa Rosa anticline [*Dibblee*, 1954, 1984a] (Figures 3-3, 3-4). Superposed upon these two large folds are many smaller, dominately east-plunging folds, with wavelengths between 1-2 km and hundreds of meters [*Dibblee*, 1954, 1984a; *Morley*, 1963; *Reitz*, 1977; *Wells*, 1986; *Feragen*, 1987; *Heitman*, 2002; *Lilly*, 2003]. Major northwest-striking dextral faults mapped by previous workers in the San Felipe Hills include the San Felipe Hills and Powerline faults, but many smaller faults have also been mapped [*Dibblee*, 1954, 1984a; *Morley*, 1963; *Reitz*, 1977; *Wells*, 1986; *Feragen*, 1987; *Heitman*, 2002; *Lilly*, 2003]. None of the previously mapped faults are continuous across the San Felipe Hills and no prior mapping has found strands of the Clark fault southeast of its mapped termination near the Truckhaven road [*Sharp*, 1972, 1975; *Bartholomew*, 1970; *Pettinga*, 1991] in the San Felipe Hills.

Explanations for the faulting and folding within the San Felipe Hills have varied and none of the previous interpretations have accounted for the kinematics of the San Jacinto fault zone to the northwest and southeast of the study area. It has been inferred that the deformation within the San Felipe Hills is the result of the dextral slip on the Clark fault, either as a blind structure at depth [*Feragen*, 1986; *Wells*, 1987] or a series of contractional stepovers which transfers slip across discontinuous faults within [*Heitman*,

2002; *Lilly*, 2003], across the San Felipe Hills [*Janecke et al.*, 2003], or around the San Felipe Hills [*Bartholomew*, 1970].

Objective

We examine the kinematics and lateral continuity of the San Jacinto fault zone using data from structures and synkinematic deposits within the San Felipe Hills. To constrain the geometry and interactions of the fault strands of the southern San Jacinto fault zone, three prior models for the geometry of the Clark fault in the San Felipe Hills and its relation to the block rotation to the south are tested. These hypotheses are presented below:

1) the Clark fault continues as a blind structure in the crystalline basement beneath the San Felipe Hills, connects at depth with the Superstition Hills fault to the south, and produces the folding deformation in sedimentary rocks the Felipe Hills above a blind portion of the fault [*Wells*, 1986; *Feragen*, 1987] (Figure 3-5).
2) the Clark Fault terminates in the folds and faults near Seventeen Palms and does not transfer slip to the Brawley seismic zone or the southern strands of the San Jacinto fault zone, including the Superstition Hills, Superstition Mountain, and Imperial faults [*Dibblee*, 1954, 1984a; *Pettinga*, 1991] (Figure 3-5).
3) the Clark fault steps 24 km to the left through the folds of the San Felipe Hills to a blind right lateral fault along the south-east margin of the Salton Sea. This

blind fault connects directly southeastward to the Imperial fault [*Janecke et al.*, 2003] (Figure 3-5).

For each kinematic model the structural relationships to the southeast are assumed to follow those described by *Hudnut et al.* [1989] and *Seeber and Armbruster* [1999]. We therefore modified each original model to include the sinistral Extra fault zone and the dextral Superstition Hills fault. Each kinematic and geometric model predicts unique structural and geophysical features in the San Felipe Hills (Figure 3-5). The actual distribution, geometry, and magnitudes of strains, and geophysical characteristics of the San Felipe Hills will be compared with those predicted by each model.

A blind connection between the Clark fault and the Superstition Hills fault to the southeast (model 1) was suggested first by *Wells* [1986] and later by *Feragen* [1987] as the primary cause of deformation within the southeastern San Felipe Hills (Figure 3-5). This model proposes that the Clark fault continues along strike to the southeast of its previously mapped termination (Figure 3-5). A zone of deformation is centered above the blind trace of the Clark fault with folding oriented oblique, roughly east west trending, to the trace of the fault (Figure 3-5). The model also implies that cross faults, like the sinistral Extra fault zone, must terminate at the blind trace of the Clark fault. The intersection zone of these faults would have more deformation (Figure 3-5).

Model 2 hypothesizes that the Clark fault does terminate at its previously mapped position, with fault-tip related deformation reaching into the San Felipe Hills [*Dibblee*, 1954, 1984a; *Sharp*, 1967; *Pettinga*, 1991] (Figure 3-5). In this model no slip is transferred to another major fault from the Clark fault. The most intense deformation should be localized very near the surficial termination of the Clark fault in the northwest

San Felipe Hills with deformation decreasing outward (Figure 3-5). Fold hinges generally trend east-west to the south and south-west of the termination and converge on the fault tip (Figure 3-5).

Model 3 proposes that the Clark fault steps over through east-west folding to a blind northwest trending dextral fault along the southwestern margin of the Salton Sea [*Janecke et al.*, 2003] (Figure 3-5). This blind structure would directly transfer slip to the Imperial fault which lies roughly along strike to the southeast. Deformation in this model would be most intense in the stepover zone and be characterized by east-west trending folds. Additional intense deformation is predicted as this blind structure interacts with and crosses several northeast trending structures at depth including the Extra fault zone and the Elmore Ranch fault (Figure 3-5).

In addition to these models one other potential geometry must be considered. This model proposes that in the past the Clark fault transferred slip via a right bend southwest of Clark Lake Valley onto the main part of the Coyote Creek fault southeast of Coyote Mountain [*Bartholomew*, 1970] (Figure 3-6). The Clark fault south of the Santa Rosa Mountains would therefore have formed later and have accumulated relatively little slip [*Bartholomew*, 1970]. In this model little or none of the 15 km of right separation on the mylonite is related to dextral slip across the Clark fault southeast of Coyote Mountain [*Bartholomew*, 1970]. This implies that the deformation in the San Felipe Hills could be unrelated to slip on the Clark fault because much of the slip across the Clark fault to the northwest may have bypassed the San Felipe Hills early in the history of the San Jacinto fault zone. The southeast-most portion of the Clark strand terminates at the surface northwest of the study area according to all prior mappers [*Bartholomew*, 1970;

Sharp, 1972; *Pettinga*, 1991] (Figure 3-6). Further structural mapping and analysis to the northwest of the San Felipe Hills are necessary to prove or disprove this fault geometry.

Methods

To assess the southeastern strands of the San Jacinto fault zone and their relations within the San Felipe Hills, new 1:48,000 scale geologic mapping, structural, and stratigraphic field studies were conducted in approximately 2.5 quadrangles in the San Felipe Hills including the Shell Reef, Kane Springs NW, and portions of Kane Springs NE, Truckhaven, and Seventeen Palms 7.5 minute quadrangles. This mapping was combined with previous 1:6,000 scale mapping in the south central San Felipe Hills [*Heitman*, 2002; *Lilly*, 2003] to produce a geologic map of the study area (Figures 3-3, 3-4; Plate 1). The map was refined using aerial photography, Landsat, and SPOT imagery courtesy of Robert Crippen and Ronald Blom (Plate 3). Five structural cross sections show structural features of the San Felipe Hills.

Folds were a particular focus of this study. Fold geometries vary across the San Felipe Hills, and folds with similar trends were grouped into distinct fold domains for geometric analysis. For each fold domain strike and dip data were plotted as poles to bedding and contoured using the Kamb method at a significance level of 1 sigma and a contour interval of 4.0 using Richard Almendinger's Stereonet for Windows 1.1 software. Best fit fold limbs were picked using the Kamb contour for each fold limb in each domain. These average folds were used to measure interlimb angles, vergence, trend, and plunge in each of the fold domains. Strain values were computed from interlimb angles. Strain rates were computed using the magnetostratigraphically determined age of

the youngest conformable strata (0.61 Ma ± 0.02 Ma and 0.52 Ma ± 0.03 Ma) deformed by the folds [*Kirby et al.*, 2004; *Chapter 2*].

Folds appear to terminate laterally at dextral faults in many parts of the San Felipe Hills (Figure 3-3, Plate 1). Thus analysis of the folds allows fault slip to be estimated. In order to characterize the total shortening and slip which the Clark strand could have produced in the study area, two transects through contiguous fold domains were analyzed. These transects cover the portion of the study area most likely affected by slip on the Clark fault and to avoid some of the larger faults in the area. Total shortening within each domain was computed from the strain and spatial extent parallel to the transects. Shortening was then resolved onto a vertical plane striking 305°, parallel to the Clark fault immediately to the northwest [*Sharp*, 1967; *Bartholomew*, 1970]. This calculation was used to estimate the amount of strike-slip offset which is required to produce the folds in the San Felipe Hills. *Feragen* [1986] first made such a calculation and extrapolated local shortening amounts from the south central San Felipe Hills across the entire San Felipe Hills. His estimate of 9 km of strike-slip [*Feragen*, 1986] is too large because folding strains in the southeast San Felipe Hills exceed those in the remainder of the study area [*this study*].

Geophysical data sets including isostatic gravity and filtered aeromagnetic anomalies were analyzed for this study and areas north and south along strike of the San Jacinto fault zone. Gravity data are from *Langenheim and Jachens* [1993] and *Langenheim* [unpublished data, 2004]. Aeromagnetic data [*U.S. Geological Survey*, 1990] were decorrugated and filtered to enhance shallow (< 1 km) magnetic sources [*Langenheim*, unpublished data, 2004]. Geophysical data sets were used to validate field

mapping and regional structural interpretations. Comparisons of isostatic gravity and magnetic anomaly maps and the geologic map provided critical information about subsurface relationships.

The three prior models for the deformation in the San Felipe Hills are compared to the geologic map, structural, and geophysical data (Figure 3-5). A new model is developed below, to better explain the diverse data sets.

Results

Overview

Structural studies in the San Felipe Hills show complex folding and faulting of the latest Miocene to Pleistocene sedimentary rocks (Figure 3-3; Plates 1, 3). The deformation is dominated by east-west tending folds but the spacing and geometry of the folds varies across the study area (Figures 3-3, 3-7; Plates 1, 3). Several faults are also apparent. Dextral faults are most common in the central and western parts of the area, whereas sinistral and normal faults are concentrated in the east and southeast San Felipe Hills. East-west striking strike-slip faults are most common in the west, east of major dextral faults. Most of the faults in the San Felipe Hills are discontinuous and less than several kilometers long.

Faults

NW striking strike-slip faults

Several large right-lateral northwest-trending strike-slip faults deform rocks in the San Felipe Hills. These include the Coyote Creek fault, the San Felipe Hills fault and the Powerline fault [*Dibblee*, 1954, 1984a; *Morley*, 1963; *Reitz*, 1977; *Heitman*, 2002; *Lilly*,

2003; *this study*]. The Coyote Creek fault is the largest fault and it passes through the extreme southwestern corner of the study area. Slip across this fault near the study area is the subject on current research and appears to be between 1 and 4 km [*Janecke et al.*, 2005*; Langenheim and Steely,* unpublished data, 2005].). The Coyote Creek fault is not is apparent as a gravity lineament in the southwestern San Felipe Hills (Figures 3-8). However, portions of this fault correspond with a strong magnetic gradient that separates less magnetic rocks to the southwest from more magnetic rocks to the northeast in the western San Felipe Hills (Figures 3-10, 3-11). The source of this large difference in magnetization is uncertain.

Both the San Felipe Hills fault and the Powerline fault are spatially limited to the San Felipe Hills [*Dibblee*, 1954, 1984a; *Reitz*, 1977; *Heitman*, 2002; *Lilly*, 2003] (Figure 3-3). The San Felipe Hills fault extends at least 8 km along a strike of approximately 310° in the western San Felipe Hills (Figure 3-3). Photogeologic studies suggest that this fault may terminate to the northwest just north of the study area in a bedding–strike parallel structure and to the southeast near the axis of the San Felipe anticline [*Dibblee*, 1984a; *Heitman*, 2002]. Dextral offset across this nearly vertical structure is unconstrained but must be small (< 2-3 km) because the fault does not offset the gravity gradient of the north limb of the San Felipe anticline (Figure 3-9). The San Felipe Hills fault corresponds well with a magnetic lineament and separates magnetic rocks to the northeast from less magnetic rocks to the southwest (Figures 3-10, 3-11). The isostatic gravity map shows slight evidence for the San Felipe Hills fault (Figures 3-8, 3-9).

The Powerline fault is located in the southern central San Felipe Hills extending some 10 km along an approximate strike of 318° NW (Figure 3-17). This fault is a single

covered strand in the south central San Felipe Hills. To the north the fault splays into at least three strands (Figure 3-3; Plate 1). These northern strands of the Powerline fault strike north-northwest and dip steeply east and west. Slickenlines indicate right-lateral motion and rake 3-5° from horizontal. Offset across the Powerline fault is unconstrained but could be up to 1-2 km. The fault correlates with a strong magnetic gradient between magnetic rocks on the southwest and much less magnetic rocks on the northeast side (Figures 3-10, 3-11). The isostatic gravity map shows a small increase in the depth of basement northeast of the Powerline fault (Figures 3-8, 3-9). The Powerline fault or the Sand Dunes fault, 4 km to the northeast, bound the east end of the bedrock high beneath the San Felipe anticline (Figure 3-9).

Many smaller dextral northwest striking faults exist within the San Felipe Hills (Figure 3-3). Dips of these smaller faults range from northeast to southwest within 30° of vertical. Rakes of slickenlines, where apparent, are within 10° of horizontal. Right-lateral motion is apparent where kinematic indicators exist.

NE striking strike-slip faults

Northeast striking sinistral faults also deform the San Felipe Hills. The Extra fault zone in the southeastern San Felipe Hills is the only laterally continuous sinistral fault (Figures 3-3, 3-12; Plates 1 and 3). The overall strike of the Extra fault zone is north 35° east, but it changes strike south of Highway 78 to north 45° east. The Extra fault zone is characterized by several discontinuous northeast-striking en echelon fault strands and adjacent small, less than 1 km long, doubly plunging anticlines and synclines near and north of state highway 78. At least one down to the west, north-striking normal fault exists within the fault zone. This fault had a strike of north 14° east and a dip of 71°

west. Lineations indicate dip slip motion. Normal separation on this fault may be 120 m based on stratigraphic correlations in Oil Well Wash [*Chapter 2*]. Farther northeast the Extra fault zone is characterized by a single fault strand striking north 25° east and dipping 82° west where it crosses state highway 86. Tool marks indicate left-lateral motion on this strand. The Extra fault zone persists along strike to the northeast to the shore of the Salton Sea and southwest to San Felipe Wash as a series of discontinuous photo lineaments and fault scarps in alluvial and eolian deposits. Total left-lateral offset across the Extra fault zone is unconstrained.

Northeast-striking magnetic and gravity gradients coincide with the surface trace of the Extra fault zone near state highway 86. Further to the southwest there is a 1-2 km offset between the surface trace and gravity and magnetic signals (Figures 3-9 to 3-11). Magnetic data shows a possible weak northeast trending gradient 2 km northwest of the Extra fault in an area of much eolian, lacustrine, and alluvial cover (Figures 3-10, 3-11). This area is the northwest-most position of a possible laterally continuous northeast-striking fault, but to date no such fault has been identified northwest of the Extra fault zone.

In general, northeast-striking sinistral faults in the San Felipe Hills are much more localized than dextral faults and may simply be cross faults between more laterally continuous northwest striking dextral faults. This is apparent between the Powerline and Sand Dunes faults where several northeast striking structures extend between these two larger faults [*Reitz*, 1977; *Heitman*, 2002; *Lilly*, 2003] (Figure 3-3). Slickenlines on a small exposure of the northwest-most of these sinistral faults indicate left lateral motion on a vertical fault plane striking 32°east of north. Other similar northeast-striking faults

exist along the eastern branch of Tarantula Wash in the central San Felipe Hills [*Reitz*, 1977; *Heitman*, 2002; *Lilly*, 2003] (Figure 3-3). These faults generally strike between and 18 and 64° east of north and dip steeply to the northwest and southeast within 25° of vertical. Kinematic indicators in a small number of exposures suggested left-lateral motion. The isostatic gravity may show a weak lineament corresponding with the northwest-most northeast striking fault between the Powerline and Sand Dunes faults (Figure 3-9). Otherwise these faults do not appear to have discernable magnetic or gravity signals (Figures 3-8, 3-9, 3-10, 3-11). In the northwestern San Felipe Hills at least one northeast striking left-lateral fault can be traced along strike to the southwest as it bends into an east-west orientation (Figure 3-3; Plates 1 and 3).

North-south striking normal faults

North-south striking normal faults are apparent in the northern, central, and eastern portions of the study area. Near the northern boundary of the mapped area several down-to-the-east fault scarps cut an elevated alluvial terrace west of Salton City and north of the Truckhaven road (Figure 3-3; Plate 1). Scarp height is between 1 and 2 meters. South-facing cross sectional views of these faults on the terrace margin north of the Truckhaven road expose small synclines in the hanging-wall of these faults. Normal faults to the south of the terraces along Arroyo Salada strike between 334 and 28° and dip between 66 and 79° east. Dip slip is apparent from lineations. Offset across each of these normal faults could be at least several meters based on stratigraphic correlations. Weak north-south magnetic anomalies south of Arroyo Salada may correlate with several of these faults (Figure 3-11). No gravity signal is apparent from these faults (Figures 3-8, 3-9).

To the south, north-northwest striking normal faults likely separate highly folded rocks on the east from less folded strata on the west side of the faults (Figures 3-3, 3-13; Plate 1). No exposures with good fault planes and slickenlines have been found for these faults which strike parallel to bedding on the west side of each fault. It is assumed that these faults strike parallel to the unfolded strata which they bound and dip east. Offset on these structures is unconstrained.

In the eastern San Felipe Hills north-south striking faults are present in a zone of north-south trending folds (Figure 3-3; Plates 1 and 3). These normal faults appear to be parallel to the dominant fold trend and in places truncate these folds (Figures 3-3; Plates 1 and 3). No measurable exposures of these faults were found during this study. Previous work by *Dronyk* [1977] documented small offset normal faults striking nearly north-south and dipping both east and west in this area.

East-west striking strike-slip faults

East-west striking steeply dipping faults are fairly common in the western San Felipe Hills, and south of Squaw Peak to the Ocotillo Badlands (Figure 3-3; Plate 1). These faults strike within 10 degrees of east. Slip sense of the faults south of Squaw Peak is assumed to be left lateral based on partly ambiguous kinematic indicators. Cross sections through these structures show at least a component of reverse motion, north side up, on these structures (Figures 3-14, 3-15). Dip directions vary over short lateral distances but faults are generally steep, within 20° of vertical. Dip of these faults was rarely measurable..

There are also several east-west striking strike-slip faults within the San Felipe Hills. In the northwestern portion of the study area at least one east-west striking fault is

continuous with a left lateral north-east striking strike-slip faults along strike to the east (Figure 3-3). Slickenlines and tool marks indicate left-lateral motion for these structures. Separations across these faults are uncertain because the faults commonly strike parallel to bedding.

East-west striking strike-slip faults are most common immediately east of major northwest striking dextral faults, including the San Felipe Hills fault and the Coyote Creek fault. They appear to extend 3-6 km east before losing definition (Figure 3-3; Plate 1). *Sharp* [1967] previously documented similar relationships east of the Coyote Creek fault in the southwestern-most part of the study area. East-west striking faults cut the anticline in the Ocotillo badlands but are incompletely mapped [*this study*].

Sand Dunes fault

In the south-central and central San Felipe Hills the mostly north-west striking Sand Dunes fault juxtaposes Diablo Formation on the southwest against the Borrego Formation and transitional unit to the northeast [*Heitman*, 2002; *Lilly*, 2003] (Figures 3-3, 3-12; Plate 1). It has a buried east-striking trace east of the southeast tip of the Powerline fault. The fault then turns north and north-northwest in an arcuate fault trace which juxtaposes older Diablo Formation on the southwest side against younger Borrego Formation on the northeast side (Figures 3-3, 3-12). Map relations imply at least partially reverse motion for this structure. Smaller left lateral northeast striking faults cut the Sand Dunes fault. The Sand Dunes fault dips steeply and is nearly vertical where observable [*Heitman*, 2002; *Lilly*, 2003]. Offset across this structure is unconstrained but may be large because it juxtaposes dissimilar rock units in most places. To the northwest the Sand Dunes fault may continue and join a large en echelon network of faults in a

complex zone of rotated blocks south of Tule Wash. Additional mapping is needed in this complex fault zone (Figure 3-3). The Sand Dunes fault correlates well with a magnetic gradient which nearly parallels its mapped position (Figures 3-10, 3-11). The San Felipe anticline loses its gravity expression east of the trace of this fault, and changes eastward from a bedrock-cored anticline to a subhorizontal undulating bedrock surface (Figures 3-8, 3-9).

En echelon strike-slip fault zone

Several previously unmapped strike-slip faults form a zone of discontinuous en echelon northwest trending strike-slip faults in the north central portion of study area (Figure 3-3). The Powerline and Sand Dunes faults are probably part of this set of faults and form the southwest margin of this fault network. This fault zone extends to the north-northwest from the Sand Dunes fault. Some faults converge northwest-ward, and the fault zone coincides with a broad, concave to the southwest, magnetic low (Figures 3-3, 3-10, 3-11). Smaller northwest-trending magnetic gradients within the 4 km wide magnetic low coincide with individual faults (Figure 3-11). These faults vary in length from 1 km to 4 km along strike and some clearly die out into east-west trending fold trains. Where fault dip is apparent it is steep between 80 and 90° for these structures. The strike of the fault strands ranges from 298 degrees to 329°. Cross section C-C' shows several of these faults which may merge at depth into a single fault (Figure 3-16). Slickenlines are uncommon but where exposed gave right-lateral motion for one of the strands and rake 7°. Spacing of these fault strands varies from 1 to 3 km perpendicular to strike. Offset is unconstrained, but we estimate that any one strand may have less than 1 km of separation. The en echelon faults are in a weak gravity low that lines up with a

prominent gravity gradient that coincides with the Clark fault to the northwest (Figures 3-8, 3-9). Immediately to the south and southeast of these faults is the east-west trending folds of fold domain K, which has the most shortening in the study area (Figure 3-7; Table 3-1). This en echelon fault zone is incompletely mapped and further field studies may show greater lateral continuity and may reveal additional faults.

Dump fault

Just north of these discontinuous en echelon strands, in the northern portion of the study area, a west-northwest striking strike-slip fault was mapped. This fault is apparent on theLandsat+Spot imagery (Plate 3). This structure is assumed to be steeply dipping and right lateral based on map relations (Figure 3-3). A west-north-west trending magnetic gradient is 1 km southwest of this structure (Figure 3-11). The strike of this fault is approximately 290°along its 6 km extent. The Dump fault defines the northeast margin of the en echelon fault array. This structure may terminate to the east and can be traced out of the study area to the west-northwest as it projects toward the southeast tip of the Clark fault.

Fault interrelations

The northwest-striking dextral faults are the largest and most continuous, cut or bound many fault blocks that also contain northeast, east-west, and north-south striking faults (Figure 3-3; Plate 1). Locally northeast-striking sinistral faults cut the northwest-striking faults including the Sand Dunes fault [*Heitman*, 2002; *Lilly*, 2003] (Figure 3-3; Plate 1). East-west-striking faults are localized primarily to the east of the major northwest striking faults such as the Coyote Creek fault and the San Felipe Hills fault

(Figure 3-3; Plate 1). The zone of en echelon dextral faults in the northern and central San Felipe Hills has a southeast-ward horsetail splaying geometry which is bounded on the northeast by the Dump fault. Along strike to the south and southeast the en echelon faults are replaced by folds and the Powerline and Sand Dunes faults which persist into the southern San Felipe Hills (Figure 3-3; Plate 1). None of the northwest striking faults except the Coyote Creek fault continue southeast of the Extra fault zone. We agree with prior mappers that the Extra fault zone is a regionally important northeast strike-slip fault zone [*Dibblee*, 1954, 1984a; *Hudnut et al.*, 1989] (Figure 3-3).

The interrelation between faults and folds within the San Felipe Hills is complex and variable. North-south striking normal faults in the northern and central San Felipe Hills separate strongly folded strata from less folded strata but not cut the folds. Elsewhere dextral faults die out into east-west-trending fold trains. Overall there is a strong interconnection between faults and folds within most of the San Felipe Hills (Figure 3-3).

Folds

Overview

Most of the exposed sedimentary section is folded in the San Felipe Hills. Folds range from open to gentle with wavelengths of 100's of m to 10's of km. Folds were grouped into domains based on the style and orientation of the folds (Figures 3-7, 3-18). Orientation of fold axes vary across the San Felipe Hills (Figures 3-7, 3-18). Most folds trend east-west in the San Felipe Hills but there are several smaller zones of north-south and southeast trending folds (Figures 3-7, 3-18).

The San Felipe and Santa Rosa anticlines are both persistent regional scale structures upon which the many smaller folds and faults of the San Felipe Hills have been superposed [*Dibblee*, 1954, 1984a]. Plunge directions of the closely spaced folds changes from east to west across the south-southeast plunging Santa Rosa anticline. The Santa Rosa and San Felipe anticlines are defined by changes in dip of bedding, plunge directions of folds, and magnetic and isostatic gravity anomalies (Figures 3-3, 3-18, 3-8 to 3-11).

San Felipe anticline

The San Felipe anticline deforms the late Miocene to Pleistocene stratigraphy of the San Felipe Hills exposing Pliocene Diablo Formation and upper Miocene-Pliocene Imperial Group near its core, and folding late Pliocene-Pleistocene Borrego Formation and middle Pleistocene Ocotillo and Brawley formations further to the east (Figure 3-3; Plate 1). Basement rocks are exposed in the core of this anticline near Squaw Peak (Figures 3-3; Plate 1). This anticline formed before the ~1.1 to 0.5Ma Ocotillo Formation lapped across its crest and has tightened since the end of Ocotillo Formation deposition (~0.5 Ma) [*Chapter 2*].Based on the subcrop beneath the Ocotillo Formation the extent of the San Felipe anticline was roughly 12 km north to south and 14 km from the western edge of the study area to the to eastern-most exposure of the sub Ocotillo Formation angular unconformity [*Kirby et al.*, 2004]. The east end of the anticline coincided with the Powerline and Sand Dunes faults prior to deposition of the Ocotillo and Brawley formations and also the extent of a prominent bedrock high [*Chapter 2*]. The San Felipe anticline likely extends to the west to a basement cored anticline at Borrego Mountain

based on the lateral continuity, similar width and amplitude of an east-west-trending gravity high there (Figures 3-8, 3-9).

The ancestral San Felipe anticline, along cross section B-B', has north and south limbs with average dips of 34 and 23°, respectively (Figure 3-15). Young east-west strike-slip faults and tilting produced the modern San Felipe anticline. It is now a faulted anticline with some superposed closely spaced folds (Figure 3-15). The interlimb angle for the San Felipe anticline is 123 ° along this cross section (Figure 3-15). The crest of the San Felipe anticline coincides with a gravity high and is 1 km north of a magnetic high (Figures 3-8 to 3-11). However there is a mismatch between the east-west extent of the gravity and magnetic signal and the mappable extent of the anticline (Figures 3-3, 3-8 to 3-11). The magnetic signal is displaced to the south 2.5 km relative to the mapped axis of the anticline and the center of the gravity high (Figures 3-10, 3-11). The gravity high disappears east of the Sand Dunes fault yet the San Felipe anticline remains a mappable fold east of the Sand Dunes fault (Figures 3-8, 3-9; Plate 1).

A reconstructed (~ 1.07 Ma) cross section of the San Felipe anticline produced from the angular unconformity beneath the Ocotillo Formation has a interlimb angle of 130°, a homoclinal north limb and a more complex south dipping limb [*Kirby et al.*, 2004] (Figure 3-19). The north-south extent of the south limb of the reconstructed San Felipe anticline is poorly known because conformable depositional contacts beneath the Ocotillo Formation occur in the Ocotillo Badlands on the southwest side of the Coyote Creek fault]. A north-dipping reverse fault is inferred at depth to explain the large difference in the subcrop of the Ocotillo Formation northward from the Ocotillo Badlands

and the presence of crystalline rocks at shallow depths near the Coyote Creek fault (*Morely*, 1963).

Preliminary offset across the Coyote Creek fault based on gravity data may be ~4 km [*Langenheim,* unpublished data, 2005; *Janecke et al.*, 2005]. Further work is necessary to verify offset amount across the Coyote Creek fault in the San Felipe Hills. Based on the reconstructed cross section (Figure 3-19) and the modern B-B' cross section (Figure 3-15) the San Felipe anticline may have tightened just 7° since the Ocotillo Formation was deposited across it. This is, however, complicated by several north-side-up east-west striking strike-slip faults which may obscure the true dimensions of the modern anticline. Other evidence for modern growth of the San Felipe anticline include the Holocene Lake Cahuilla shoreline which defines a large embayment south of the San Felipe anticline and a smaller embayment north of the San Felipe anticline (Plate 1). These relationships suggest that the anticline may still be growing and deflecting the shoreline.

Santa Rosa anticline

The southeast plunging Santa Rosa anticline is less well defined than the San Felipe anticline and it may not persist south of Tule Wash (Figure 3-3). It is best expressed in the northern portion of the field area where the east limb dips up to 19 degrees and the west limb dips up to 20°. Cross section C-C' shows the faulted limbs of the southern-most Santa Rosa anticline (Figure 3-16) and an industry seismic data imaged the east dipping limb (Figure 3-20). The fold extends 7 km along trend south-southeast into the northern San Felipe Hills and is up to 4 km across (Figure 3-3). South of Tule Wash this regional structure may be defined by fold plunges which change from east to

west near the Powerline Fault (Figure 3-7). The Santa Rosa anticline coincides with a gravity high in the northern portion of the study area but to the south this signal is less clear because the Santa Rosa and San Felipe anticlines intersect there (Figures 3-8, 3-9). The Santa Rosa anticline correlates with a magnetic high north of Tule Wash but farther to the south arcing anomalies associated with the southeast end of the Clark fault obscure possible continuations of the Santa Rosa anticline (Figures 3-10, 3-11). The age of initial growth of the Santa Rosa anticline is uncertain but most of the growth was after deposition the Brawley Formation. This unit dips east on the east limb of the anticline nearly as much as the underlying Borrego and Diablo formations (Figures 3-16, 3-20).

Fold domains

Folds with similar orientation and style of folding were grouped into 11 domains. Where possible, fold domains are directly abutted with one another unless separated by covered areas, homoclinally dipping rocks, or faults (Figure 3-7). Domains C and D have noncontiguous subdomains which are separated by areas of cover or other fold domains (Figure 3-7). Geometric data for each fold domain are shown in tables 3-1 and 3-3 and figures 3-7 and 3-18.

All but two of the fold domains have upright axial surfaces on average (Figure 3-15). Fold wavelength varies among fold domains from a minimum of several hundred meters to a maximum of several kilometers (Figure 3-3). Fold style varies considerably from kink folding (domain D) to cylindrical folding which dominated most of the other fold domains (Figures 3-7, 3-18).

The trend and plunge of folds vary somewhat across the study area but east-west folds dominate (Figure 3-18; Table 3-1). Folds in domains B, E, G, J,and K all trend and

plunge to the east with folding in domains E and J plunging slightly north of east, and folds in domain D plunging slightly south of east (Figures 3-7, 3-18). Fold domains F, H, and I plunge west (Figure 3-18). Folds in domain C plunge to the east-southeast (Figure 3-18). Folds in domain A, just west of the Salton Sea trend north (Figures 3-7, 3-18). Plunge values range from 3° in domain H to 21° in domain E (Table 3-1). Average plunge was approximately 8°. Folds in the southeast San Felipe Hills bend from their dominant east-west trend to east-northeast trends as they approach the Extra fault zone.

Vergence varies slightly among the fold domains but the difference may not be statistically significant (Table 3-1). Folds on the south limb of the San Felipe anticline verge to the north [*Wells*, 1986; *Heitman*, 2002; *Lilly*, 2003] (Figures 3-15, 3-16). Folds on the north limb of the San Felipe anticline may verge southward in domain F (Figure 3-15; Table 3-1). Folds in domain A show possible east vergence (Figure 3-15; Table 3-1). Larger data sets may show additional patterns but most axial surfaces are close to vertical.

Interlimb angles among fold domains range from 164.4° for the north plunging domain A in the northeastern portion of the field area to 81.8° for the east plunging folds in domain K (Table 3-1). Other fold domains have interlimb angles between 107.4 and 143.4° (Table 3-1).

The shortening direction in each domain is assumed to be perpendicular to the dominant trend of the folds (Figure 3-14; Table 3-1). Across the San Felipe Hills the dominant shortening direction is nearly north-south (Figure 3-18). Several fold domains vary slightly from north-south shortening (Figure 3-7; Table 3-1).

Strain

Strain magnitudes were computed for each fold domain and the homoclinal dip domains using interlimb angles (Tables, 3-1, 3-2). Limbs were assumed to be initially horizontal and of a unit length. Change of horizontal length parallel to the shortening direction was then trigonometrically calculated from the change in initial and final limb angles (Figure 3-21). Strain ranges from a low of 0.009 for fold domain A to a high of 0.345 for fold domain K (Table 3-1). The other fold domains have strain magnitudes between 0.050 and 0.195 (Table 3-1). The homoclinal dip domains reflect strains of 0.034 and 0.073 for the south and north limbs of the San Felipe anticline (Table 3-2).

Strain rates were calculated using the strain magnitudes and magnetostratigraphic age constraints from the Brawley Formation in the southeastern San Felipe Hills (Table 3-1). The Brawley Formation is the youngest internally conformable deposit that contains no evidence for active deformation on local structures during its deposition. Growth strata were not observed in this or any other unit in the San Felipe Hills but may be present farther to the north and west in the Borrego and Diablo formations [*Dorsey*, unpublished data, 2003]. Seismic lines in the north San Felipe Hills also show little evidence of lateral thickening of the Pliocene to Quaternary strata in the San Felipe Hills (Figure 3-20). Magnetostratigraphic correlation and sedimentation rates applied to a measured section yield ages which range from 0.61 Ma $\pm$ 0.02 Ma to 0.52 Ma $\pm$ 0.03 Ma for the end of deposition of the Brawley Formation in the San Felipe Hills. Paleomagnetic data show clockwise vertical axis rotation of ~ 8.5° for the uppermost Borrego Formation and Brawley Formation in the southeastern San Felipe Hills [*Kirby et al.*, 2004].

Our data support earlier interpretations that all deformation except growth of the basement-cored part of the San Felipe anticline occurred since the deposition of the Brawley Formation [*Dibblee*, 1954, 1984a]. Deformation is assumed to be equally distributed across a given fold or dip domain. Age constraints yield two distinct end member strain rates and shortening rates for each fold domain. Strain rates ranged from a high of $66.40 \pm 3.62\ 10^{-8}$/yr for fold domain K assuming the youngest onset of deformation at 0.52 Ma $\pm$ 0.03 Ma to a low of $1.52 \pm 0.04\ 10^{-8}$/yr for fold domain A assuming the older onset of deformation at 0.61 Ma $\pm$ 0.02 Ma (Table 3-1).

Shortening

Shortening rates were calculated using the strain values, spatial extent of fold domains, and age constraints for the onset of folding. These values ranged from 3.98 ± 0.22 mm/yr for the east-plunging folds in domain K to 0.11 ± 0.003 mm/yr for the north-plunging folds in domain A. Shortening rates for each fold domain are shown in table 3-1.

We calculate total shortening from folding along two structural transects (Figure 3-7). The transects are oriented approximately north-south and exactly normal to the trend of each contiguous fold and homoclinal dip domain (Figure 3-7). Transect 1 includes fold domains B and K and is located in the east central portion of the study area (Figure 3-14). Shortening across the homoclinal north and south limbs of the San Felipe anticline was grouped with fold domains F, G, and H in transect 2, which covers a north-south section in the central San Felipe Hills (Figure 3-14). The amount of shortening was calculated for each fold and dip domain by multiplying the spatial extent of each domain, parallel to the direction of shortening, by the calculated percent shortening. Shortening is

calculated separately for each fold domain and then summed for all fold and dip domains in a given transect (Table 3-2). Shortening was then projected on an idealized vertical Clark fault plane striking 305°NW to calculate the equivalent dextral slip recorded in each transect.

Equivalent dextral slip across transect 1, likely related to the Clark fault in the eastern San Felipe Hills, is 5.62 $\pm$ 0.2 km. This value is a minimum and assumes that all the Clark related slip is transferred to east-west trending folds in transect 1. In the central San Felipe Hills, including the San Felipe anticline, transect 2 has 1.32 $\pm$ 0.2 km of equivalent slip. A maximum estimate sums the strain in transects 1 and 2 for equivalent slip of 6.95 $\pm$ 0.4 km. We prefer the lower estimate of 5.62 km $\pm$ 0.2 km based on transect 1 alone, because transect 2 is at least partially structurally isolated from the influence of the Clark fault by the intervening Sand Dunes and Powerline faults (Figure 3-7). Either the nearby San Felipe Hills fault and or the more distant Coyote Creek fault is a more likely source of the shortening observed along transect 2.

Error estimates for each transect result from potential measurement error of the spatial extent of fold domains within a given transect. Different spatial extents can be measured within a given transect. Error resulting from the calculation of strain for each fold domain is unconstrained. Our method does not detect slip on discrete faults unless the faults terminate into zones of folding. Rotation about vertical axes can significantly affect the end result. Total rotation about vertical axes in the southeastern San Felipe Hills is up to 8° clockwise since about 1 Ma.

To the north, shortening was calculated in a similar manner for a north-south transect which stretches north from the study area to Travertine Ridge (Figure 3-3). This

transect should record any additional shortening by folding that could have been produced by slip on the Clark fault. North and south homoclinal dip domains, dipping 8.5 and 14° respectively, define this transect. Total shortening across the 6.5 km transect was minor at just 0.04 km.

5.62 ± 0.4 km of dextral slip likely related to the Clark fault, on a plane striking 305° NW, is preserved in the folds of the eastern San Felipe Hills. Some unknown amount of dextral slip is preserved on the strike-slip faults in the San Felipe Hills, but without offset markers this value is poorly constrained. Faults with potential for the greatest offset and slip within the San Felipe Hills include the San Felipe Hills, Sand Dunes, Powerline, and Dump faults, but most of these faults appear to die out and transfer some or all of their slip to folds [*Heitman*, 2002; *Lilly*, 2003; *this study*].

Discussion

Faults

Based on our new mapping, the Clark fault continues 18 km southeast of its previously mapped termination as a series of en echelon faults and horsetail splays which terminate in the folded stratigraphy of the central and southeastern San Felipe Hills (Figure 3-3). The northernmost newly mapped fault strand which may be related to the Clark fault is the Dump fault (Figure 3-3). It strikes west-northwest and coincides with the southwest edge of gravity and magnetic highs which curve along strike into the strong gravity and magnetic gradient along the Clark fault farther to the northwest (Figures 3-3, 3-8,3-9,3-10,3-11). To the south of the Dump fault are discontinuous and complex northwest striking dextral faults that are likely related to the Clark fault farther to the

northwest (Figures 3-3; Plate 1). Magnetic gradients from these faults turn and connect directly with gradients along the Clark fault farther to the northwest (Figures 3-10,3-11). The gravity and magnetic data are consistent with a single fairly large Clark fault at basement level that splays southeastward into the northwest edge of the study area. Surface geology shows a much less organized fault zone in the same area [*Dibblee*, 1954, 1984a; *Bartholomew*, 1970; *Pettinga*, 1991]. We infer that the Clark fault changes from a single fault at depth to multiple strands at shallower levels northwest of the study area and distributes slip southeastward along the Dump, Powerline, and en echelon faults into the San Felipe Hills.

Several other major dextral northwest-striking faults including the Powerline and Sand Dunes faults have been mapped northwest of their previously mapped positions [*Reitz*, 1977; *Heitman*, 2002; *Lilly*, 2003] by our study. These faults likely transmit slip from the Clark fault into the central and south-central San Felipe Hills. None of these faults, however, are continuous across the study area. It is therefore likely that slip on these faults, is balanced by folds near their terminations.

New mapping shows the Extra fault zone to be the only through-going northeast-striking sinistral fault zone in the San Felipe Hills. This fault is unlike other sinistral faults in the San Felipe Hills but quite similar to sinistral faults to the southeast including the Elmore Ranch fault [*Hudnut et al.*, 1989; *Janecke et al.*, 2004]. The Extra fault zone represents a kinematic and geometric change from the rest of the study area. The fold and fault patterns apparent in the San Felipe Hills are best represented by a new model shown in figure 3-22. Models 1,2, & 3 predict fault and fold geometries that are not apparent in the San Felipe Hills (Table 3-4; Figure 3-5).

Folds

Strain intensity due to folding is distributed unevenly across the San Felipe Hills. Highest strain is localized in the southeastern San Felipe Hills in fold domains K,J, and B (Table 3-1). Fold domains B and K lie just to the east and south respectively of the Powerline, Sand Dunes and discontinuous fault strands which penetrate the central San Felipe Hills from the southeast end of the Clark fault (Figure 3-7). Both of these domains likely reflect strain transmitted to the southeastern San Felipe Hills by slip on the strands of the Clark fault and its interaction with the province of block rotation and sinistral faulting to the south. Fold domain K has the highest strain magnitude (35 %) of all domains examined by a factor of two (Table 3-1). Strain magnitudes for the remainder of the fold domains, excluding domain A, lie in the middle of the calculated range. None of the prior models examined predict that the most intense folding would be localized in the southeastern San Felipe Hills (Figure 3-5).

Fold domain A with its north-south trending folds and low apparent strain, is an anomaly compared with the folding apparent in the rest of the San Felipe Hills. Domain A may be the result of east-west extensional strain resulting from the continued subsidence of the floor of the Salton Trough. The position of some of the north-south trending folds in the hanging walls of north striking normal faults suggests these folds may be extensional fault propagation folds. This fold domain is only accounted for by model 3 that proposes these folds developed over a blind northwest striking dextral fault near the margin of the Salton Sea [*Janecke et al.*, 2003] (Figure 3-5) . The low

magnitude of strain present in fold domain A is however not predicted by this model and model 3 does not predict high strains in the south central to southeast San Felipe Hills.

Fold domain J along the Extra fault zone had the second highest strain rate and is located east of domain K. There is a strong spatial correlation of these folds with the left-lateral Extra fault zone. Strands of the Extra fault zone cut and interact with the doubly plunging anticlines and synclines characteristic of this domain. Fold domain J likely represents strain resulting from slip along the left-lateral Extra fault zone and not from slip transferred from the north on strands of the Clark fault. The folds of domain J provide further evidence of a change in structural kinematics along the Extra fault zone relative to most of the San Felipe Hills. Previous workers have concluded that the Extra fault is part of the province of sinistral faulting and clockwise block rotation farther to the southeast of the San Felipe Hills, but some models included the southeast San Felipe Hills northwest of the Extra fault, in the zone of block rotation [*Hudnut et al.*, 1989; *Seeber and Armbruster*, 1999].

Preferred model

The structural data do not support any of the prior models for the structure of the San Felipe Hills (Figures 3-5). Fault distributions and orientations are closely matched by model 3; however none of the models predict the high strain values found in domain K. Based on this we present a modified kinematic model to account for the data (Figure 3-23; Table 3-4). In the modified model the extent of folding in the San Felipe Hills and the presence of a previously unmapped en echelon dextral fault strands in the north central San Felipe Hills and other large northwest-striking faults including the Powerline, Sand Dunes, and Dump fault are best explained by slip which enters the San Felipe Hills

from the Clark fault to the northwest (Figure 3-23). These faults transmit dextral strain to most of the northern, central, and south-central San Felipe Hills, producing the high strain found in fold domains B and K. The highest strain magnitude found in domain K may be produced by the interaction of slip from the Clark fault and the northwestern edge of the province of sinsitral faulting and block rotation to the southeast. Our field studies show clearly that the Extra fault is the northwest-most laterally continuous sinistral fault of the transrotating domain because we have mapped a virtually unfaulted Borrego and Brawley contact across the southern and eastern San Felipe Hills just northwest of there. Previous workers have shown the province block rotation extending northwest into the San Felipe Hills [*Hudnut*, 1987, 1988; *Seeber and Armbruster*, 1998]. The preferred model limits the northwestward extent of laterally continuous sinistral faults to the zone between the Extra fault zone and Domain K. Deformation along the Extra fault zone and block rotation in the San Jacinto fault zone to the southeast must have begun contemporaneously at 0.61 Ma $\pm$ 0.02 Ma to 0.52 Ma $\pm$ 0.03 Ma, the age of the youngest pre-growth strata deformed by the Extra fault zone.

San Felipe anticline

The large San Felipe anticline is geometrically distinct from the younger closely spaced folds that also shortened the San Felipe Hills. Reconstructed cross sections of the San Felipe anticline based on angular relations at the basal contact of the Ocotillo formation define the extent of the San Felipe anticline at about 1.07 Ma (Figure 3-19). Development of the San Felipe anticline immediately preceded or coincided with a basin-wide change in deposition and facies recorded by the Brawley and Ocotillo formations [*Chapter 2*]. The interlimb angle of the reconstructed San Felipe anticline east of Squaw

Peak is 130° whereas the current interlimb angle is 123°. This shows minor tightening of the San Felipe anticline since ~1.07 Ma in the central San Felipe Hills, and much of tightening may be localized tilting adjacent to east-west-striking strike-slip faults.

The modern stress field and slip on strands of the modern San Jacinto fault zone are unlikely to have produced the San Felipe anticline because the fold has barely tightened since ~1 Ma and the currently active Coyote Creek fault crosscuts and offsets the anticline. Instead, slip on a kinematically different early San Jacinto fault zone is hypothesiszed to have produced this fold. The poorly understood San Felipe and Veggie Line faults to the west may also be related to formation of the San Felipe anticline (Figure 3-2). A similar bedrock cored fold has been described by *Dibblee* [1954, 1984a, 1984b] southeast in the Coyote Mountains adjacent to a contractional bend in the Elsinore fault. The orientation, scale, structural and stratigraphic context of that fold resembles the San Felipe anticline [*Dibblee*, 1984b].

Shortening from Folding

Feragen [1986] calculated ~ 9 km of north-south fold related shortening across the San Felipe Hills by assuming that shortening percentages equal to those in domain K apply to the entire San Felipe Hills. This is equivalent to 14 km of dextral slip on the Clark fault plane (305° NW) [*Wells and Feragen*, 1987]. Our work suggests lower values of fold-related shortening because the actual strain magnitudes are significantly less than *Feragen* [1987] inferred across much of the San Felipe Hills. We calculate that at least 5.62 $\pm$ 0.4 km of dextral slip likely related to the Clark fault, on a plane striking 305° NW, is preserved in the folds of the eastern San Felipe Hills (Table 3-2). If the discontinuous dextral faults in the area accommodated additional slip, the total-slip in the

San Felipe Hills could be ~ 1-3 km greater. The absence of correlatable markers across many of the dextral faults makes more detailed estimation of fault offset untenable, and there may be large errors associated with the current estimate.

A fraction (about 1/3) of the 15 km of dextral separation across the Clark fault is recorded in the folds of the San Felipe Hills. Further work is needed to determine if the remaining ~ 9-10 km of separation is preserved on small faults in the San Felipe Hills and/or on faults northeast of the Clark fault between Travertine Ridge and the Truckhaven Road, or is not evident in near-surface sedimentary deposits. Some of this slip deficit may be accounted for if earlier geometries of the Clark fault were similar to those presented by *Bartholomew* [1970] (Figure 3-6). If his model is partially correct significant amounts of the slip on the Clark fault to the north of the San Felipe Hills could have been transferred to the south, bypassing the San Felipe Hills. Slip could have been transferred to the Coyote Creek fault [*Bartholomew,* 1970] or the Fish Creek Mountain fault [*Janecke et al.*, 2004]. Another possible explanation for the slip deficit may be suggested by recent work by *Fialko et al.* [2005] that show large differences between slip magnitudes at 3-5 km depths and slip magnitudes near the surface. Further work is necessary to explain the apparent slip deficit.

The absence of growth strata in the Brawley Formation of the San Felipe Hills suggests that all of the folding on transect 1 occurred since deposition of the Brawley Formation at 0.61 Ma $\pm$ 0.02 Ma to 0.52 Ma $\pm$ 0.03 Ma (Figure 3-7). Therefore at least ~5-6 km of slip has been transferred into the San Felipe Hills along strands of the Clark fault in less than 0.5 Ma.

Slip Rates

Folding along transect 1 may have begun no earlier than the end of deposition of the internally conformable Brawley Formation in the southeastern San Felipe Hills at 0.61 ± 0.02 Ma to 0.52 ± 0.03 Ma [*Chapter 2*].. Two slip rates of 9.5 ± 0.3 mm/yr and 10.8 ± 0.7 mm/yr are calculated based on shortening in transect 1 and the age of the youngest Brawley Formation (Table 3-2). These minimum slip rates are calculated only for fold domains B and K in transect 1 that are most likely to be the result of slip on the Clark fault. These slip rates likely are likely minima because potential slip on faults including the Sand Dunes, Powerline, and Dump faults is not included in this estimate (Figure 3-3). Fold domains D and E could also record slip on the Clark fault but are likely to be structurally isolated by faults and or may record duplicate slip already captured in transect 1 (Figure 3-7). Actual slip rates may be somewhat lower if some of the folding across transect 1 is the result of deformation stepping left from the Coyote Creek fault, and somewhat higher if there was significant clockwise rotation of the fold axes within the San Felipe Hills. A rotation of 10° could increase the slip rate by roughly 10%, assuming that 2 km long blocks rotate coherently.

This rate represents a significant amount of plate boundary slip when compared with slip rates of ~ 25 mm/yr for the southernmost San Andreas fault south of the Transverse Ranges [*Weldon and Sieh*, 1985; *Bennett et al.*, 1996]. Total slip across the San Jacinto fault zone in the western Salton Trough will be at least 9.5 to10.8 mm/yr plus the slip rate on the Coyote Creek fault. Recent estimates of the slip rate across the Coyote Creek fault [10 mm/yr; *Dorsey*, 2002] appear too high by a factor of 2. Follow-up studies

suggest slip rates of 4-6 mm/yr in the same area [*Janecke et al.*, 2005]. Combining these estimates with our data gives a slip rate of at least 15 mm/yr for the San Jacinto fault zone over at least the last 0.5 Ma.

Recent trilateration data support similar strain rates (32.0 to 2.4 10^{-8}/yr) across both the San Jacinto fault zone and the San Andreas fault at the latitude of the San Felipe Hills [*Anderson et al.*, 2003]. Such high rates are surprising given the lower neotectonic rates of ~10-12 mm/yr found farther to the northwest along the San Jacinto fault zone based on dated Quaternary deposits offsets and GPS studies [*Sharp*, 1981; *Rockwell et al.*, 1990; *Wesnouski et al.*, 1991; *Bennett et al.*, 1996] but agree with higher rates in other studies [*Kendrick et al.*, 1994].

Conclusions

The middle Pleistocene to recent structural history of the San Felipe Hills is complex and shows the interaction of several different fault geometries and deformation styles produced by the evolution of the southern San Jacinto fault zone. Early structures, including the large east-trending basement cored San Felipe anticline are different from the smaller, tighter, and more numerous folds that deform much of the study area. Magnetostratigraphically dated rocks of the Brawley Formation are internally conformable and provide age constraints on both the San Felipe anticline and the onset of the later smaller scale folding. An angular unconformity beneath the Ocotillo Formation in western the San Felipe Hills shows that the basement cored portion of the San Felipe anticline developed slightly before or at ~1.07 Ma. Using the modern strain rate of 32.0 $\pm$ 2.4^10^{-8} per year from GPS data sets [*Anderson et al.*, 2003] over a similar spatial area

and orientation to that of the reconstructed anticline the anticline could have formed in 285,500 ± 19,700 years [*Chapter 2*]. Farther to the east at this time no folding is apparent during the deposition of the Brawley Formation. Development of the many smaller folds in the eastern San Felipe Hills could not have begun until after deposition of the internally conformable deposition of the Brawley Formation at 0.61 Ma ± 0.02 Ma to 0.52 Ma ± 0.03 Ma [*Chapter 2*]. Thus the current configuration of the San Jacinto fault zone at the latitude of the San Felipe Hills can be no older than the youngest Brawley Formation. An earlier change, around 1.1 Ma, evidenced by the growth of the San Felipe anticline and the arrival of coarse clastics in a former lake basin probably records another reorganization. This event appears to be the initiation of the San Felipe and Fish Creek-Vallecito faults [*Chapter 2; Steely et al.*, 2005], and perhaps also the initiation of the ancestral San Jacinto fault zone [*Lutz*, 2005; *Janecke et al.*, 2005]. The relatively high slip rates found by this study are also consistent with this interpretation. Slip rates slightly higher than those found by this study could account for the total right separation across the southern San Jacinto fault zone [*Sharp*, 1967; *Janecke et al.*, 2005] in just over 1 Ma.

Since the end of deposition of the Brawley Formation (~0.5 Ma) at least 5-6 km of slip has occurred on the Clark fault plane. This value represents a portion of the 15 km separation across the Clark fault northwest of the study area, but still leaves a slip deficit of at least ~ 9-10 km. Some of the slip deficit could disappear if the Clark fault had a significant southwest-side-down component in Clark Lake Valley. Some of this deficit can be accounted for by earlier geometries of the San Jacinto fault zone, which bypassed the San Felipe Hills [*Bartholomew*, 1970; *Janecke et al.*, 2004] (Figure 3-6).

The rest of the slip may reside in undocumented fault slip across structures northeast of the Clark fault, like the Truckhaven fault, and faults in the San Felipe Hills like, the Sand Dunes, Powerline, and Dump faults. Offset across these faults could total up to 3-4 km and account for some of the slip deficit. Finally, permanent near-surface slip deficits, like those recently documented on strike-slip faults, could explain the observed slip deficit [*Fialko et al.*, 2005]. Further detailed work on the faults in the San Felipe Hills and the possibility of Clark fault step-around to the south is warranted. Slip rates based on the resolved shortening and the paleomagnetic time constraints are calculated at 9.5 ± 0.3 mm/yr and 10.8 ± 0.7 mm/yr for the Clark fault over the last ~0.5 Ma. These values are quite conservative and actual rates may be higher.

The overall geometry of folding and deformation within the San Felipe Hills is likely the result of slip on the Clark fault and its interaction with province of block rotation to the southeast and the Coyote Creek fault to the west. This interpretation is further supported by the localization of the highest strain within the San Felipe Hills in fold domain K. This folding is not the direct result of block rotation because of the lack of major (>10°) vertical axis rotation documented in concurrent paleomagnetic studies [*Housen et al.*, 2004; *Chapter 2*]. Instead this folding may be produced by slip on the Clark fault transferred into the southern San Felipe Hills, which interacts with the province of clockwise block rotation to the south. The geometry and spatial extent of the folding in domain K is also different from that of fold domain J which is related to sinistral slip on the northeast striking Extra fault zone.

Of the three prior models presented for the formation of the closely-spaced folds and smaller faults in the San Felipe Hills, none exactly match the structural, map, and

geophysical data (Figure 3-5). Instead we propose a variant which better incorporates the data, in which the Clark fault terminates as series of en echelon horse-tail splays which transfer slip southward to the northern edge of the province of sinistral faulting and block rotation (Figure 3-23). Deformation is most intense where the en echelon strands of the Clark fault interact with the northern boundary of the block rotation.

Our model for the kinematics of the southern San Jacinto fault zone near the San Felipe Hills has several important implications. First, the Brawley Zone which bounds the province of block rotation on the east [*Hudnut et al.*, 1989] and transfers dextral slip north from the Imperial fault may be no older than the onset of folding in the Brawley Formation. Second, the southern San Jacinto fault zone has undergone major kinematic changes in just the last 1 Ma. Third, the transfer of slip and strain across the province of block rotation is linked to slip and strain changes along the Coyote Creek and Clark fault to the northwest. Fourth, the San Felipe Hills lie astride a complex zone of kinematic transfer in the southern San Jacinto fault zone with the Extra fault zone lying near or on the northwest boundary between sinistral faulting and block rotation to the southeast and dextral strike-slip along the Coyote Creek and Clark faults to the northwest.

Deformation in the San Felipe Hills is driven by previous (~1.1 Ma) and recent (< 0.5 Ma) along strike changes in the fault kinematics and geometries of the San Jacinto fault zone. Evidence for at least two geometries of the San Jacinto fault zone is shown by the ~ 1.1 Ma San Felipe anticline and the (< 0.5 Ma) closely spaced folds and faults. The modern San Jacinto fault zone displays major kinematic changes southeastward along strike, from the en echelon strands of the Clark fault to province of sinistral faulting and block rotation to the southeast.

References

Anderson, G. C., D. C. Agnew, and H. O. Johnson (2003), Salton Trough regional deformation estimated from combined trilateration and survey-mode GPS Data, *Bull. Seismol. Soc. Am.*, *93*, 2402-2414.

Atwater, T. (1989), Plate tectonic history of the northeast Pacific and western North America, in *The Eastern Pacific Ocean and Hawaii: Geological Society of America, The Geologyof North America*, edited by E. L. Winterer, D. M. Hussong, and R. W. Decker, N, 21-72, GSA, Boulder, Co.

Axen, G. J., and J. M. Fletcher (1998), Late Miocene-Pleistocene extensional faulting, northern Gulf of California, Mexico and Salton Trough, California, *International Geology Review*, *40*, 217-244.

Bartholomew, M. J. (1970), San Jacinto Fault Zone in the northern Imperial Valley, *GSA Bulletin*, *81*, 3161-3166.

Bennett, R. A., W. Rodi, and R. E. Reilinger (1996), Global Positioning System constraints on fault slip rates in Southern California and northern Baja, Mexico, *J. Geophys. Res.*, *101*, 21,943-21,960.

Dibblee, T. W. (1954), Geology of the Imperial Valley region, California, in Jahns, R. H., ed., Geology of southern California, *California Division of Mines Bulletin* 170, 21-28.

Dibblee, T. W. (1984a), Stratigraphy and tectonics of the San Felipe Hills, Borrego Badlands, Superstition Hills and vicinity, in *The Imperial Basin; tectonics, sedimentation and thermal aspects*, v. 40, edited by C. A. Rigsby, Pacific Section SEPM Field Trip Guidebook, p. 31-44.

Dibblee, T. W. (1984b), Stratigraphy and tectonics of the Vallecito-Fish Creek mountains, Vallecito badlands, Coyote mountains, Yuha desert, southwestern Imperial basin,in *The Imperial Basin; tectonics, sedimentation and thermal aspects*, v. 40, edited by C. A. Rigsby, Pacific Section SEPM Field Trip Guidebook, p. 59-79.

Dorsey, R.J. (2002), Stratigraphic record of Pleistocene initiation and slip on the Coyote Creek fault, lower Coyote Creek, southern California, in *Contributions to Crustal Evolution of the Southwest United States*, edited by A. Barth, GSA Special Paper 365, p. 251-269, Boulder, Co.

Dronyk, M. P. (1977), Stratigraphy, structure and a seismic refraction survey of a portion of the San Felipe Hills Imperial Valley, California, M.S. Thesis, Univ. of Calif.,

Riverside. Riverside, Ca.

Feragen, E.S. (1986), Geology of the southeastern San Felipe Hills, Imperial Valley, California, M.S. Thesis, San Diego St. Univ., San Diego, Ca.

Fialko, Y., D. Sandwell, M. Simmons, and P. Rosen (2005), Three-dimensional deformation caused by the Bam, Iran, earthquake and the origin of shallow slip deficit, *Nature*, *435*, 295-299.

Frost, E. G., M. J. Fattahipour, and K. L. Robinson (1996), Emerging perspectives on the Salton Trough region with an emphasis on extensional faulting and its implications for later San Andreas deformation. in *Sturzstroms and Detachment Faults, Anza-Borrego Desert State Park, California*, edited by P. L. Abbott, and D. C. Seymour, South Coast Geological Society Annual Field Trip Guide Book, No. 24, 81-122.

Heitman, E. A. (2002), Characteristics of the structural fabric developed at the termination of a major wrench fault, M.S. Thesis, San Diego St. Univ., San Diego, Ca.

Housen, B. A., R. J., Dorsey, S. U. Janecke, S. M. Kirby, and A. T. Lutz (2004), Magnetostratigraphy and Rotation of Pleistocene Sedimentary Rocks in the San Jacinto Fault zone, Western Salton Trough, CA, *Eos Trans. AGU, 85*, Fall Meet. Suppl., Abstract, GP43A-0841.

Hudnut, K. W., L. Seeber, J. Pacheco, J. G. Armbruster, L. R. Sykes, C. G. Bond, and M. A. Kominz, (1989), Cross faults and block rotation in Southern California; earthquake triggering and strain distribution, *Yearbook Lamont –Doherty Geological Observatory of Columbia University*, p. 44-49.

Janecke, S.U., S. M. Kirby, and R. J. Dorsey (2003), New strand of the San Jacinto fault zone SW of the Salton Sea and a possible contractional step-over in the San Felipe Hills; a model to be tested, *Geological Society of America,* Abstracts with Programs, *35*, 26.

Janecke, S.U., S. M. Kirby, V. E. Langenheim, B. Housen, R. J. Dorsey, R. F. Crippen, and R. G. Blom (2004), Kinematics and evolution of the San Jacinto fault zone in the Salton Trough: progress report from the San Felipe Hills Area, *Geological Society of America,* Abstracts with Programs, *36*, 37.

Janecke, S.U., S. M. Kirby, V. E. Langenheim, R. J. Dorsey, B. Housen, A. N. Steely, and A. Lutz (2005), High geologic slip rates on the San Jacinto fault zone in the SW Salton Trough, and possible near-surface slip deficit in sedimentary basins, *Geological Society of America,* Abstracts with Programs, in press.

Jennings, C. W. (1977), Geologic Map of California, *State of California, Resources*

Agency, Dept. of Conservation, scale 1:750,000.

Kendrick, K., L. McFadden, and D. Morton (1994), Soils and slip rates along the northern San Jacinto Fault, in Geological investigations of an active margin, edited by S. F. McGill, and T. M. Ross, *Geological Society of America*, Cordilleran Section Annual Meeting Field trip Guidebook., v. 27, 146-151.

Kirby, S. M., S. U. Janecke, R. J. Dorsey, B. Housen, and K. McDougall (2004), A 1.07 Ma change from persistent lakes to intermittent floodning and dessication in the San Felipe Hills, Salton Trough, Southern California, *Geological Society of America,* Abstracts with Programs, 36, 37.

Langenheim, V. C. and R. C. Jachens (1993), Isostatic residual gravity map of the Borrego Valley 1:100,000 scale quadrangle, California, *U.S. Geol. Surv.,* Open-File Report 93-2461, scale 1:100,000.

Lilly, D. R. (2003), Structural geology of a transitory left step in San Felipe Hills fault, M.S. Thesis, San Diego St. Univ., San Diego, Ca.

Lutz, A.T. (2005), Tectonic controls on Pleistocene basin evolution in the central San Jacinto fault zone, southern California, M.S. Thesis, Univ. of Oregon, Eugene, Or.

Magistrale, H. (2002), The Brawley Seismic Zone, Imperial Valley, Southern California, *AGU Eos. Trans., 83*, F1034-1035.

Meade, B. J., and B. H. Hager (2005), Block models of crustal motion in southern California constrained by GPS measurements, *J. Geophys. Res., 110*, B03403.

Meisling, R., and R. J. Weldon (1989), Late Cenozoic tectonics of the northwestern San Bernardino Mountains, Southern California, *GSA Bull., 101*, 106-128.

Morley, E. R. (1963), Geology of the Borrego Mountain quadrangle and the western portion of the Shell Reef quadrangle, San Diego County, California, M.S.Thesis, Univ.of South. Calif., Los Angeles, Ca.

Morton, D. M., and Matti, J.C. 1993. Extension and Contraction within an evolving divergent strike-slip fault complex: the San Andreas and San Jacinto fault Zones at their convergence in Southern California, in *The San Andreas fault system: displacement, palinspastic reconstruction, and geologic evolution*, edited by R. E. Powell, R. J. Weldon, and J. C. Matti, Geological Society of America, Memoir 178, 217-230.

Nicholson, C., L. Seeber, P. Williams,and L. R. Sykes (1986), Siesmic evidence for conjugate slip and block rotation within the San Andreas fault system, southern California, *Tectonics, 5*, 629-648.

Oskin, M., and J. Stock (2003), Marine incursion synchronous with plate-boundary localization in the Gulf of California, *Geology*, *1*, 23-26.

Petersen, M. D., L. Seeber, L. R. Sykes, J. L. Nabelek, J. G. Armbruster, J. Pacheco, and K. W. Hudnut, (1991), Seismicity and fault interaction, southern San Jacinto fault zone and adjacent faults, Southern California: implications for seismic Hazard, *Tectonics*, *10*,1187-1203.

Pettinga, J. R. (1991), Structural styles and basin margin evolution adjacent to the San Jacinto fault zone, Southern California: *Geological Society of America*, Abstracts with Programs, 23, 257.

Reitz, D. T. (1977), Geology of the western and central San Felipe Hills, northwestern Imperial County, California, M.S. Thesis, Univ. of South. Calif., Los Angeles, Ca.

Remeika, P., and R. Beske-Diehl (1996), Magnetostratigraphy of the western Borrego Badlands, Anza-Borrego Desert State Park, California: Implications for stratigraphic age control, in *Sturzstroms and Detachment Faults, Anza-Borrego Desert State Park, California*, edited by P. L. Abbott and D. C. Seymour, South Coast Geological Society Annual Field Trip Guide Book, No. 24, 209-220.

Rockwell, T., C. Loughman, and P. Merifield (1990), Late Quaternary rate of slip along the San Jacinto fault zone near Anza, Southern California, *J. Geophy. Res., 95*, 8593-8605.

Seeber, L., and J. G. Armbruster (1999), Earthquakes, Faults, and Stress in Southern California, *SCEC Annual Progress Report* accessed online at http://www.scec.org/research/99research/99seeberarmbruster.pdf.

Severson, L. C. (1987), Analysis of seismic reflection data from the Salton Trough, M.S. Thesis, Univ. of South. Calif., Los Angeles, Ca.

Sharp, R. V. (1967), San Jacinto fault zone in the Peninsular Ranges of Southern California, *GSA Bull.*, *78*, 705-729.

Sharp, R. V. (1972), Map showing recently active breaks along the San Jacinto fault zone between the San Bernardino area and Borrego Valley, California, *USGS*, IMAP 675, 3.

Sharp, R.V. (1975), En echelon fault patterns of the San Jacinto fault zone,in *San Andreas fault in southern California,* edited by J. C. Crowell, J.C., California Division of Mines and Geology Special Report 118, 147-152.

Sharp, R.V., (1979), Some characteristics of the eastern Peninsular Ranges mylonite zone, in Proceedings, Conference VIII, Analysis of actual fault zones in bedrock *U.S. Geol. Surv.,* Open File Report 79-1239, 258–267.

Sharp, R. V. (1981), Variable rates of late Quaternary strike slip on the San Jacinto fault zone, Southern California, *J. of Geophys. Res.*, *86*, 1754-1762.

Steely, A., S. U. Janecke, R. J. Dorsey, and G. J. Axen (2004), Evidence for Late Miocene-Quaternary low-angle oblique strike-slip faulting on the West Salton detachment fault, southern California, *Geological Society of America,* Abstracts with Programs, 36, 37.

Steely, A., S. U. Janecke, G. J. Axen, and R. J. Dorsey (2005), Pleistocene (~1Ma) Transition from West Salton Detachment Faulting to Cross-Cutting Dextral Strike-Slip Faults in the SW Salton Trough, *Geological Society of America,* Abstracts with Programs, in press.

U.S. Geological Survey. (1990), Aeromagnetic map of parts of the San Diego, Santa Ana, and 1 by 2 degree adjacent quadrangles, California. *U.S. Geol. Surv.,* Open-File Report 90-206, scale 1:250,000.

Wagoner, J. L. (1977), Stratigraphy and sedimentation of the Pleistocene Brawley and Borrego formations in the San Felipe Hills area, Imperial Valley, California, U.S.A., M.S. Thesis, Univ. of Calif., Riverside. Riverside, Ca.

Weldon, R. J., K. E. Meisling, and J. Alexander (1993), A speculative history of the San Andreas fault in the central Transverse Ranges, California, in *The San Andreas Fault System: Displacement, Palinspastic Reconstruction, and Geologic Evolution*, edited by R. E. Powell, R. J. Weldon, and J. C. Matti, Geological Society of America, Memoir 178, 161-198.

Weldon, R. J., and K. E. Sieh (1985), Holocene rate of slip and tentative recurrence interval for large earthquakes on the San Andreas Fault, Cajon Pass, Southern California. *GSA Bull.*, *96*, 793-812.

Wells, D.L. (1987), Geology of the eastern San Felipe Hills, Imperial Valley, California: implications for wrench faulting in the southern San Jacinto fault zone, M.S. Thesis, San Diego St. Univ., San Diego, Ca.

Wells, D. L., and E. S. Feragen (1987), Percent strain and slip rate estimates for a proposed buried extension of the Clark fault, southern San Jacinto fault zone, Imperial Valley, California. *Geological Society of America* Abstracts and Programs, 19, 6.

Wesnouski, S. G., C. S. Prentice, K. E. Sieh (1991), An offset Holocene stream channel and the rate of slip along the northern reach of the San Jacinto fault zone, San Bernardino Valley, California. *GSA Bull.*, *103*, 700-709.

Winker, C. D., and S. M. Kidwell (1996), Stratigraphy of a marine rift basin: Neogene of

the western Salton Trough, California, in *Field Conference Guide 1996 Pacific Section AAPG*, edited by P. L. Abbot, J. D. Cooper, GB 73, Pacific Section S.E.P.M., Book 80, 295-336.

Table 3-1. Table of fold domain data. Summary of fold domains showing plunge and trend, interlimb angle, percent shortening, orientation of shortening, spatial extent, strain rate, and shortening rate. Shortening orientation isperpendicular to trend of folding. Strain rates were calculated by assuming all folding post dates the deposition of the Brawley Formation in the eastern San Felipe Hills. This assumption may be incorrect for fold domains in the western San Felipe Hills, including domains E, F, and G. Fold categories include o (open folds), g (gentle folds).

Fold domain	Orientation (plunge and trend)	Interlimb angle	Percent shortening	Shortening orientation (azimuth)	Spatial extent of fold domain perpendicular to trend (km)	Strain rates 10^{-8} yr^{-1} since 0.52 Ma	Strain rates 10^{-8} yr^{-1} since 0.61 Ma	Rate of shortening perpendicular to trend (mm/yr) since 0.52 Ma	Rate of shortening perpendicular to trend (mm/yr) since 0.61 Ma
Domain A	5, 359	164.4 g	1 %	269	7	1.78 ± 0.10	1.52 ± 0.04	0.12 ± 0.01	0.11 ± 0.00
Domain B	11, 91	116.4 o	15 %	181	6	28.87 ± 1.58	24.61 ± 0.78	1.73 ± 0.09	1.48 ± 0.05
Domain C	11, 127	140.2 g	6 %	217	1	11.15 ± 0.63	9.79 ± 0.31	0.12 ± 0.01	0.10 ± 0.00
Domain D	12, 101	143.4 g	5 %	191	5	9.73 ± 0.53	8.29 ± 0.26	0.49 ± 0.03	0.42 ± 0.01
Domain E	21, 76	129.0 g	10 %	346	1	18.73 ± 1.02	15.97 ± 0.51	0.19 ± 0.01	0.16 ± 0.00
Domain F	5, 271	128.9 g	10 %	181	2	18.81 ± 1.03	16.03 ± 0.51	0.38 ± 0.02	0.32 ± 0.01
Domain G	10, 94	140.2 g	6 %	184	4	11.48 ± 0.63	9.79 ± 0.31	0.46 ± 0.03	0.39 ± 0.01
Domain H	3, 273	136.7 g	7 %	183	4	13.57 ± 0.74	11.56 ± 0.37	0.54 ± 0.03	0.46 ± 0.01
Domain I	5, 268	135.0 g	8 %	358	5	14.64 ± 0.80	12.48 ± 0.40	0.73 ± 0.04	0.62 ± 0.02
Domain J	4, 80	107.3 o	20 %	350	3	37.42 ± 2.04	31.90 ± 1.01	1.12 ± 0.06	0.96 ± 0.03
Domain K	7, 94	81.8 o	35 %	184	6	66.40 ± 3.62	56.60 ± 1.80	3.98 ± 0.22	3.40 ± 0.11
homocline N	n/a	n/a	7 %	180	2	n/a	n/a	n/a	n/a
homocline S	n/a	n/a	3 %	180	2	n/a	n/a	n/a	n/a

Table 3-2. Shortening transect summary. Location of transects is shown in figure 3-14. Spatial extent of fold domains is measured parallel to the orientation of shortening. North and south limbs are the homoclinal limbs of the San Felipe anticline. Total north-south shortening was resolved onto a vertical plane parrallel to the Clark fault plane northwest of the study area (305° NW).

Transect	Fold or dip domain	Interlimb angle or homocline dip	Orientation of shortening axis from north	Percent shortening	Spatial extent (km)	Total shortening across domain (km)	Slip resolved on 305 NW (km)
Transect 1	b	116.4°	181°	15 %	6.20	0.93	1.66
	k	81.8°	184°	35 %	5.90	2.04	3.96
					Shortening on transect 1	2.97	5.62 ± 0.2 km
Transect 2	f	128.9°	181°	9.7 %	2.50	0.24	0.44
	g	140.2°	184°	5.9 %	2.70	0.16	0.31
	h	136.7°	183°	7 %	2.80	0.20	0.37
	N limb	34°	180°	4.3 %	1.70	0.07	0.13
	S Limb	23°	180°	2 %	1.90	0.04	0.07
					Shortening on transect 2	0.71	1.32 ± 0.2 km

Table 3-3. Cylindrical best fit eigen vectors and confidence intervals for fold domains a-k. For values of n > 25 confidence intervals were computed.

Fold domain	n	Eigen vector	Eigen value	Trend	Plunge	Confidence max	Confidence min
A	38	1	0.9153	220.8	85.1	6.5	2.6
		2	0.0723	90.9	3.2		
		3	0.0125	0.7	3.8	12.3	2.5
B	33	1	0.7233	223.8	74.1	20.0	4.0
		2	0.2561	3.2	12.2		
		3	0.0206	95.4	10.1	8.2	3.9
C	21	1	0.8688	297.1	83.6		
		2	0.1194	36.4	1.0		
		3	0.0118	126.5	6.3		
D	17	1	0.8237	295.9	78.2		
		2	0.1599	195.4	2.2		
		3	0.0165	105.0	11.5		
E	16	1	0.7329	138.8	81.3		
		2	0.2514	2.5	6.3		
		3	0.0157	271.8	5.9		
F	10	1	0.7582	268.6	68.7		
		2	0.2206	168.6	3.9		
		3	0.0212	77.1	20.9		
G	18	1	0.8101	266.5	81.7		
		2	0.1498	359.0	0.4		
		3	0.0401	89.0	8.3		
H	27	1	0.7956	23.0	82.7	14.7	4.3
		2	0.183	184.0	6.9		
		3	0.0214	274.3	2.3	11.2	3.7
I	21	1	0.7959	88.3	82.6		
		2	0.167	357.3	0.1		
		3	0.0372	267.3	7.4		
J	17	1	0.6181	5.5	81.1		
		2	0.2978	166.6	8.4		
		3	0.0841	257.1	2.8		
K	230	1	0.5234	356.9	44.2	21.2	3.9
		2	0.4048	187.9	45.3		
		3	0.0718	92.3	5.6	4.1	3.6

Table 3-4. Table of prior tectonic models. Summary of the fit between observed relationships and those predicted by prior tectonic models for the San Felipe Hills and the southern Clark fault. (1) = *Wells* [1986] and *Feragen* [1987], (2) = *Dibblee* [1954,1984], *Sharp* [1967], and *Pettinga* [1991], (3) = *Janecke et al.* [2003]. Figure 3-5 corresponds with models 1 thru 3. Bolded entries represent significant mismatches between actual data and predictions.

Observed data	Predictions of Model 1: blind Clark fault (1)	Predictions of Model 2: Clark fault term. (2)	Predictions of Model 3: Clark fault stepover (3)
E-W trending folds in most of the San Felipe Hills (SFH) except in the east where NS trending folds exist	E-W trending folds	E-W to SE trending folds fold trend changes across folded zone	E-W trending folds throughout SFH except in the east where NS trending folds are developed
folding is distributed across the entire SFH	**folds are developed primarily above the blind trace of the Clark fault**	**folds are developed only near the tip of the Clark fault in the NW SFH**	folds are distributed broadly across the entire SFH
highest strain is located in the SE SFH	**strain is equally distributed in deformed zone above the blind fault**	**highest strain is expected near the tip of the Clark fault NW of the SFH**	**highest strain is expected in stepover zone in the central and northern SFH**
several NW-striking dextral faults possbly related to the Clark fault	**no large surface faults predicted in the SFH**	**no surface faults predicted in the SFH**	**NW striking faults should be discontinuous and bound folded stepover zones**
Extra fault zone is a major through-going NE striking sinstral fault zone	**no major NE striking faults should cross the Clark fault**	**no major NE striking faults are predicted**	**Extra fault is not predicted and must cross a major buried NW striking fault zone at depth**

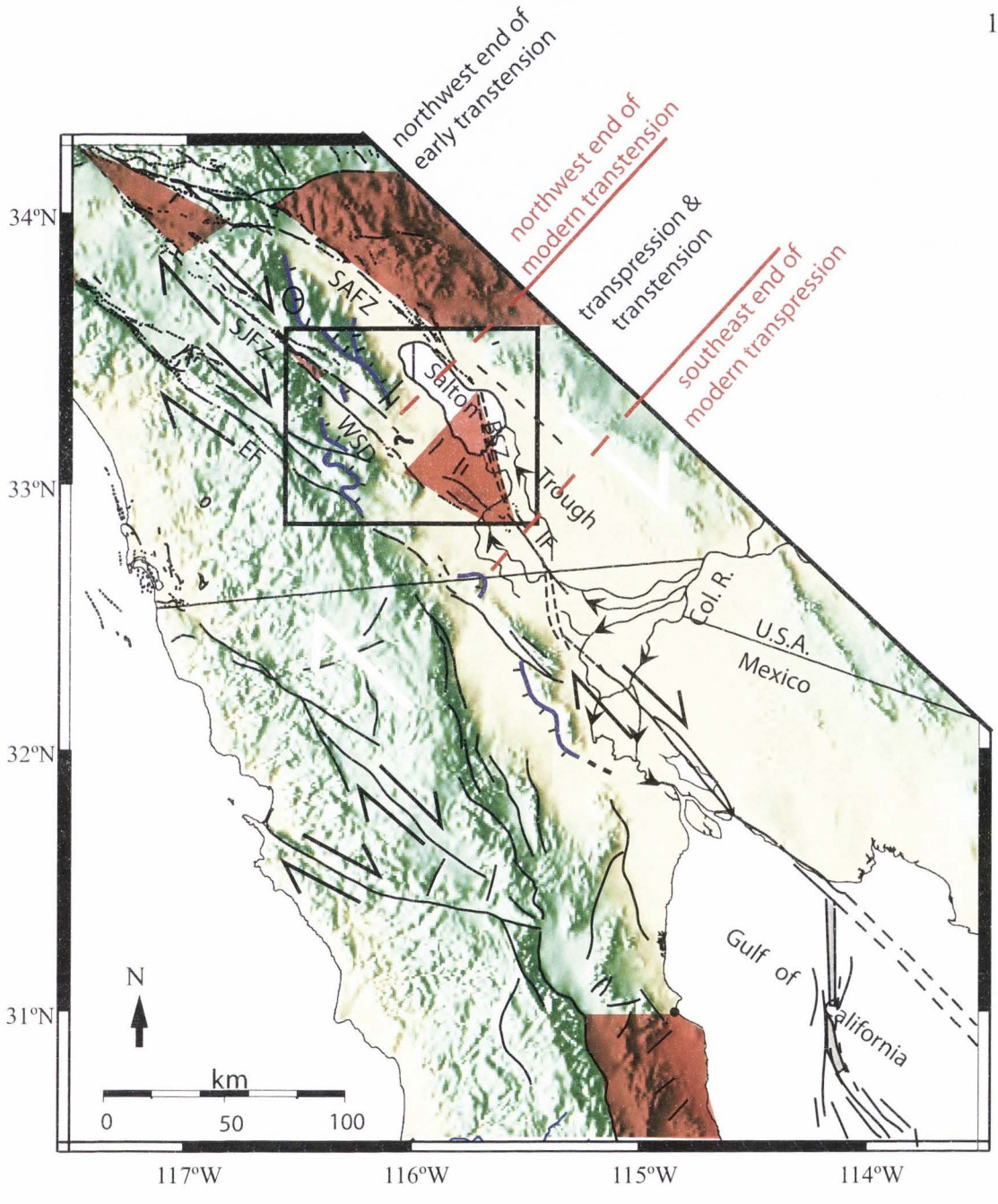

Figure 3-1. Tectonic overview of southern California. Areas of active block rotation are shaded red [*Nicholson et al.*, 1986; *Hudnut et al.*, 1989; *Oskin and Stock*, 2003]. Strike-slip faults are in black; SAFZ=San Andreas fault zone, SJFZ=San Jacinto fault zone, IF=Imperial fault, SJFZ=San Jacinto fault zone, EF=Elsinore fault. BSZ=Brawley Seismic Zone. Oblique-slip detachment faults are in blue including the WSD=West Salton detachment. Fault locations are from *Jennings* [1977], and *Axen and Fletcher* [1998]. Box is approximate location of figure 3-2.

Figure 3-2. Overview of the western Salton Trough. Black box is extent of gravity map in figure 3-8. Red box is the extent of magnetic anomaly map in figure 3-10. Dashed black box is the extent of the study area figure 3-3. CCF, Coyote Creek fault; CF, Clark fault; SAF, San Andreas fault; SHF, Superstition Hills fault; SMF, Superstition Mountain fault; EF, Extra fault; ERF, Elmore Ranch fault; IF, Imperial fault; BSZ, Brawley Seismic zone; DH, Durmid Hills; SFH, San Felipe Hills; OC, Ocotillo Badlands; BB, Borrego Badlands; FCB, Fish Creek-Vallecitos basin; FCM, Fish Creek Mts.; PM Pinyon Mountains; ; CM, Coyote Mountain; C Mts.,Coyote Mountains; SM, Split Mt.; SYM, San Ysidro Mts.; VM,Vallecito Mts.; TBM, Tierra Blanca Mountains; WP, Whale Peak; YR, Yaqui Ridge. Modified from *Axen and Fletcher* [1998].

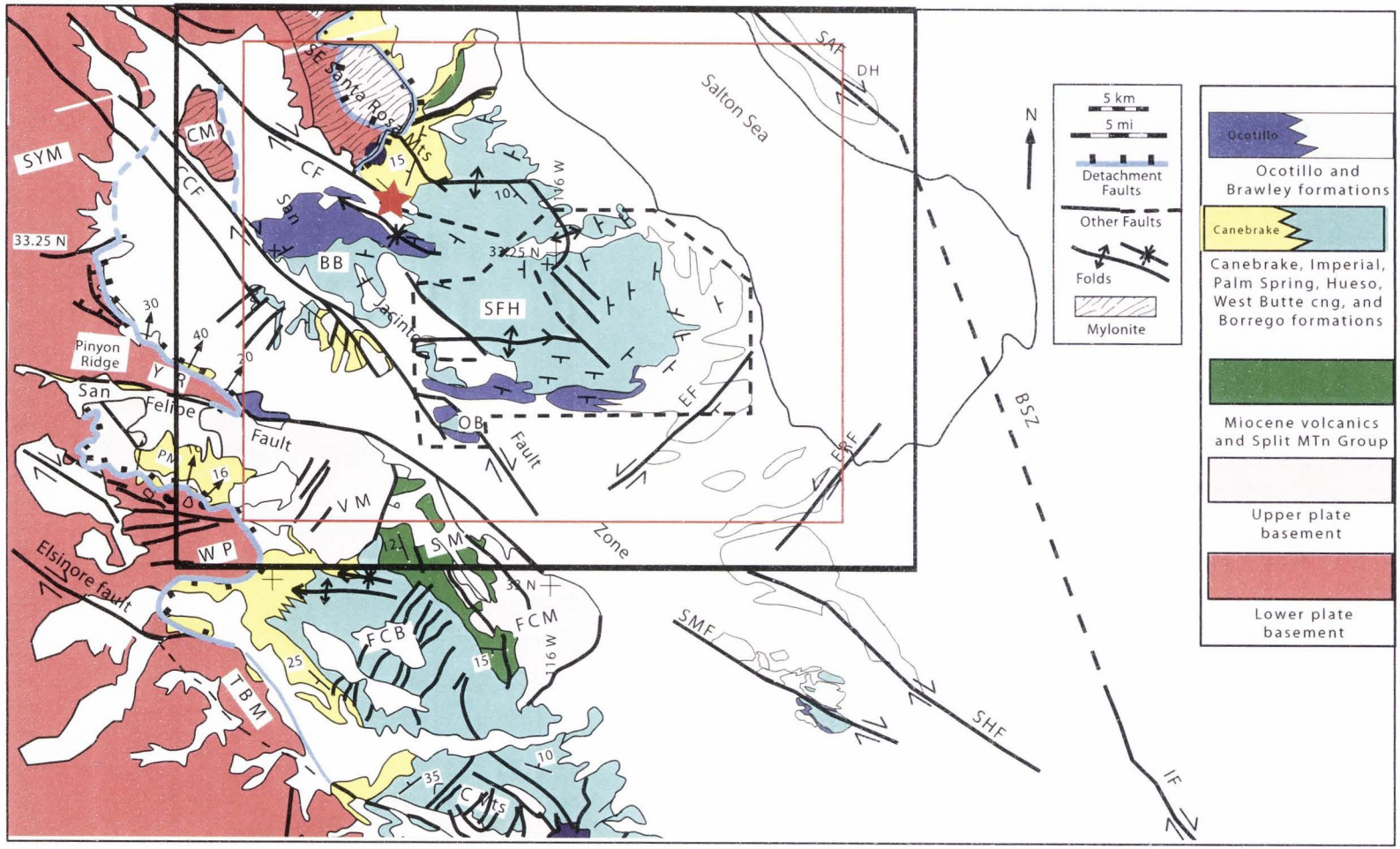

Figure 3-2. Overview of the western Salton Trough.

Figure 3-3. Simplified geology of the San Felipe Hills. Geologic mapping by *Kirby, Janecke, Dorsey and Steely* unpublished mapping [2003], area of compilation from *Girty, Heitmann, and Lilly* unpublished mapping [2002] shown by dashed blue box. Faults are shown in blue and folds in black. Major strike-slip faults within the study area include the San Felipe Hills fault (SFHF), the Dump fault (DF), the Coyote Creek fault (CCF), the Powerline fault (PWF), and the Sand Dune fault (SDF). The trend of the major San Felipe Anticline (SFA) is shown in thicker black line. Locations of cross sections shown by solid black lines. Approximate position of San Felipe wash is shown by the black dashed line. Red dashed lines are state highways. See figure 3-4 for unit descriptions.

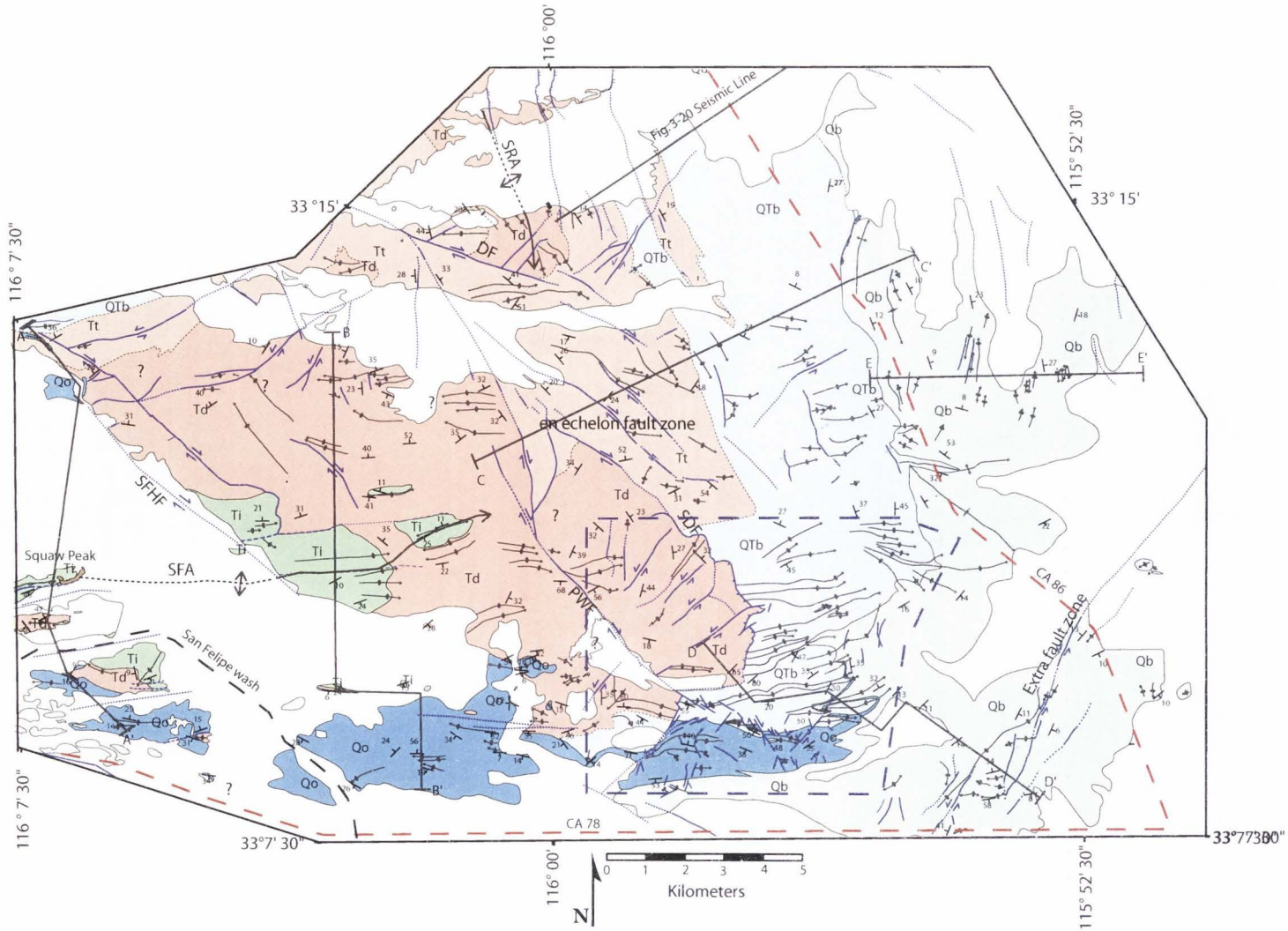

Figure 3-3. Simplified geology of the San Felipe Hills.

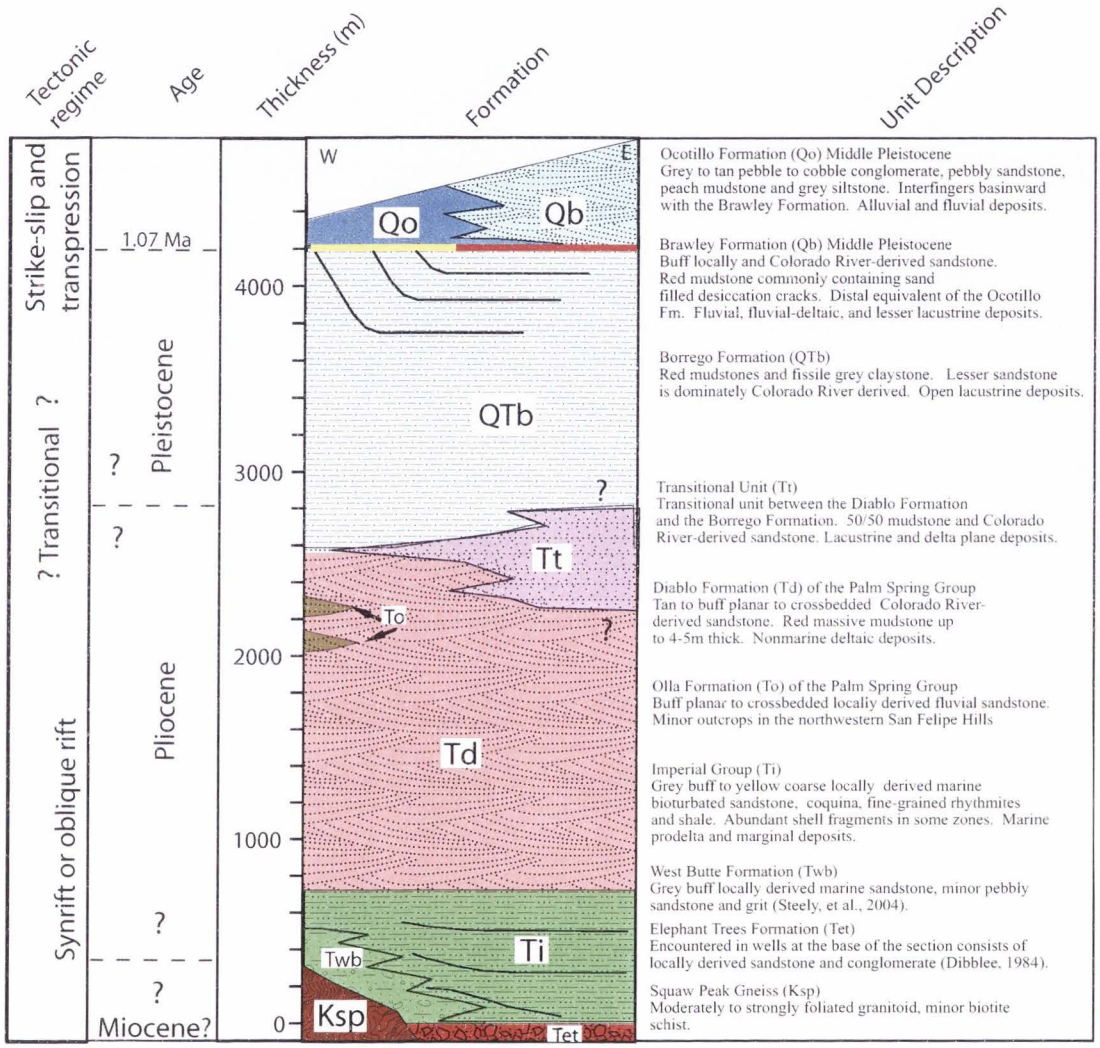

Figure 3-4. Stratigraphic column. Early synrift succession is the Imperial Group to Diablo Formation. The Borrego Formation is a transitional unit. Above these units, across an angular unconformity (shown in yellow) in the west and disconformity (shown in red) in the east are the Ocotillo and Brawley formations which were likely deposited during onset or reorganization of slip on strands of the San Jacinto fault zone. The coarse Ocotillo Formation conglomerate and sandstone interfinger with the finer sandstone of the Brawley Formation to the east within the San Felipe Hills. The 1.07 Ma age of the unconformity was determined paleomagnetically by this study. Other ages are approximate based on work of this study and previous work nearby by *Johnson et al.* [1983], *Remieka and Beske-Diehl* [1996], *Winker and Kidwell* [1996], and *Steely et al.* [2004]. Growth may be apparent in the Imperial-aged deposits just to the west [*Steely et al.*, 2004]. Unit thickness's are minima based on mapping from this study. Units match those in figure 3-3.

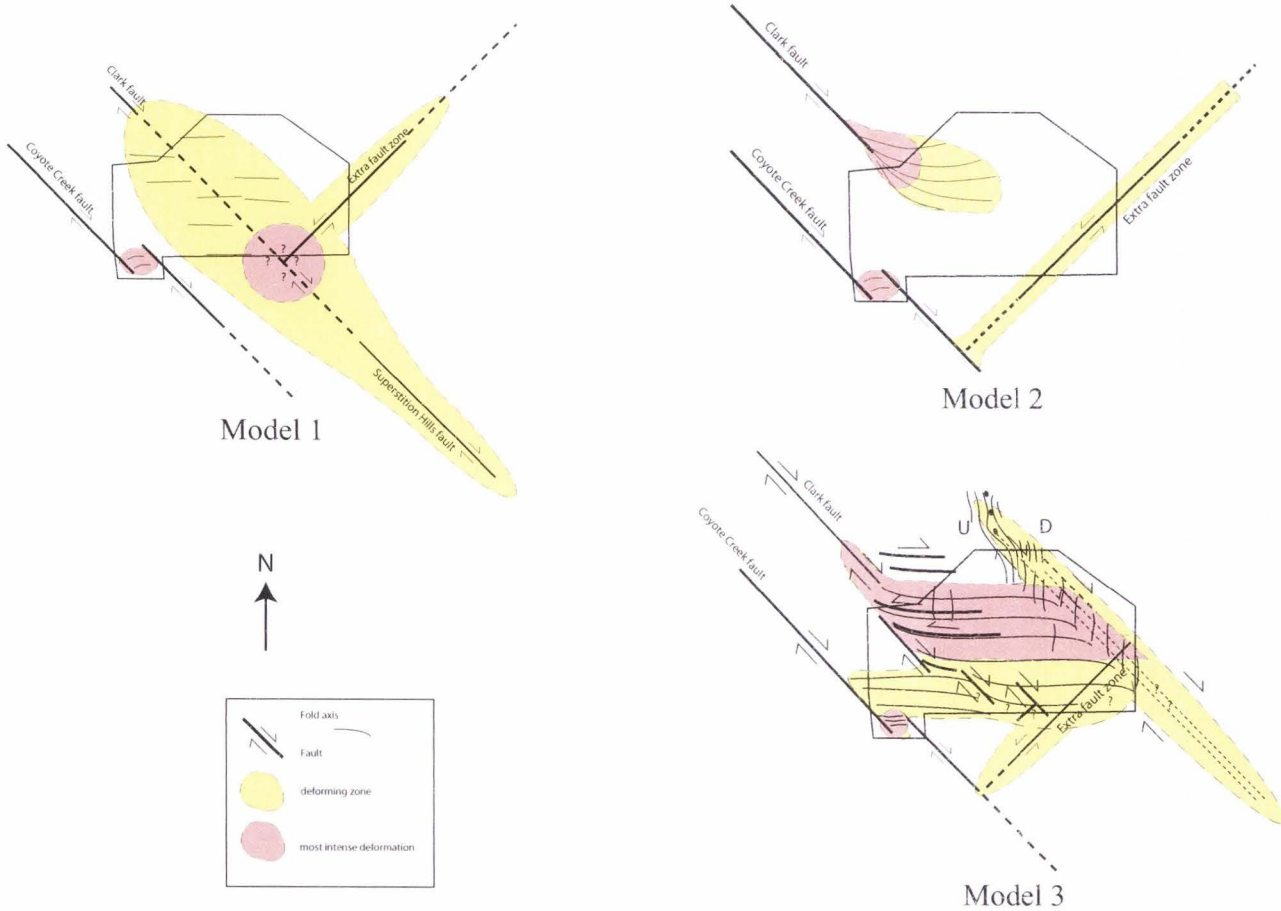

Figure 3-5. Previous kinematic models. The approximate extent of the study area is shown by the black boxes. Model 1 shows a blind continuation of the Clark fault at depth beneath the San Felipe Hills after *Feragen* [1986] and *Wells* [1987]. Model 2 shows the Clark fault terminating within the northern San Felipe Hills as proposed by both *Dibblee* [1954, 1984a], *Sharp* [1972], and *Pettinga* [1991]. Model 3 shows a contractional stepover of the Clark fault onto a blind northwest striking dextral fault zone located near the shore of the Salton Sea after *Janecke et al.* [2003]. See Chapter 3 text for details of each model.

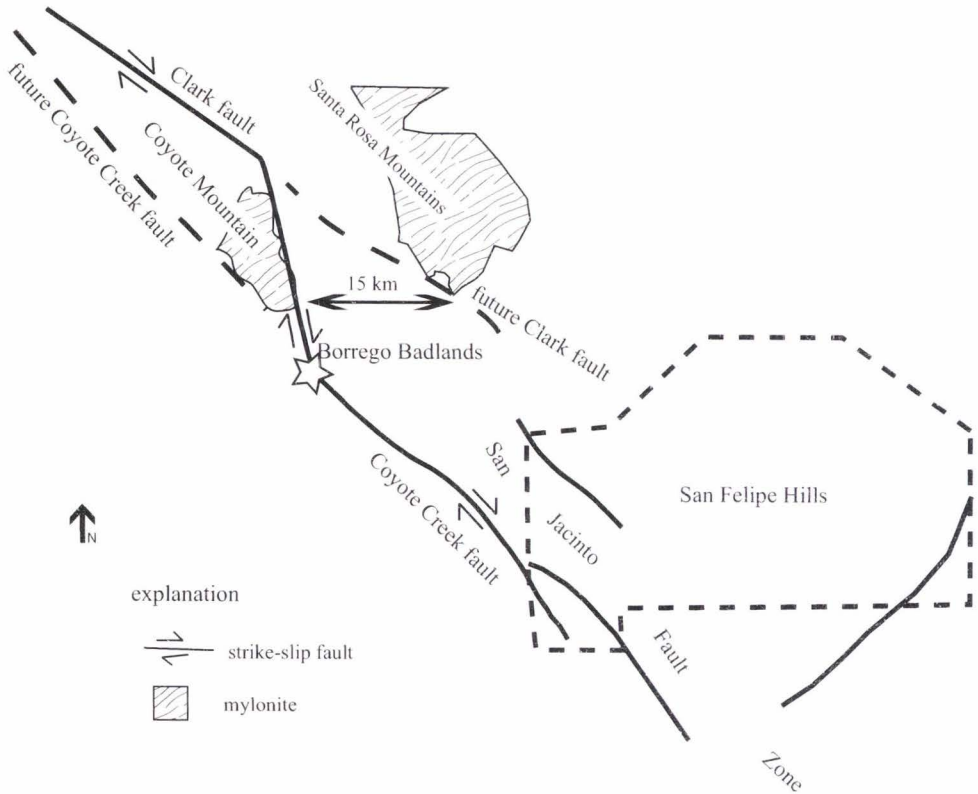

Figure 3-6. Clark fault bend model. Model of an extensional bend in the Clark fault after Bartholomew [1970]. Most of the apparent offset of the mylonite is produced by slip on an older geometry of the Clark fault which transfers slip along the the eastern edge of Coyote Mountain. This model was not directly tested by data in this study, further work in the Borrego Badlands and along the Coyote Creek fault is necessary to determine whether the Coyote Creek fault southeast of the star has more slip than the Coyote Creek fault northwest of the star. Dashed box is the extent of the study area.

Figure 3-7. Fold domain map of the San Felipe Hills. Fold characteristics for domains A-J were computed from field mapping. Data for fold domain K was compiled from *Heitmann* [2002]. Azimuthal orientation of average shortening direction for each domain is shown by black arrows. Average trend and plunge of fold domains is shown by large black arrows. Extent of two transects used to compute total shortening (Table 3.2) most likely related to the Clark fault are shown in black. Faults are shown in blue and folds in black. Major strike-slip faults within the study area include the San Felipe Hills fault (SFHF), the Dump fault (DF), the Powerline fault (PWF) , and the Sand Dunes fault (SDF). The axes of the major San Felipe anticline (SFA) and Santa Rosa anticline (SRA) are shown in black. Major state routes and highways shown by red dashed lines.

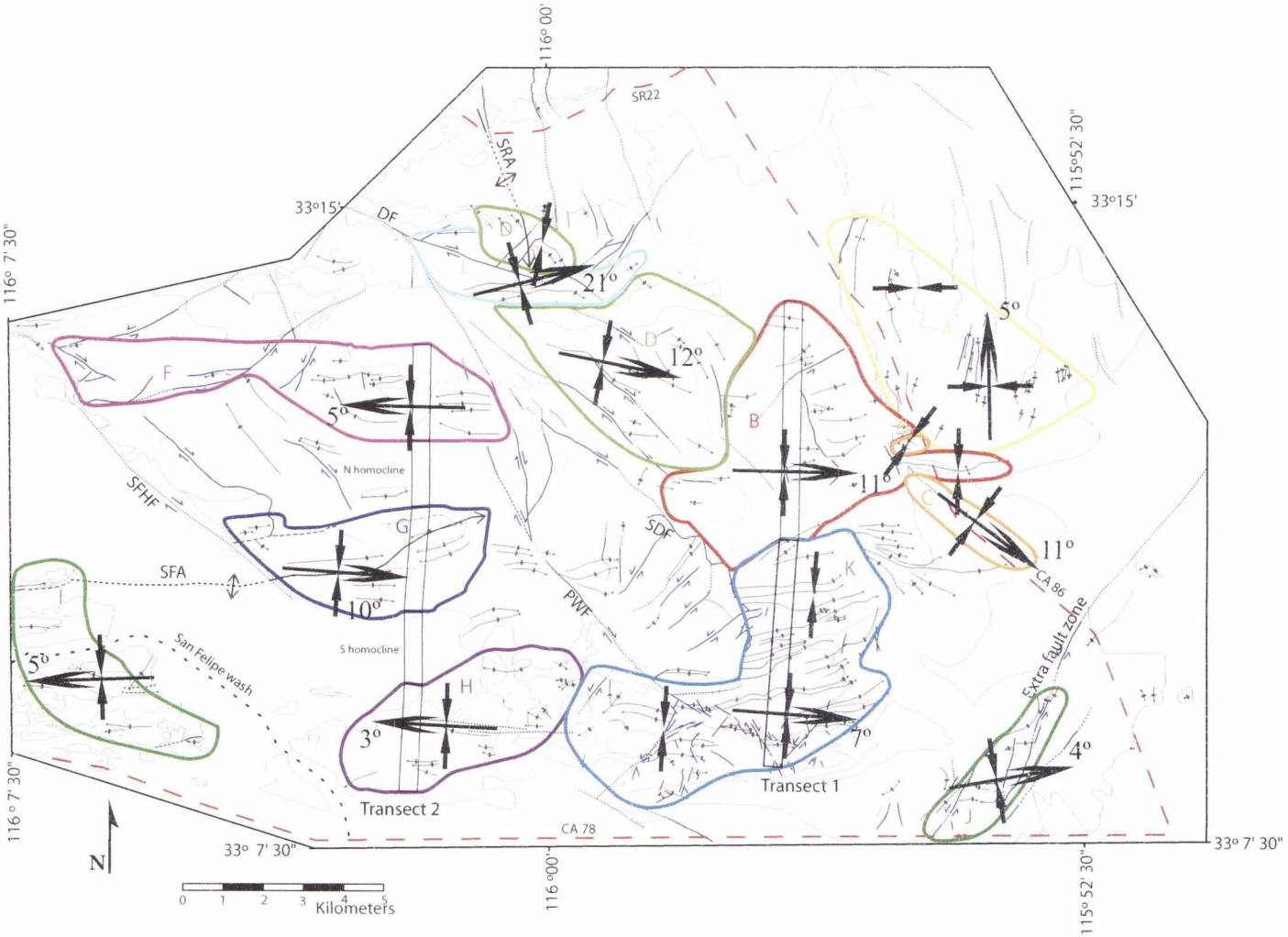

Figure 3-7. Fold domain map.

Figure 3-8. Isostatic gravity anomaly map of the western Salton Trough. Approximate extent of the study area is shown by black dashed box. The gravity signal of the San Felipe anticline (SFA) extends east past the Powerline fault (PWF). The gravity signal of the composite south-plunging Santa Rosa anticline (SRA) is apparent for the northern and central parts of the anticline. Major faults are shown in white including the Clark fault (CF), Coyote Creek fault (CCF), Extra fault zone (EFZ), Elmore Ranch fault (ERF) and the Superstition Hills fault (SHF). Relevant exposures of Plio-Quaternary rocks include the Borrego badlands (BB) and the Ocotillo badlands (OB). State highways are shown by the red dashed lines. Gravity data are from *Langenheim and Jachens* [1993] and *Langenheim* unpublished data [2004].

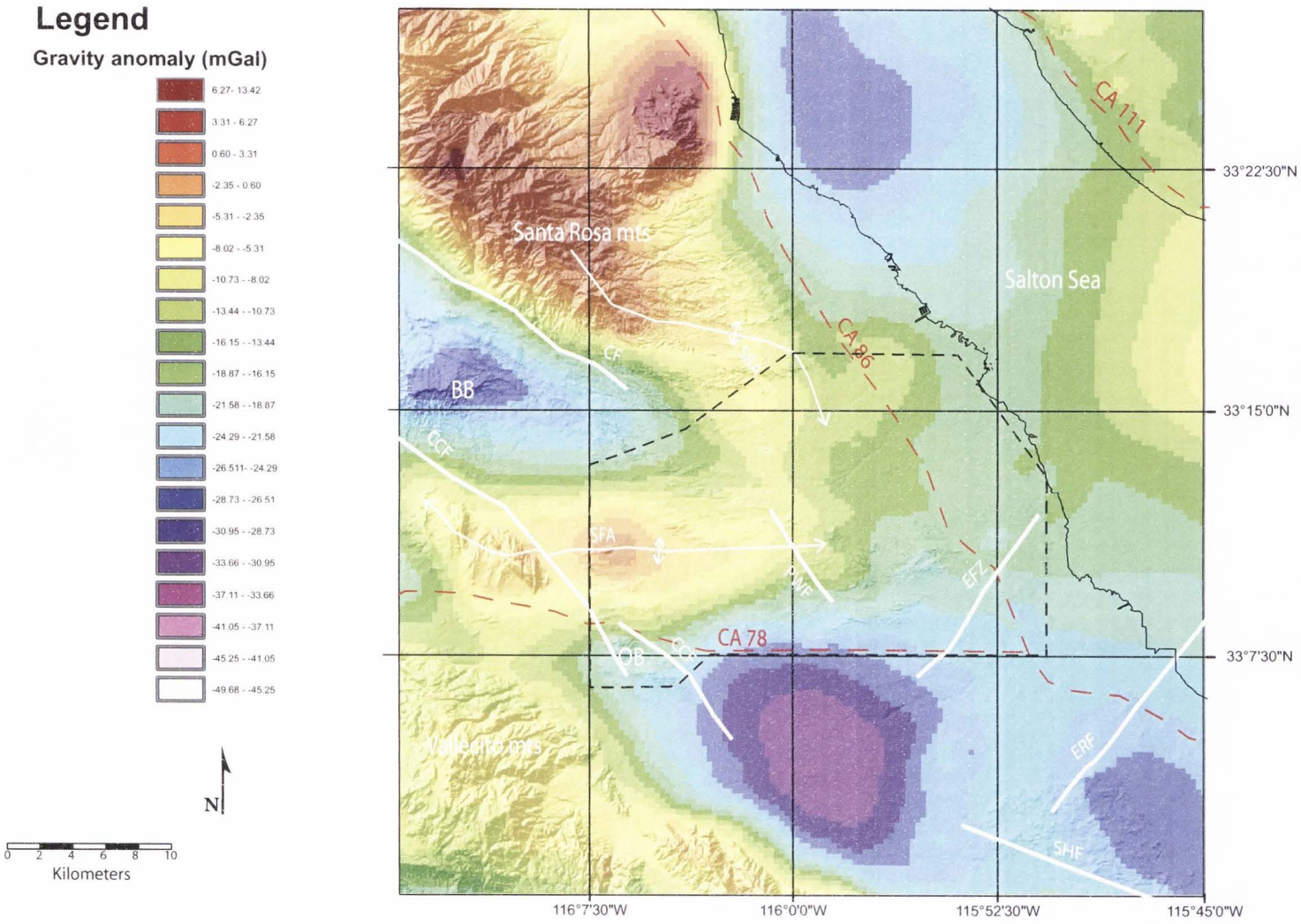

Figure 3-8. Isostatic gravity anomaly map of the western Salton Trough.

Figure 3-9. Isostatic gravity and surficial geology of the San Felipe Hills. Gravity extent of the San Felipe anticline corresponds well with mapped San Felipe anticline (SFA). Gravity signal of the Santa Rosa anticline (SRA) is offset from the mapped axis of this fold. Faults are shown in blue and folds in black. Major strike-slip faults within the study area include the SFHF (San Felipe Hills fault), the DF (Dump fault), the PWF (Powerline fault), and the SDF (Sand Dunes fault). The trends of the major SFA (San Felipe Anticline) and SRA (Santa Rosa Anticline) are shown in black. Approximate position of San Felipe Wash is shown by the black dashed line. Red dashed lines are state highways. Gravity data are from *Langenheim and Jachens* [1993] and *Langenheim* unpublished data [2004].

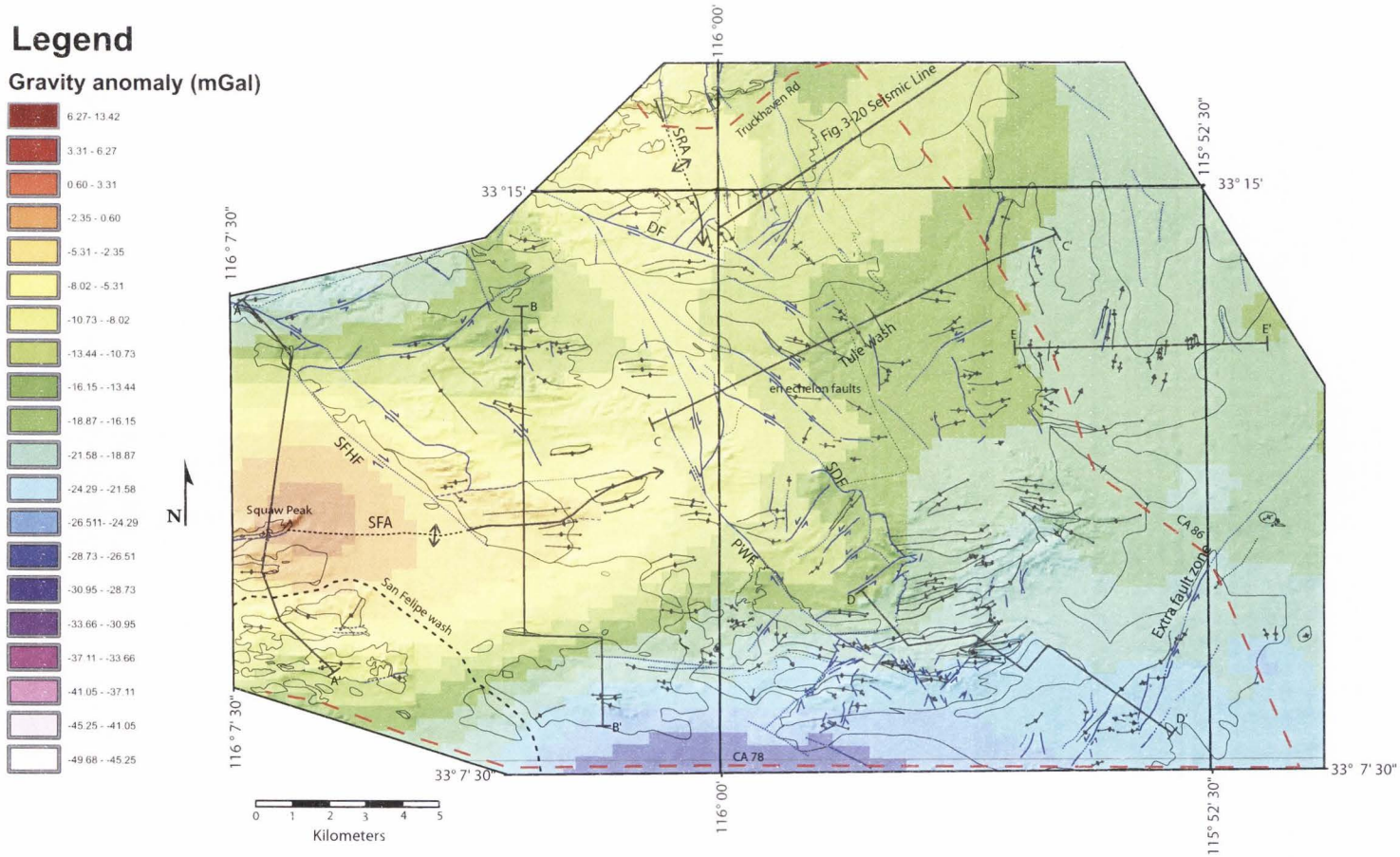

Figure 3-9. Isostatic gravity and surficial geology of the San Felipe Hills.

Figure 3-10. Magnetic anomaly map of the western Salton Trough. Magnetic anomaly has been filtered to enhance shallow sources [*Langenheim*, unpublished data, 2004]. Edge of color shade is the edge of available detailed data. Black dashed box is the approximate extent of the study area. Major structures apparent on the magnetic anomaly include the Coyote Creek fault (CCF), Clark fault (CF), San Felipe Hills fault (SFHF), Extra fault zone (EFZ), and Powerline fault (PWF). Several magnetic lineaments represent the magnetic signal of the diffuse strands of the Clark fault (CFS) found by this study in the field area. The expression of the San Felipe anticline (SFA) and the Santa Rosa anticline (SRA) is apparent. Magnetic signal of the SFA across the CCF is much lower west of the fault p does not show this juxtaposition. Nearby exposures of Plio-Quaternary strata include the Ocotillo badlands ()B) and Borrego badlands (BB). State highways are the red dashed lines.

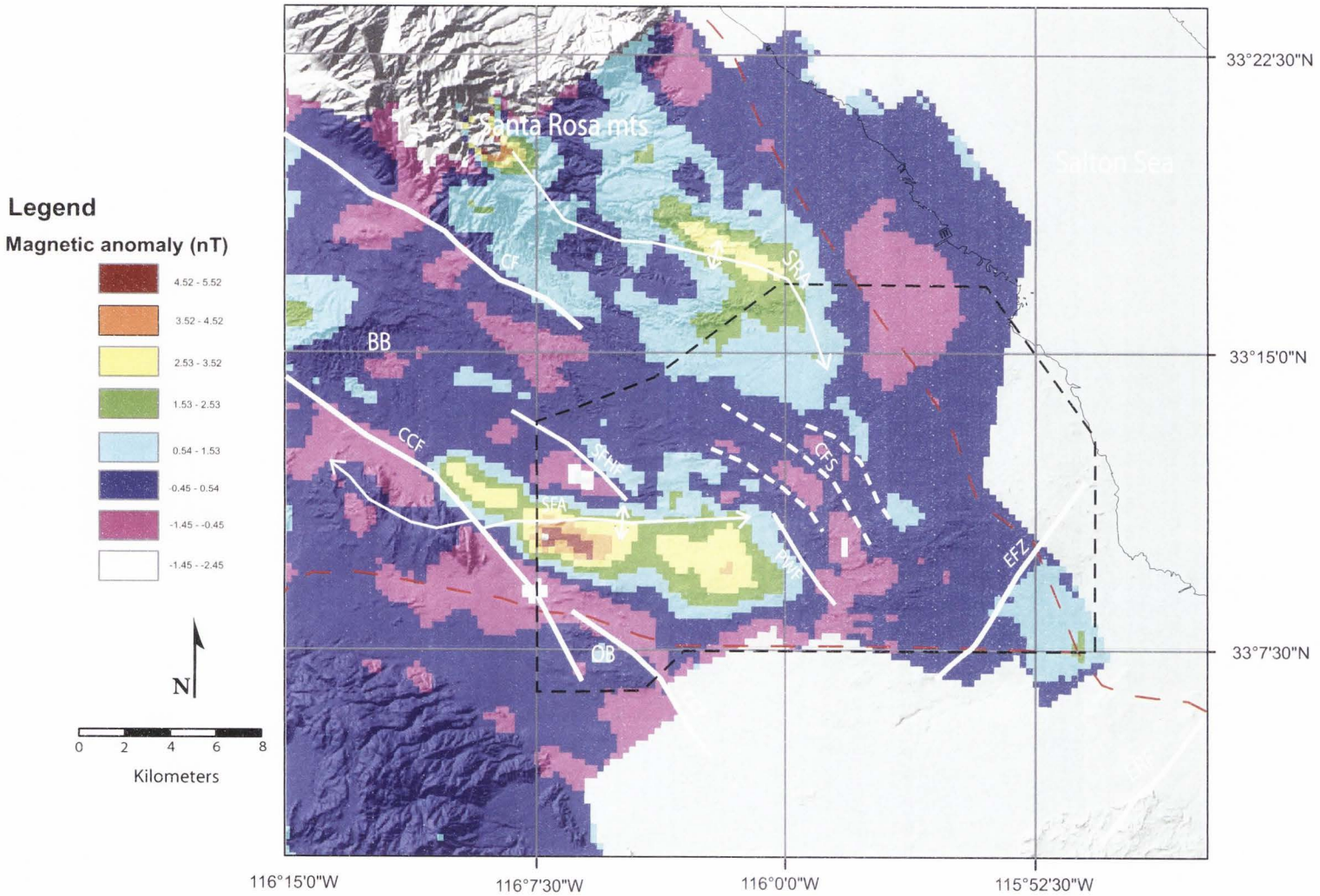

Figure 3-10. Magnetic anomaly map of the western Salton Trough.

Figure 3-11. Filtered magnetic anomaly and surficial geology of the San Felipe Hills. Magnetic gradients correlate with the surficial Sand Dunes fault (SDF) and the en echelon northwest trending faults just to the north. Faults are shown in blue and folds in black. Major strike-slip faults within the study area include the San Felipe Hills fault (SFHF), the Dump Fault (DF), the Powerline fault (), and the Sand Dunes fault (SDF). The trends of the major San Felipe Anticline (SFA) and Santa Rosa Anticline (SRA) are shown in black. Approximate position of San Felipe Wash is shown by the black dashed line. Red dashed lines are state highways. Locations of cross sections shown in black.

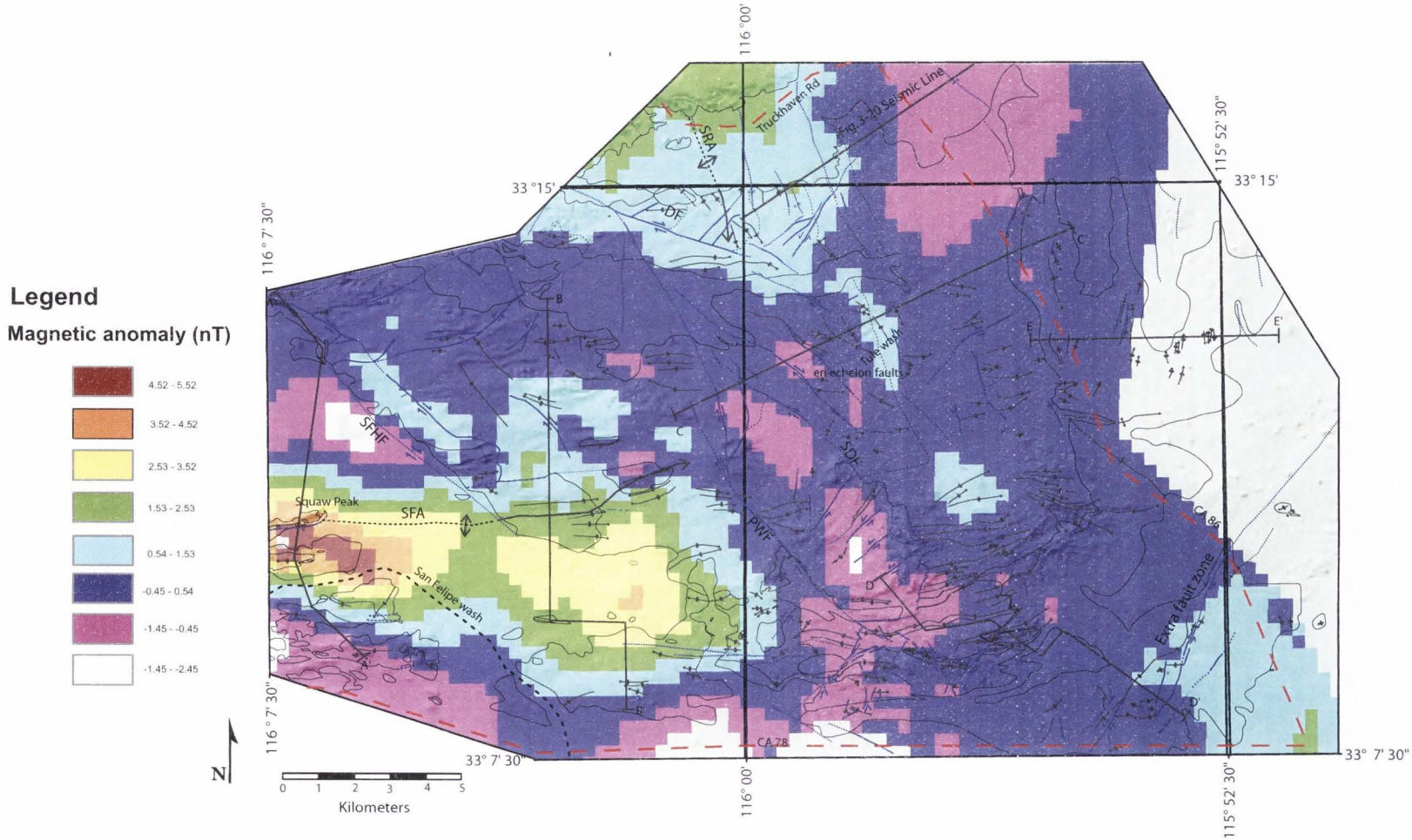

Figure 3-11. Magnetic anomaly and surficial geology of the San Felipe Hills.

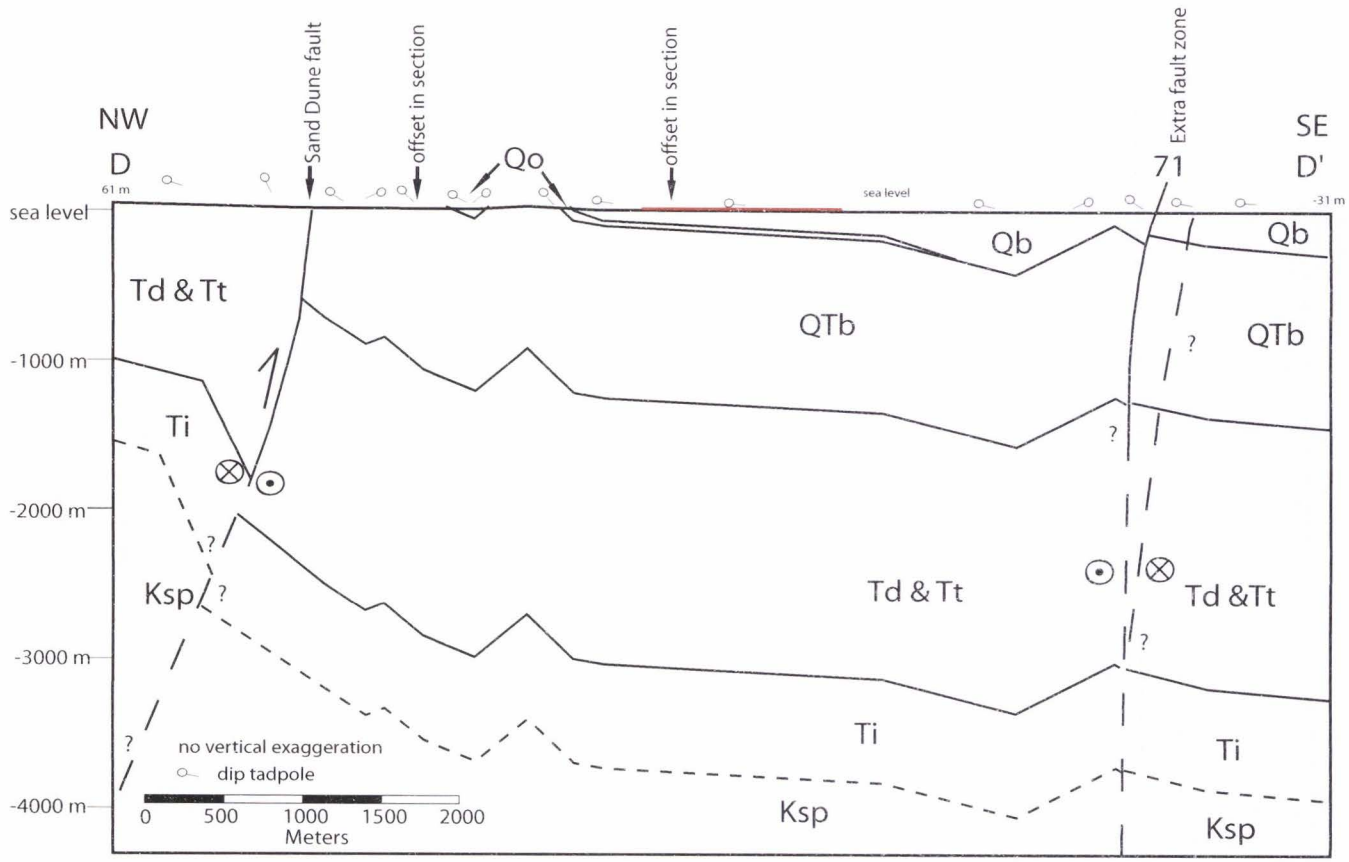

Figure 3-12. Cross section D-D'. Cross section through the southeastern San Felipe Hills from southeast to northwest. Two offsets of the section were made to the west; see figure 3-3. Units are Ksp (Squaw Peak gneiss), Ti (Imperial Group), Td (Diablo Formation), Tt (transitional unit), QTb (Borrego Formation), Qo (Ocotillo Formation), and Qb (Brawley Formation). Vertical offset across the Sand Dunes fault is uncertain. Red line is the extent of surficial cover.

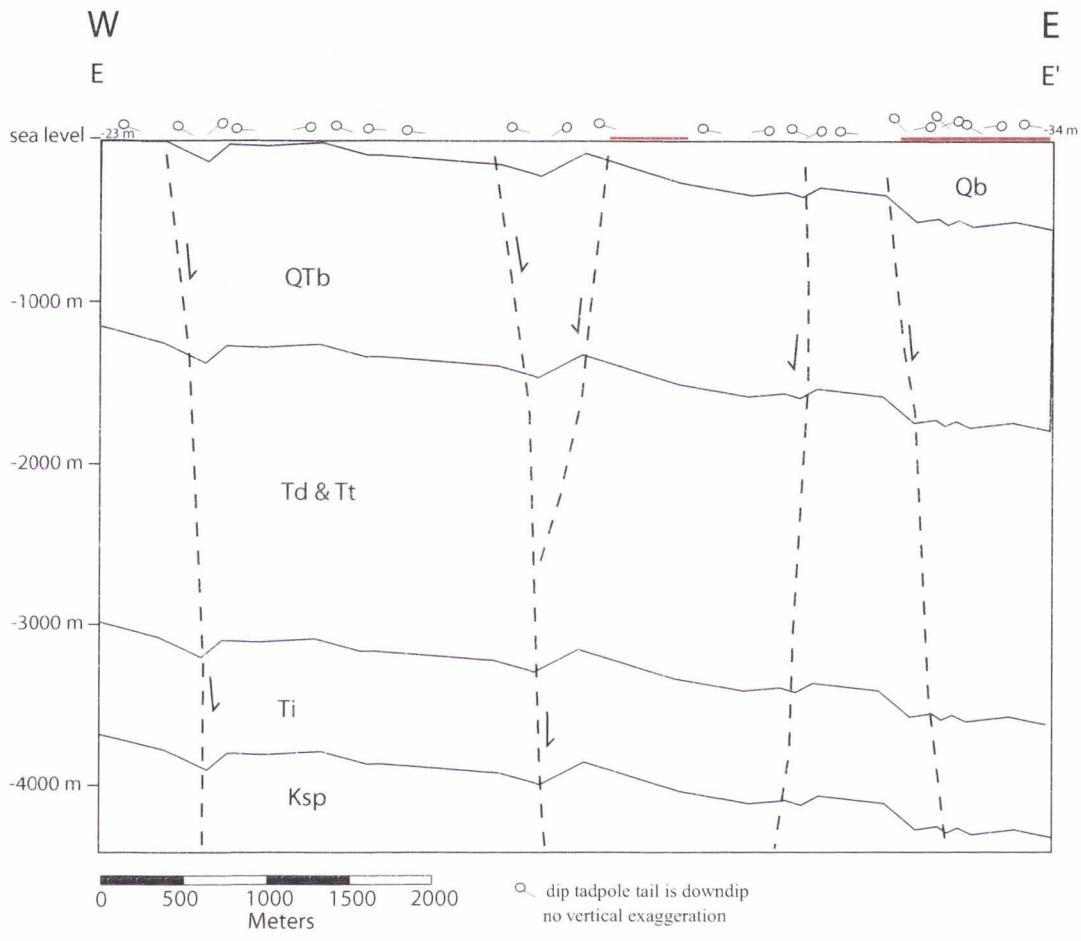

Figure 3-13. Cross section E-E'. East-west cross section through the north-plunging folds of fold domain a in the eastern San Felipe Hills. Units are Ksp (Squaw Peak gneiss), Ti (Imperial Group), Td (Diablo Formation), Tt (transitional unit), QTb (Borrego Formation), and Qb (Brawley Formation). Folding along this section may be related to east-west extension andsubsidence of the Salton Trough, dashed faults are inferred. Red line shows covered areas. See Plate 1 for location of strike-and-dips along eastern portion of cross section. See figure 3-3 for cross section location.

Figure 3-14. Cross section A-A'. North-south cross section in the western San Felipe Hills through the east-plunging San Felipe anticline. Units include the Ksp (Squaw Peak gneiss), Ti (Imperial Group), Td (Diablo Formation), Tt (transitional unit), QTb (Borrego Formation), and the Qo (Ocotillo Formation). Black tadpoles represent the dips of all units except the Ocotillo Formation. Red tadpoles represent the dip of the Ocotillo Formation. Red line represents the extent of surficial coverage. Blue dashed line is the west Salton detachment fault (WSD) which in this orientation has upper plate motion into the page. It is inferred that the detachment fault was folded by the San Felipe anticline and then faulted by east-west strike-slip faults which are driven by slip on the nearby Coyote Creek fault and San Felipe Hills fault. Separation across the San Felipe Hills fault is uncertain. Relative thickness of upper plate basement is inferred to show a persistent bedrock high located beneath Squaw Peak. See figure 3-3 for location.

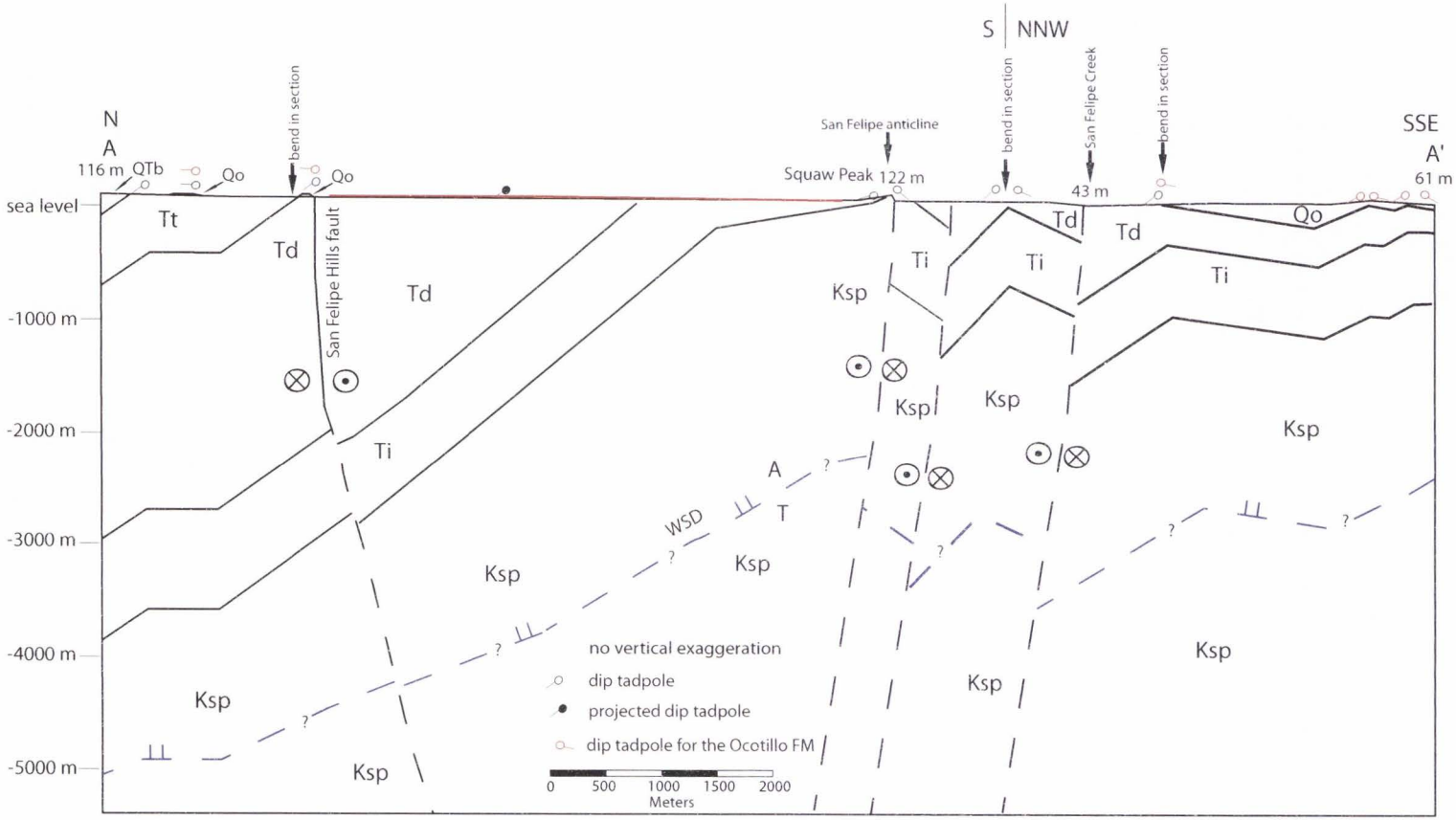

Figure 3-14. Cross section A-A'.

Figure 3-15. Cross section B-B'. North-south cross section through the San Felipe anticline. Units include Ksp (Squaw Peak gneiss), Ti (Imperial Group), Td (Diablo Formation), and Qo (Ocotillo Formation). Black tadpoles are dips for all units except the Ocotillo Formation. Red tadpoles are the dips for the Ocotillo Formation. The Ocotillo Formation lies in angular unconformity on the Diablo Formation on the south end of the cross section. The blue line is the west Salton detachment fault. Red line is the extent of surficial cover. Upper plate motion is into the page. The detachment is inferred to have been folded and faulted after it ceased slipping. The thickness of the upper plate basement is uniform across this cross section. Several high angle east-west striking strike-slip faults in this section are assumed to be left lateral faults based on kinematic indicators on east-west striking faults in the northwest portion of the study area. See figure 3-3 for cross section location.

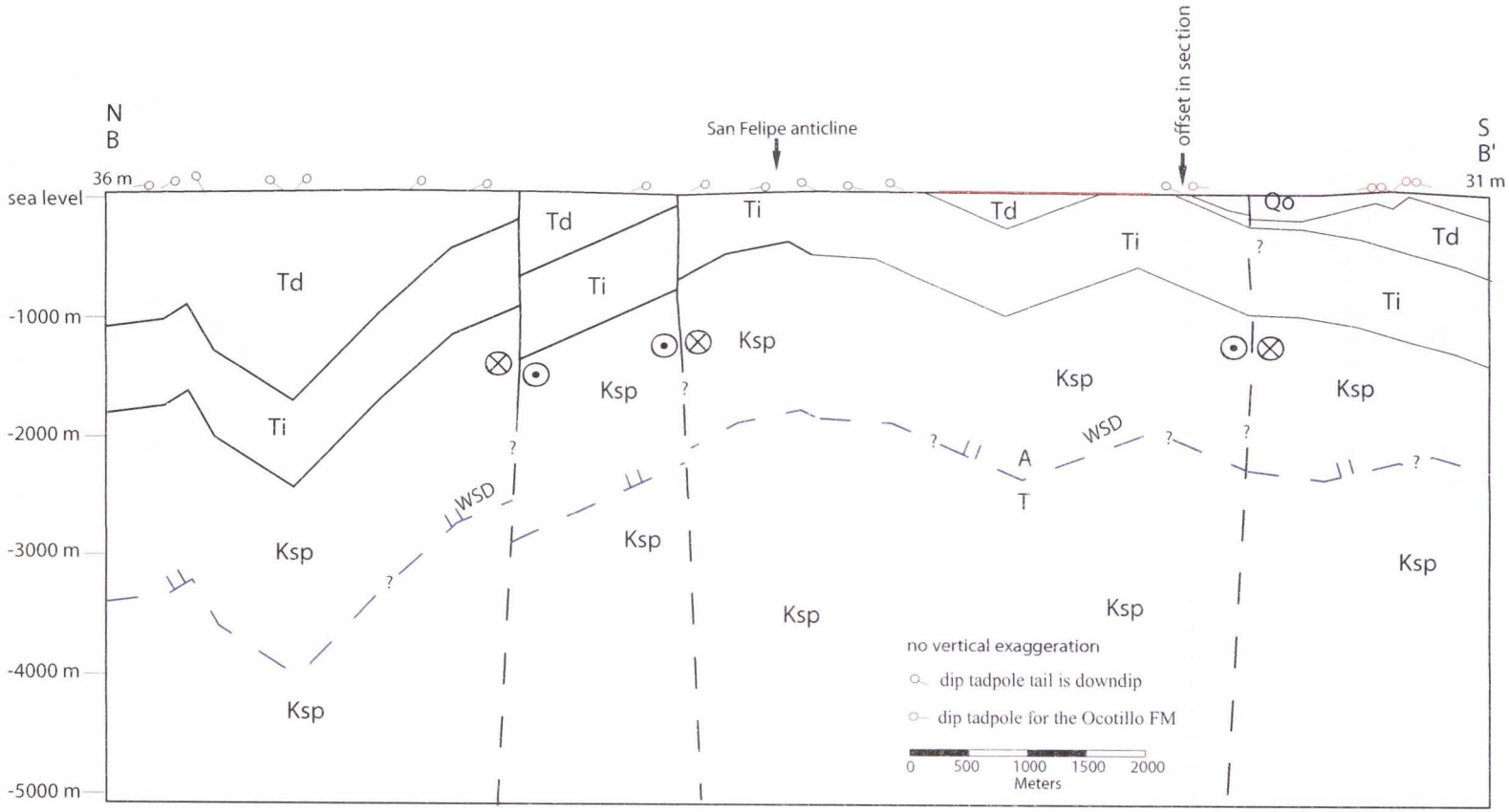

Figure 3-15. Cross section B-B'.

Figure 3-16. Cross section C-C'. Cross section through the en echelon strands of the Clark fault in the central San Felipe Hills. Subsurface geometries and structure inferred from seismic reflection data from *Severson* [1987] ~7 km to the northeast. See figure 3-20 for interpreted seismic line. Cross-cutting relationships shown in the cross section imply that the detachment stopped slipping at the end of deposition of the Diablo Formation. Black-dashed strike-slip fault strands correspond with magnetic linaments in figure 3-11. Dashed blue lines are normal faults and the west Salton detachment fault (WSD). Red line represents a regional disconformity at the base of the Brawley Formation [*Chapter 2*]. Units Peak gneiss), Ti (Imperial Group), Td (Diablo Formation), Tt (transitional unit), QTb (Formation), and Qb (Brawley Formation), QTu (undivided QT sediments). See figure 3-3 for cross section location.

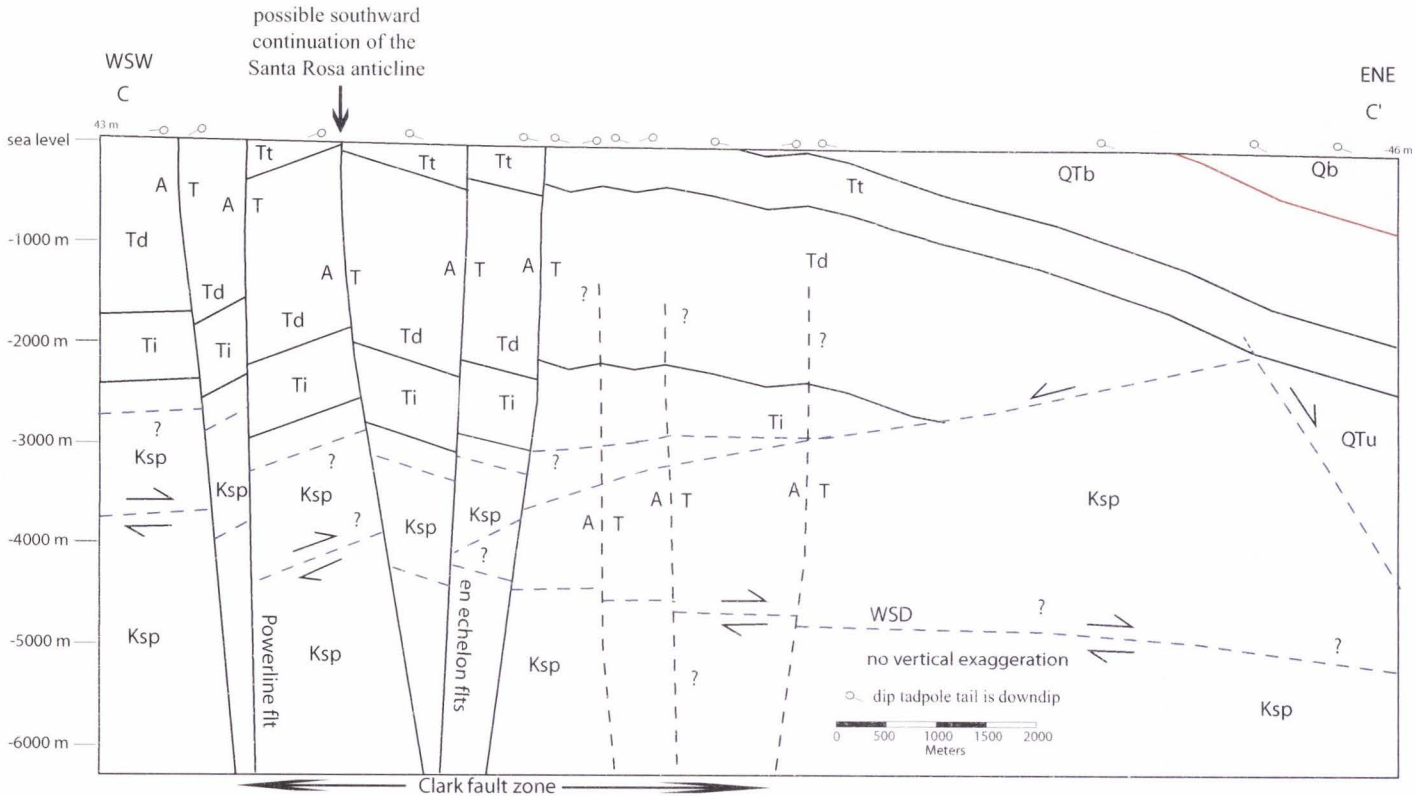

Figure 3-16. Cross section C-C'

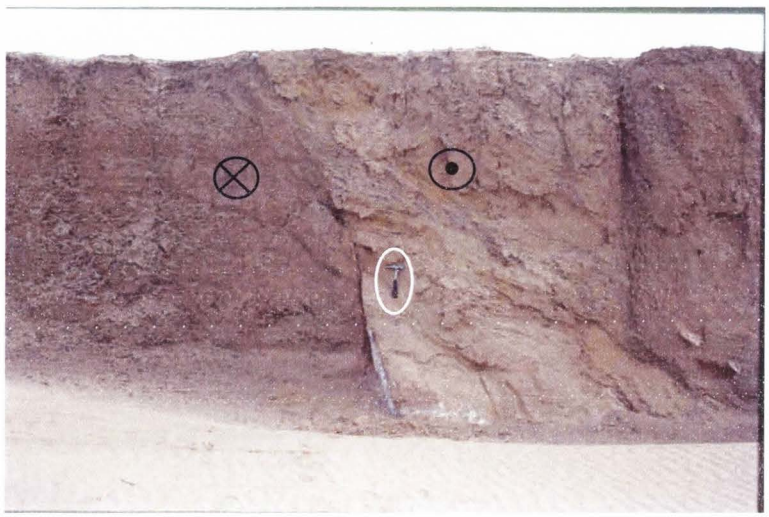

Figure 3-17. Photograph of the Powerline fault. View is to the south along Tule Wash. Right lateral fault motion places red mudstones against tan sandstones of the transitional unit (Td-m). Hammer for scale.

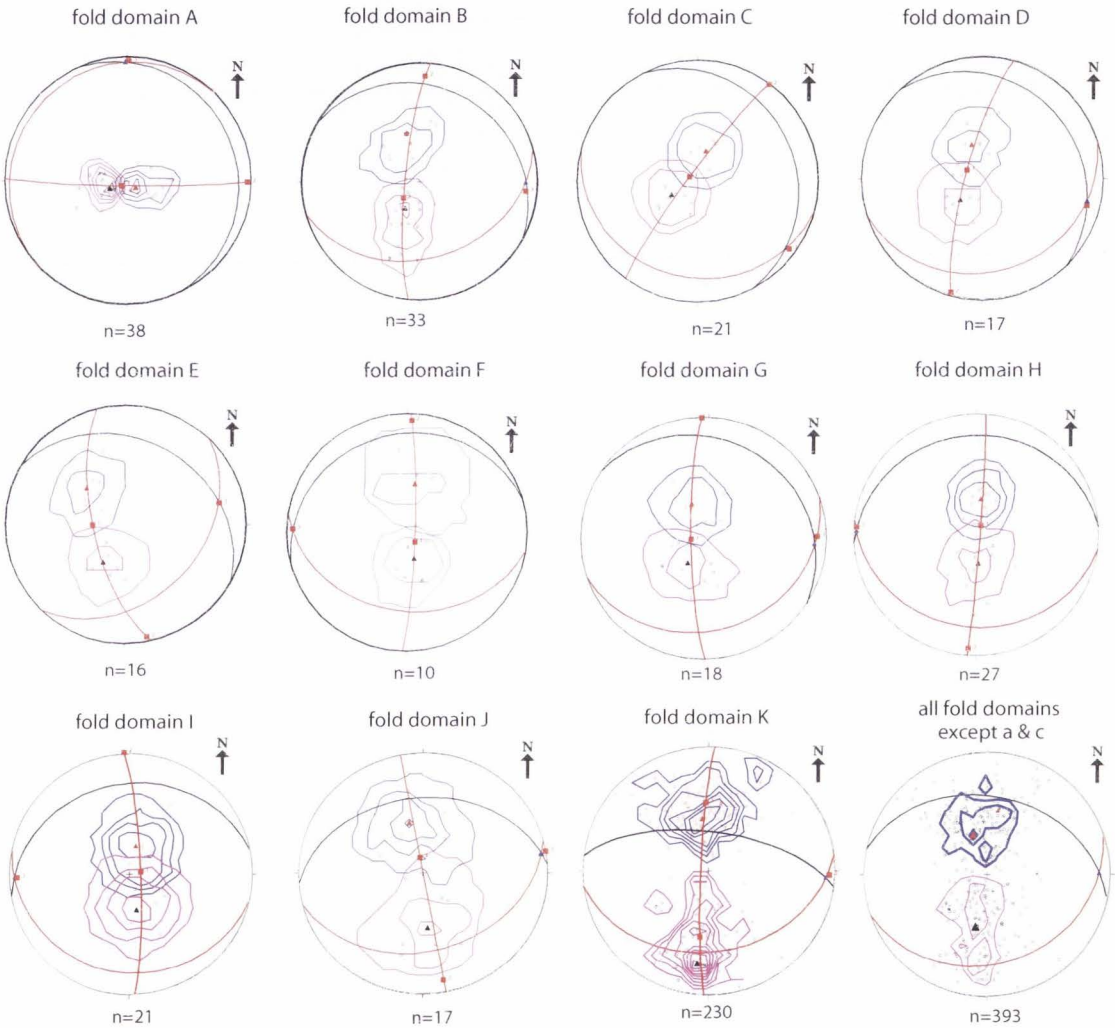

Figure 3-18. Stereonets for fold domains. For each fold domain shown in figure 3-7 strike and dip data were plotted as poles to planes and kamb contoured using a significance level of 1 sigma and a contour interval of 4.0 using stereonet software. Kamb contour of poles to fold limbs shown in purple and blue. Average fold limb picks are in red and black. Blue triangle represents the average trend and plunge in each fold domain. Cylindrical bestfit shown in red. Eigen vectors are shown by red boxes. Numerical data are summarized in tables 3-1 and 3-3.

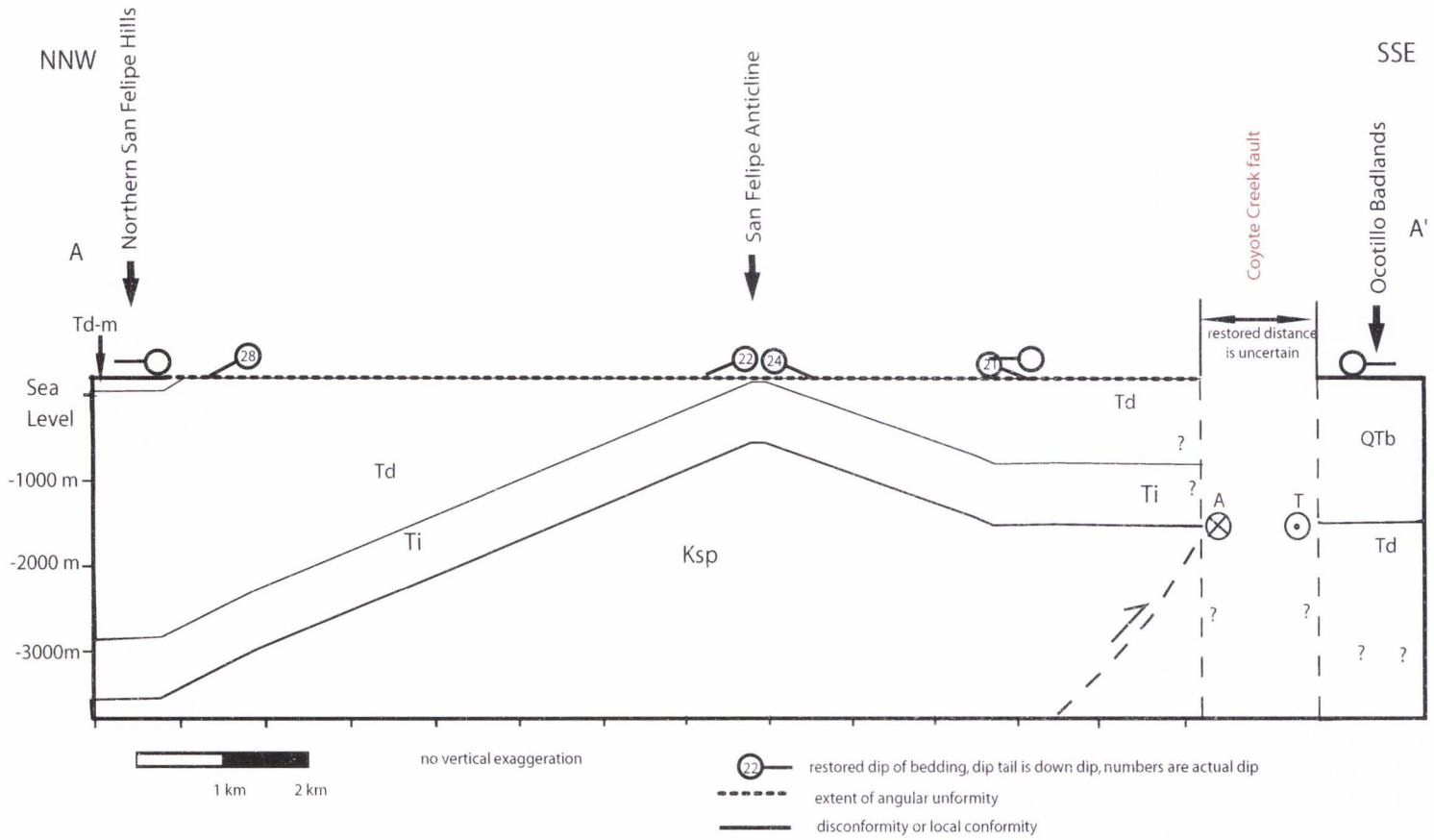

Figure 3-19. Reconstructed cross section of the San Felipe anticline at 1Ma created from the angular relations between the Ocotillo Formation and the older units beneath it. Offset across the Coyote Creek fault along the south limb of the San Felipe anticline is unconstrained. Offset across the Coyote Creek fault on the north limb of the San Felipe anticline may be 4 km based on offset gravity anomalies (*Janecke and Langenheim pers. comm.*). Units correspond with those used in figures 3-3, 3-4. Dip tadpoles without numbers indicate flat sub-Ocotillo Formation bedding. Location of cross section is shown on figure 2-3.

Figure 3-20. Seismic line in the northeast San Felipe Hills. Industry seismic line from *Severson* [1987]. Seismic interpretation shows faults as dashed red lines, the solid red line represents top of basement and probable faults, prominent sedimentary reflectors are shown in blue. Basement interpretation for cross section C-C' (figure 3-16) is from this seismic line. Location of seismic line is shown on figure 3-3. Depth to basement for Pure Oil #1 well is 2000 m [*Severson*, 1987; *Layman* unpublished data, 2005]. Units are QTb (Borrego Formation), Qb (Brawley Formation) and pT (preTertiary basement).

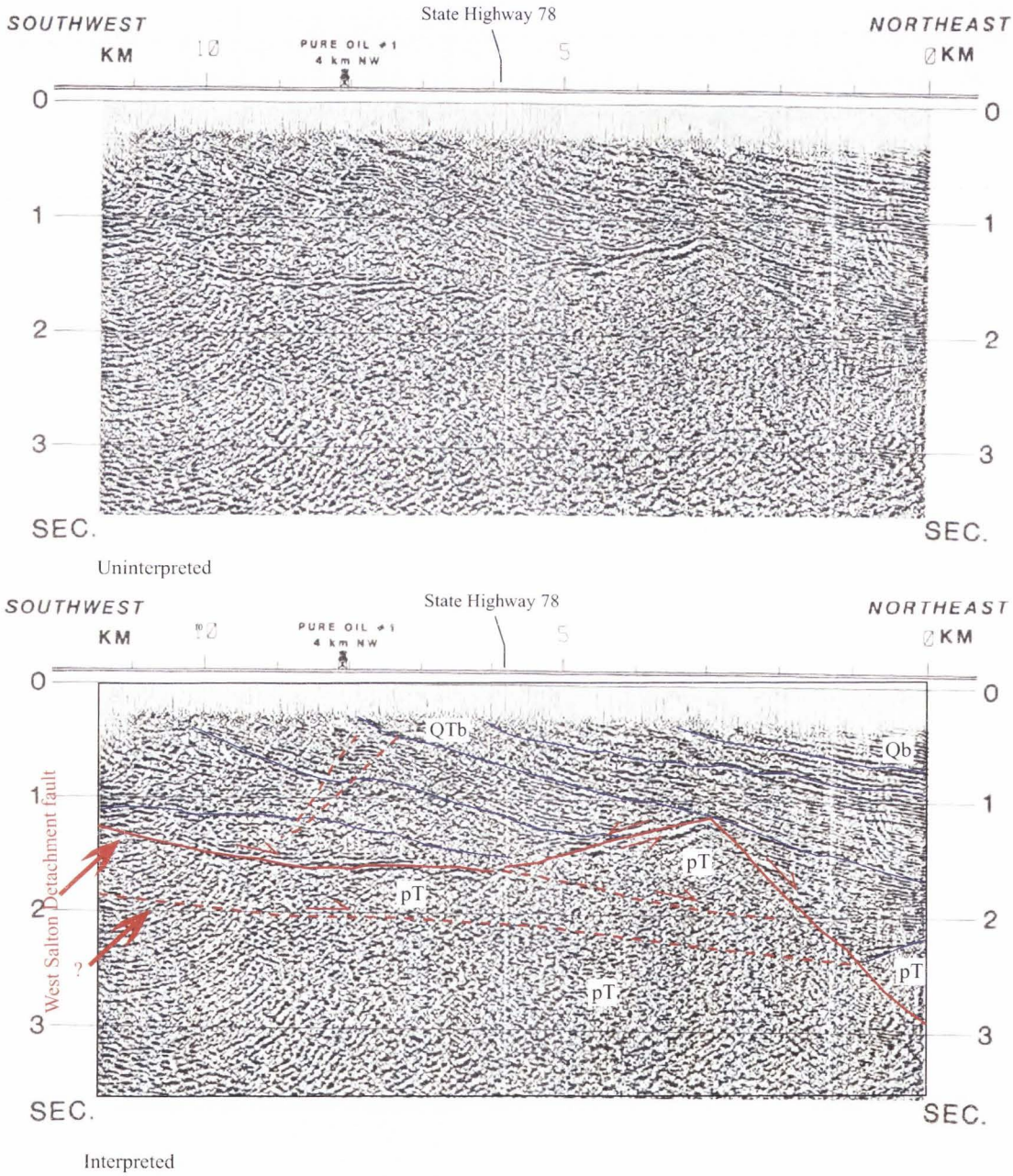

Figure 3-20. Seismic line in the northeast San Felipe Hills.

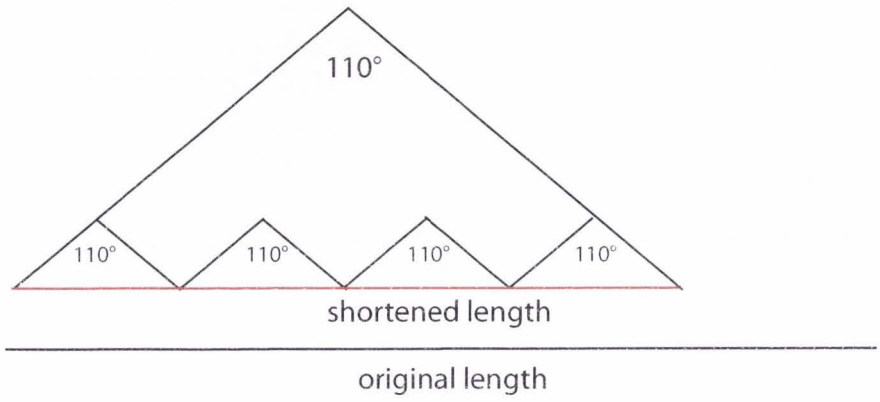

Figure 3-21. Shortening from folding diagram. Diagram shows unit length of a given fold domain before shortening in black. Shortened length is calculated from mean interlimb angle for each fold domain. Folds are assumed to have kink fold geometry.

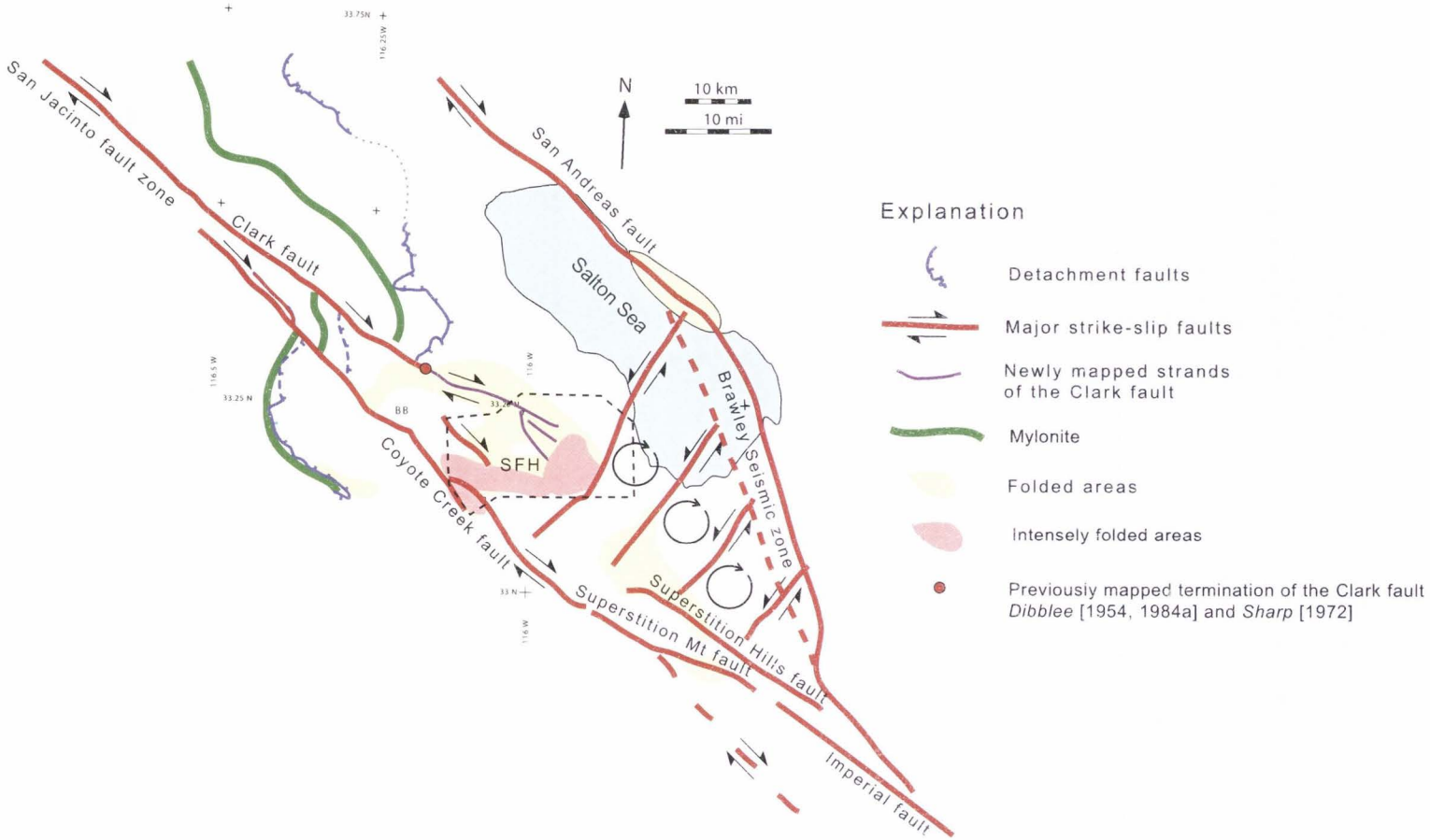

Figure 3-22. Preferred geometryof the Clark fault. This model shows the Clark fault transferring slip to a province sinstral faults and clockwise rotation to the southeast. Black dashed box is the extent of the study area. The highest strain and most intense deformation occurs where the discontinuous strands of the Clark fault interact with the northwest-most rotating block shown by red shade. Strain and deformation throughout the rest of the San Felipe Hills are moderate. Orientation of folding is generally east-west in the San Felipe Hills (SFH).

CHAPTER 4

CONCLUSIONS

We examined stratigraphic and structural relationships well exposed in the Plio-Quaternary rocks of the San Felipe Hills, in order to characterize the evolution of the North American-Pacific plate boundary in the Salton Trough area. Early extension localized on the West Salton detachment fault was replaced sometime after ~1.5 to 1.1 Ma by slip on cross cutting strike-slip faults. Our work provides detailed constraints on the timing and kinematic evolution of strike-slip faulting including fault strands of San Jacinto fault zone in the western Salton Trough.

Stratigraphic analysis of the Ocotillo and Brawley formations and their relations with the underlying units provides constraints on the evolution of the San Jacinto fault zone between ~ 1 and 0.5 Ma. Our work accurately constrains the age and depositional environment of the Brawley Formation in the San Felipe Hills for the first time. We measures 550 m of the Brawley Formation in the southeastern San Felipe Hills. Magneto-stratigraphy along this section shows that the Brawley Formation was deposited between 1.07 Ma and 0.61 Ma $\pm$ 0.02 Ma and 0.52 Ma $\pm$ 0.03 Ma (Chapter 2). A 245 m section of the coarse lateral equivalent of the Brawley Formation, the Ocotillo Formation, described in the Ocotillo badlands shows rapid westward coarsening relative to the and Brawley Formation to the east (Chapter 2). Plio-Pleistocene sedimentary rocks in the San Felipe Hills, Salton Trough record an abrupt change from older, open, perennial lake beds to cyclic alluvial fan, fluvial-deltaic, and marginal lacustrine deposits at 1.07 Ma. The ~1680 m thick lacustrine claystone, mudstone, and sandstone of the Borrego Formation in the San Felipe Hills preserve almost no marginal lacustrine deposits and formed in a

large perennial lake. A regional disconformity and laterally equivalent angular unconformity at the crest of a 15 km long east-west trending bedrock-cored anticline separate the Borrego Formation from the overlying Ocotillo Formation and its fine-grained equivalent, the Brawley Formation (Chapter 2). This east-west trending anticline is interpreted as the first evidence for transpressional deformation within the previously transtensional southwest Salton supradetachment basin.

The Ocotillo Formation is dominated by alluvial fan and braided stream facies, with lesser fluvial and minor lacustrine facies deposited conformably on the underlying Borrego Formation in the Ocotillo Badlands (Chapter 2). Sediment is locally sourced from nearby uplifts in the Fish Creek and Vallecitos Mountains and contains clasts recycled from older early to middle Pliocene basin fill. Paleoflow was to the east. The Ocotillo Formation fines and thins to east-northeast as in interfingers with the Brawley Formation in the eastern San Felipe Hills (Chapter 2).

The Brawley Formation consists of 3 interbedded lithofacies: fluvial to deltaic sandstone with cross-bedding and weak calcic paleosols; lacustrine mudstone, claystone, and marlstone with 0.5 to 1.5 m deep desiccation cracks, rare evaporite minerals, and locally abundant microfossils; and eolian sandstone with large scale (~ 3-4 m high) high-angle cross stratification (Chapter 2). Microfossils include marine to lagoonal forams, and lacustrine ostracods, micromollusks, and charophytes. Sandstones include ~60 % biotite-rich arkose derived from local tonalite plutons (L suite), and ~ 40 % sublitharenite derived from the Colorado Plateau (C suite). Sediment transport was to the E to NNE in the San Felipe Hills. Sedimentation rates in the Brawley Formation range from 1.0 ± 0.1 to 1.2 ± 0.2 mm/yr (Chapter 2). Clastic Brawley Formation sediments accumulated in an

ephemeral stream and delta system on the western margin of the Salton Trough while evaporites accumulated offshore in the southeast Salton Sea. Most water in the Brawley lake was derived from the Colorado River to the SE, but paleocurrents show that sand was derived from local sources in the W and SW. C suite sand was recycled from the uplifted Pliocene Diablo Formation, Imperial Group, and/or Borrego Formation. Flooding of the basin occurred when channel switching in the Colorado River delta delivered water north into the Brawley basin (Chapter 2).

Starting at 1.07 Ma the lake margin shifted to the NE and nearly modern depositional environments were established. These environments include the alluvial facies of the Ocotillo Formation in the west and southwest and grading eastward into the fluvial, fluvial-deltaic, eolian, lacustrine, and evaporite facies of the distal Brawley formation. Deposition of the Ocotillo and Brawley formations occurred in a basin controlled by geometries kinematics of the San Jacinto fault zone that differ from those of the current San Jacinto fault zone. Folding after the end of Brawley and Ocotillo formation deposition between 0.61 Ma $\pm$ 0.02 Ma and 0.52 Ma $\pm$ 0.03 Ma shifted the depocenter even farther to the east as the active strands of the San Jacinto fault zone changed to their modern geometries. The depositional basin was localized on the floor of the Salton Trough and uplift and pedimentation became the dominant process in the western Salton Trough. This abrupt change at ~0.5 to 0.6 Ma reflects reorganization of the basin due to initiation or reorganization of the San Jacinto fault zone in the San Felipe Hills.

Our work found no definitive evidence of stratigraphic growth relations in the stratigraphy pre-dating the Ocotillo and Brawley formations. Rocks of the Imperial

Group, Diablo and Olla formations, and Transitional unit were apparently deposited in a conformable sequence across the San Felipe Hills. Landsat imagery showing convergent bedding traces in the lower Borrego Formation in the central San Felipe Hills in an area of incompletely mapped dextral faults (Plate 3). To the south a single laterally continuous bed of recycled clast conglomerate in the Borrego formation provide possible evidence of pre-Ocotillo Formation inter-basin deformation in the San Felipe Hills (Chapter 3). Further field studies are needed in the lower and middle Borrego Formation in the central and south-central San Felipe Hills to quantify these observations. The stratigraphic position of these features implies that they are not the result of slip along strands of the Pleistocene San Jacinto fault zone because it were not active during deposition of the lower Borrego Formation.

Within the San Felipe Hills, Plio-Quaternary sediments of the previously described and dated Borrego, Ocotillo, and Brawley formations are strongly deformed by a complex series of folds and faults southeast of the previously mapped termination of the surface trace of the Clark fault. To the south, the Superstition Hills and Superstition Mountain faults may be accommodating slip in broad zone of clockwise transrotation (Hudnut et al. 1989). To constrain the geometries and interactions of the fault strands of the southern San Jacinto 3 prior models for the geometry of the Clark fault in the San Felipe Hills and its relation to the Superstition Hills fault to the south are considered. It has been suggested that the Clark fault terminates, continues as a blind fault in the subsurface, or steps left ~ 25 km to the blind northwest continuation of the Imperial fault (Chapter 3). Our field studies refute these three models. New data suggest, instead. that the Clark fault probably persists into the central San Felipe Hills as an incompletely

mapped horsetail fan and en echelon fault zone, and the San Jacinto fault zone recently began to accommodate strain in a broad transrotational zone southeast of the San Felipe Hills (Chapter 3). Gravity data show a southwest-deepening step in the bedrock surface coincident with the Clark strand near the Santa Rosa Mountains (Chapter 3). The bedrock step persists southeast into the central San Felipe Hills, southeast of the tip-line identified by prior surface mapping (Dibblee 1954, 1984; Sharp 1972).

The southeast San Felipe Hills preserve the most intensely folded sedimentary rocks in the area (Heitman 2002; Lilly 2003; Chapter 3). This highly folded belt is interpreted as the boundary zone between the domain of dextral slip and wrench folding to the northwest and a broad domain of clockwise transrotation to the southeast. The transrotational domain transfers slip from the Coyote Creek and Superstition strands to the Imperial and Brawley zones in the east and southeast (Hudnut et al. 1989; Seeber and Armbruster 1999), our work shows that it also captures slip from the Clark strand. The current configuration of the San Jacinto fault zone appears to be less than 0.6 ± 0.02 to 0.5 ± 0.03 Ma (Chapter 3).

The folding in the San Felipe Hills was divided into fold domains based on similar fold geometries. Average trend and plunge, interlimb angles, strain rates, shortening, and shortening rates were calculated for each domain. Transects through relevant fold domains were used to calculate the total shortening and amount of equivalent dextral slip on the Clark fault plane oriented 305° NW (Chapter 3). Total equivalent slip on the Clark fault plane for transect 2 is 5.62 km. Total equivalent dextral slip on transect 1 is 1.32 km, but is likely produced by slip on faults to the southwest of the Clark fault, including the Coyote Creek and or San Felipe Hills faults (Chapter 3).

Folding along transect 2 may have begun no earlier than the end of deposition of the internally conformable Brawley Formation in the southeastern San Felipe Hills at 0.61 ± 0.02 to 0.52 ± 0.03 Ma. Our analysis based on the spatial extent and amount of shortening from folding and the time constraints gives possible minimum slip rates between 9.5 ± 0.3 mm/year and 10.8 ± 0.7 mm/year for the Clark strand in and near the San Felipe Hills (Chapter 3). This suggests a significant component of plate boundary motion at this latitude has been localized on the Clark strand of the San Jacinto fault zone since at least 0.5 Ma.

Basin-scale structural and stratigraphic analyses can provide critical details of plate boundary evolution and geometry. In the San Felipe Hills our work shows the evolution of the southern San Jacinto fault zone from ~1 Ma to recent time period is complex and involves at least 2 major basin wide stratigraphic and structural transitions. An early change is recorded by a spatially extensive angular unconformity and lateral disconformity which separates the middle Pleistocene aged alluvial to fluvio-lacustrine Brawley and Ocotillo formations from the underlying persistently lacustrine Borrego Formation. A later change at 0.5 Ma complexly folded and faulted these rocks as the Clark strand transmitted slip southward into the San Felipe Hills and interacted with the developing zone of block rotation to the southeast. This geometry appears to have persisted into the present day.

References

Dibblee, T.W., Jr. 1954. Geology of the Imperial Valley region, California. *In* R.H. Jahns ed, Geology of southern California. California Division of Mines Bulletin 170: 21-28.

Dibblee, T.W. 1984. Stratigraphy and tectonics of the San Felipe Hills, Borrego Badlands, Superstition Hills and vicinity. *In* , C.A. Rigsby ed, The Imperial Basin; tectonics, sedimentation and thermal aspects. Pacific Section SEPM Field Trip Guidebook 40:31-44.

Heitman, E. A. 2002. Characteristics of the Structural Fabric Developed at the Termination of a Major Wrench Fault. [M.S. thesis], San Diego State University. San Diego CA, 77p.

Hudnut, K. W.; Seeber, L.; Pacheco, J.; Armbruster, J. G.; Sykes, L. R.; Bond, G. C.; and Kominz, M. A. 1989. Cross faults and block rotation in Southern California; earthquake triggering and strain distribution. Yearbook Lamont–Doherty, Geological Observatory of Columbia University, p. 44-49.

Lilly, D. R. 2003. Structural geology of a transitory left step in San Felipe Hills fault. [M.S. Thesis], San Diego State University. San Diego CA, 91 p.

Seeber, L., and Armbruster, J. G. 1999, Earthquakes, faults, and stress in Southern California. SCEC Annual Progress Report accessed online at http://www.scec.org/research/99research/99seeberarmbruster.pdf.

Sharp, R. V. 1972, Map showing recently active breaks along the San Jacinto fault zone between the San Bernardino area and Borrego Valley, California. USGS, IMAP 675, 3.

APPENDIX

July 11, 2005
Stefan Kirby
9535 Raintree Dr.
Sandy, UT 84092
801-910-8131

Dear Coauthor:

I am requesting your permission to include you as a coauthor on for Chapter 2 of my thesis. A copy of the text is included with this letter. Please advise me of any changes you require.

Please indicate your approval of this request by signing in the space provided, attaching any other form or instruction necessary to confirm permission. If you have any questions, please call me at the number above. I hope you will be able to reply immediately.

Thank you for your cooperation,

I hereby acknowledge coathorship of Stratigraphy and Depositional Setting of the Brawley Formation: Insights into Initial Strike-Slip Deformation in the Western Salton Trough, Chapter 2 of The Quaternary Tectonic and Structural Evolution of the San Felipe Hills, CA [M.S. Thesis] 178 p. with the following authors; Stefan M. Kirby, Susanne U. Janecke, Rebecca J. Dorsey, Bernard A. Housen, Victoria Langenheim, and Kristin McDougall-Reid.

July 11, 2005
Stefan Kirby
9535 Raintree Dr
Sandy, UT 84092
801-910-8131

Dear Coauthor:

I am requesting your permission to include you as a coauthor on for Chapter 2 of my thesis. A copy of the text is included with this letter. Please advise me of any changes you require.

Please indicate your approval of this request by signing in the space provided, attaching any other form or instruction necessary to confirm permission. If you have any questions, please call me at the number above. I hope you will be able to reply immediately.

Thank you for your cooperation,

I hereby acknowledge coathorship of Stratigraphy and Depositional Setting of the Brawley Formation: Insights into Initial Strike-Slip Deformation in the Western Salton Trough, Chapter 2 of The Quaternary Tectonic and Structural Evolution of the San Felipe Hills, CA [M.S. Thesis] 178 p. with the following authors; Stefan M. Kirby, Susanne U. Janecke, Rebecca J. Dorsey, Bernard A. Housen, Victoria Langenheim, and Kristin McDougall-Reid.

July 11, 2005

Stefan Kirby
9535 Raintree Dr.
Sandy, UT 84092
801-910-8131

Dear Coauthor:

I am requesting your permission to include you as a coauthor on for Chapter 2 of my thesis. A copy of the text is included with this letter. Please advise me of any changes you require.

Please indicate your approval of this request by signing in the space provided, attaching any other form or instruction necessary to confirm permission. If you have any questions, please call me at the number above. I hope you will be able to reply immediately.

Thank you for your cooperation,

I hereby acknowledge coathorship of Stratigraphy and Depositional Setting of the Brawley Formation: Insights into Initial Strike-Slip Deformation in the Western Salton Trough, Chapter 2 of The Quaternary Tectonic and Structural Evolution of the San Felipe Hills, CA [M.S. Thesis] 178 p. with the following authors; Stefan M. Kirby, Susanne U. Janecke, Rebecca J. Dorsey, Bernard A. Housen, Victoria Langenheim, and Kristin McDougall-Reid.

July 11, 2005
Stefan Kirby
9535 Raintree Dr.
Sandy, UT 84092
801-910-8131

Dear Coauthor:

I am requesting your permission to include you as a coauthor on for Chapter 3 of my thesis A copy of the text is included with this letter. Please advise me of any changes you require.

Please indicate your approval of this request by signing in the space provided, attaching any other form or instruction necessary to confirm permission. If you have any questions, please call me at the number above. I hope you will be able to reply immediately.

Thank you for your cooperation,

I hereby acknowledge coathorship of Middle Pleistocene to Recent Evolution of the San Jacinto Fault Zone in the San Felipe Hills Area, CA, Chapter 3 of The Quaternary Tectonic and Structural Evolution of the San Felipe Hills, CA [M.S. Thesis] 178 p. with the following authors; Stefan M. Kirby, Susanne U. Janecke, Victoria Langenheim, Rebecca J. Dorsey, and Bernard A. Housen.

July 11, 2005

Stefan Kirby
9535 Raintree Dr.
Sandy, UT 84092
801-910-8131

Dear Coauthor:

I am requesting your permission to include you as a coauthor on for Chapter 3 of my thesis A copy of the text is included with this letter. Please advise me of any changes you require.

Please indicate your approval of this request by signing in the space provided, attaching any other form or instruction necessary to confirm permission. If you have any questions, please call me at the number above. I hope you will be able to reply immediately.

Thank you for your cooperation,

I hereby acknowledge coathorship of Middle Pleistocene to Recent Evolution of the San Jacinto Fault Zone in the San Felipe Hills Area, CA, Chapter 3 of The Quaternary Tectonic and Structural Evolution of the San Felipe Hills, CA [M.S. Thesis] 178 p. with the following authors; Stefan M. Kirby, Susanne U. Janecke, Victoria Langenheim, Rebecca J. Dorsey, and Bernard A. Housen.

Plate 1 Geologic map of the San Felipe Hills, CA.

by S. Kirby, S. U. Janecke, R. Dorsey and, A. Steely 2005

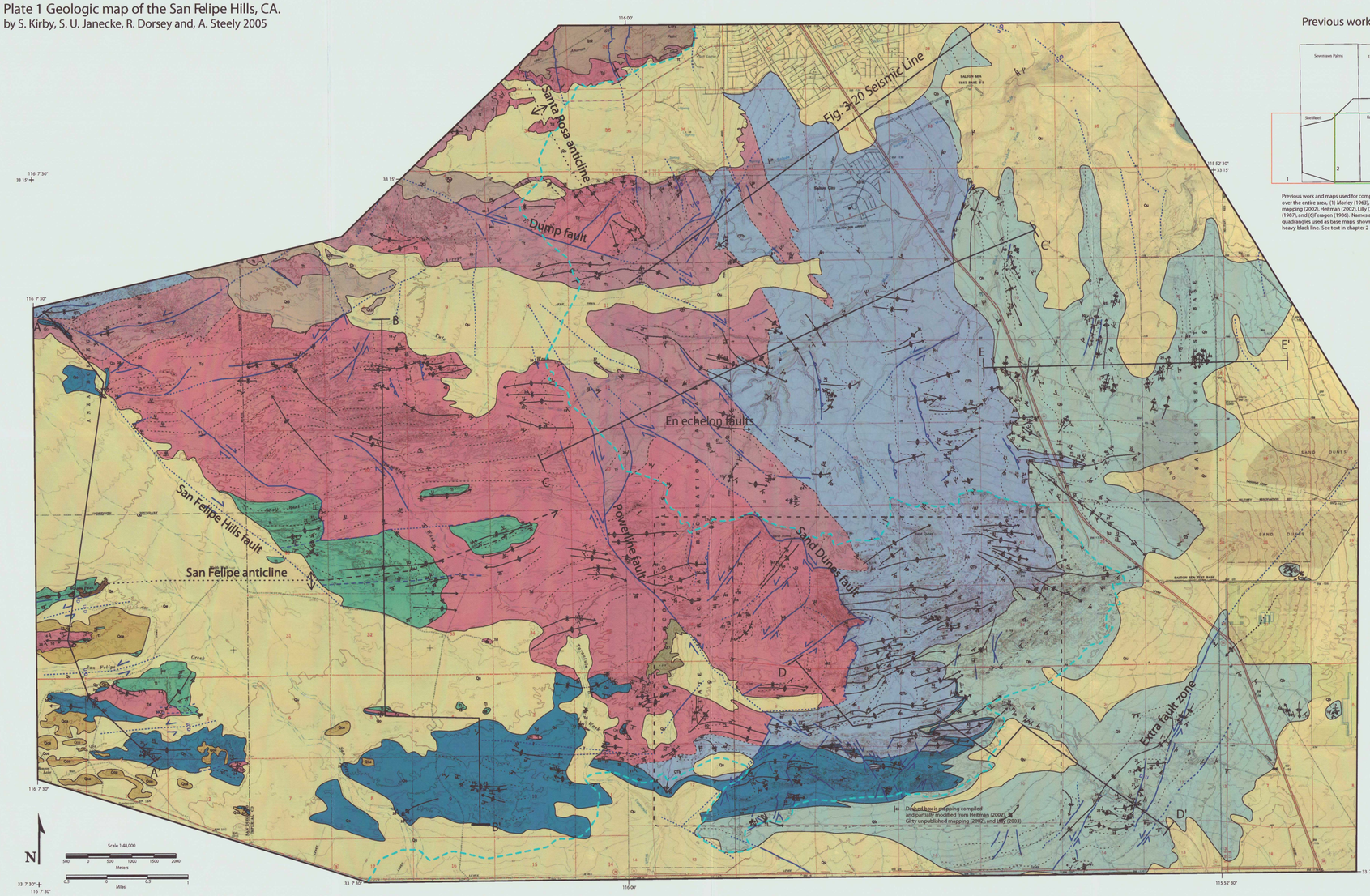

Previous work

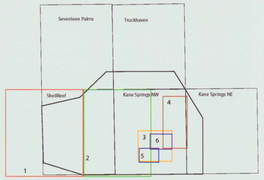

Previous work and maps used for compilation include Dibblee (1954, 1984) over the entire area, (1) Morley (1963), (2) Reitz (1977), (3) Girty unpublish ed mapping (2002), Heitman (2002), Lilly (2003), (4) Dronyk (1977), (5) Wells (1987), and (6)Fieragen (1986). Names and locations of USGS 1:24,000 quadrangles used as base maps shown relative to study area shown by heavy black line. See text in chapter 2 for references.

Correlation of units

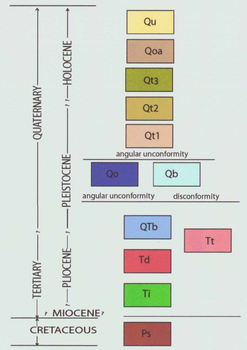

Geologic Symbols

Contacts

- Definite
- Gradational or approximately located
- Concealed

Faults

(solid where definitely located, dashed where approximately located, dotted where concealed)

- Strike-slip fault (arrows give slip sense)
- Normal fault (u is on footwall)
- Oblique-slip fault
- Thrust or reverse fault (barb is on hanging wall)
- Normal fault scarp (hatch is on down-thrown block)
- Bedding plane strike parrallel fault (inferred to separate highly folded from less folded rocks)

Folds

- Syncline (direction of arrow is direction of plunge)
- Anticline (direction of arrow is direction of plunge)

Miscellaneous Symbols

- Strike and dip of bedding
- Bedding trace from air photos
- Lake Cahuilla highstand ~ 48 ft above sea level

Unit Descriptions

Qu Undivided surficial deposits (Qu). Unit consists of all remaining late Holocene age deposits including; stream alluvium, colluvium, vegetated and active dunes, and lake Cahuilla deposits in the east. Lake Cahuilla deposits anecharacterized by poorly consolidated dull brown silt, sand, mud, and occasional white marls. Broken lacustrine gastropod fossils are common. Pumice clasts are locally common in the Cahuilla sediments. Total thickness of the Cahuilla deposits is up to ~ 4-5 m but is generally less ~ 2-3 m.

Qoa Older alluvium (Qoa). Dark weathering cobble to sandy-gravel deposits. Deposits form small low hills south of Squaw Peak in the western San Felpe Hills. Poorly consolidated deposit which is dominated by plutonic clasts derived from the Eastern Peninsular Ranges. Unit maybe weakly folded in some areas. Total thickness is ~ 2-4 m.

Qt3 Youngest terrace deposit (Qt3). Dark weathering gravel to sandy gravel and cobble terrace. Clast composition is similar to Qt2. Unit is deposited along the upper portions of Arroyo Salada and Tule washes near the western edge of the map area. Overlies all older rocks in angular unconformity.Several fault scarps and lineaments are apparent in this unit. Total thickness 2-3 m.-

Qt2 Terrace deposit (Qt2). Dark brown weathered cobble to sandy-gravel terrace deposit. Clasts consist of metamorphic rocks including marble and quartzite, and plutonic rocks of the Eastern Peninsular Ranges. Unit forms high terrace along the northern edge of the map area overlying the Diablo Formation and Transitional unit in angular unconformity T errace is cut by several down to the east ~ 2-3 m high fault scarps. Total thickness is ~ 4-5 m.

Qt1 Oldest terrace deposit (Qt1. Weathered tan to brown gravel and sandy terrace deposit with moderately developed calcic soil horizon. Clasts are dominated by plutonics derived from the Eastern Peninsular Ranges. Isolated south sloping high terrace exposure just west of the Powerline fault north of Tarantula Wash. Overlies older units in angular unconformity. Total thickness is ~ 2-3 m. Maybe correlative with the Fonts Point sandstone of Ryter (2002) further to the west.

Qb Brawley Formation (Qb). Buff-tan to orange weathering, locally-derived and Colorado River-derived sandstone and mudstone. Formation is characterized by moderately to poorly lithified, medium- to fine-grained sandstone with abundant sedimentary structures including large scale high angle cross stratification, trough and planar cross bedding, climbing ripples, channel fills, and soft sediment deformation. Red mudstone and claystone, containing downward tapering sand filled desiccation cracks up to 1-2 m deep are common. Also includes locally abundant sandstone concretions, gray fossiliferous marls up 0.4 m thick, and minor siltstone. Microfossil assemblages show deposition in fresh to brackish water conditions. Distal equivalent of the conglomeratic Ocotillo Formation. The basef formation is a regional disconformity in the eastern San Felipe Hills dated at 1.07 Ma. Total thickness is up to ~ 550 m in the eastern San Felipe Hills. Fluvial, fluvial-deltaic, lacustrine, and eolian deposits. Lower to middle Pleistocene age.

Qo Ocotillo Formation (Qo) (formerly the Ocotillo Conglomerate of Dibblee, 1954). Gray to tan, pebble to cobble conglomerate, pebbly sandstone, arkose, gritty sandstone, peach mudstone, and gray siltstone. Recycled clasts of the Diablo Formation and the Imperial Group are locally common. Overlies older units in angular unconformity in the western San Felipe Hills and disconformity in the southeastern San Felipe Hills. Interfingers basinward with the Brawley Formation. Total thickness is ~ 225 m to the south in Ocotillo Badlands, exposed thickness in the southwest San Felipe Hills is significantly less ~ 75-100 m. A thin tongue (~ 10-20 m thick) of Ocotillo Formation underlies the Brawley Formation in the southeastern San Felipe Hills, where this contact is dated at 1.07 Ma. Alluvial and fluvial deposits. Lower to middle Pleistocene age.

QTb Borrego Formation (QTb). Red laminated to massive mudstone and fissile gray claystone dominate over buff to tan colored, moderately lithified, fine to medium grain tabular to crossbedded sandstone. Minor grey siltstones and fossiliferous marls. Yellow argillicceous calcite nodules up 10 cm in length common in the gray claystones. Fossil assemblages indicate fresh to brackish water conditions. Sediment is dominantly Colorado River derived. Records deposition in open water to marginal lacustrine conditions. Total thickness is ~ 1800 m just south of Salton City. Upper Pliocene to lower Pleistocene age.

Tt Transitional Unit (Tt). Transitional unit between the Diablo Formation and the Borrego Formation. Approximately subequal amounts of red massive to laminated mudstone and buff to tan colored Colorado River-derived sandstone Total thickness in the north-central San Felipe Hills may be up to 500 m. Transitional unit is uncommon on the south flank of the San Felipe anticline in part because of younger faulting and erosion. Most outcrops are complexly folded and faulted. Unit interfingers with both fully lacustrine deposits of the Borrego Formation and fluvial to fluvial deltaic deposits of the Diablo Formation. Lacustrine and delta-plain deposits. Dibblee (1954,1984) included this within the Palm Spring Formation. Middle to upper Pliocene age.

Td Diablo Formation (Td) of the Palm Spring Group. Tan to buff, planar to crossbedded, Colorado River-derived sandstone. Includes beds of red massive mudstone up to 4-5 m thick, commonly at the top of 3-4 m thick fining upward channel sandstone intervals. Resistant, black to varicolored pebble size siliceaous clasts are common at the base of some sandstone packages. Gray to gray-blue calcite crusts and nodules and large spherical sandstone concretions are common in the north-central portion of the San Felipe Hills. Petrified palm wood is common. Total thickness on the north limb of the San Felipe anticline is ~ 2000 m. Nonmarine deltaic deposits. Pliocene age.

Ti Imperial Group (Ti). Gray buf f to yellow, coarse-grained locally derived marine bioturbated sandstone, coquina, fine-grained rhythmites and shale. Abundant oyster shell fragments in some zones. Very coarse-grained locally derived arkose lies in buttress unconformity on basement rock at Squaw Peak. Sandy and fossiliferous gray limestone is charcteristic of the lower portions of the Imperial Group. T otal thickness near the core of the San Felipe anticline is ~900 m. Marine prodelta and marginal deposits. Upper Miocene to lower Pliocene age.

Ksp Squaw Peak Gneiss (Ksp). Moderately to strongly foliated, dark weathering granitoid, minor biotite schist. Exposed at Squaw Peak whereellation dips ~ 50-60 north and strikes west-northwest. Cretaceous age.

Plate 2. Measured section and magnetostratigraphy of the Brawley Formation, Oil Well Wash, San Felipe Hills, CA.

S. Kirby, S. U. Janecke, R. Dorsey, and B. Housen 2005.

Preferred correlation to magnetic polarity timescale

no data; uncertain polarity, but probably normal

Brunhes Ch.

0.780 Ma

400 m

Jaramillo Ch.

0.990 Ma

265 m

Olduvai Ch.

1.070 Ma

185 m of section

Matuyama Ch.

Ocotillo Fm

Borrego Fm

Brawley Fm

Yellow marker unit on spot image

Correlation of projected yellow marker units does not produce reasonable correlations of lithostratigraphy and polarity

Preferred correlation of marls beneath 610m and marls beneath 480m

Alternate correlation of marls beneath 610m and marls at 415m

normal or most likely reverse polarity

Paleocurrents from Brawley Formation N=36 taken throughout the Brawley Formation in the eastern San Felipe Hills.

Calculation Method ....Frequency
Class Interval .....20 Degrees
Length Filtering ....Deactivated
Azimuth Filtering ....Deactivated
Data Type .....Unidirectional
Population 36
Maximum Percentage ....21.4 Percent
Mean Percentage .....9.1 Percent
Standard Deviation ....4.73 Percent
Vector Mean .....50.1 Degrees
Confidence Interval ....15.48 Degrees
R-mag 0.73

Legend

All UTM coordinates are in NAD 27

Grain Size
M Mud
S Silt
VFSd Very fine sand
F Fine sand
MSd Medium sand
C Coarse sand
VC Very coarse sand
Pb Pebble

Environment of Dep.
F Fluvial
FD Fluvial-deltaic
Eolian
L Lacustrine

Symbols

Magnetic polarity white is reverse and black is normal

Sandstone
Siltstone
Mudstone
Claystone
Marl

Pebbly sandstone
Tabular bedded sandstone
Crossbedded sandstone
Rippled sandstone

Plate 3. Landsat image and geology of the San Felipe Hills, CA.

by S. Kirby, S. U. Janecke, R. Dorsey and, A. Steely 2005